NEW MEXICO BUREAU OF GEOLOGY AND MINERAL RESOURCES

Sunshine Valley Hydrogeology Study

Geoffrey Rawling and Shari Kelley

Open-File Report 607
February 2020

Sunshine Valley Hydrogeology Study

Geoffrey Rawling and Shari Kelley

Open-File Report 607
February 2020

New Mexico Bureau of Geology and Mineral Resources
A Research Division of New Mexico Institute of Mining and Technology

PROJECT FUNDING

Healy Foundation, New Mexico Bureau of Geology and Mineral Resources, and Aquifer Mapping Program.

New Mexico Bureau of Geology and Mineral Resources

A Research Division of New Mexico Institute of Mining and Technology

Socorro, NM 87801
(575) 835 5490
www.geoinfo.nmt.edu

CONTENTS

Executive Summary 1

I. Introduction 3

II. Climate and Precipitation 5

III. Previous Work 7
- Geology 7
- Hydrogeology 7
- Geophysics 10

IV. Regional Geology 11

V. Regional Hydrogeology 13

VI. Methods 15
- A. Physical and chemical hydrologic data collection 15
  - Water-level measurements 15
  - Water samples 15
  - General ion and trace metal chemistry 19
  - Stable isotopes 19
  - Carbon isotopes and tritium 19
- B. Geophysical Methods 19
  - Temperature logging 19
  - TEM Surveys 20
- C. Historical Data Evaluation 21
  - Water-level data 21
  - Geochemistry data 21
  - Streamflow data 21
  - Subsurface geology 21

VIII. Results 25
- Water-level elevations 25
- Groundwater chemistry 26
- Temperature-depth Measurements 31
- TEM Survey 32

IX. Discussion 35
- Processes controlling water chemistry 35
- Stable isotopic compositions, location, and seasonality of recharge 37
- Age of recharge and mixing, and potential irrigation return 37
- Temperature and mixing of hydrothermal waters 38
- Subsurface interpretations from TEM surveys 41

X. Hydrogeologic Conceptual Model 43

XI. Water Budget 45
- Components of the water budget 45
- Chloride mass balance 49
- Inflow from streams 52
- Outflow to streams 53
- Discussion 54

XII. Conclusions 59

Acknowledgments 60

References 61

Figures

1. Map of the study area in northern Taos County, New Mexico 2
2. Plots of water usage and irrigated acreage in Sunshine Valley region over time 4
3. Climate and streamflow data for the Sunshine Valley region 5
4. Geologic map and geologic cross sections of the Sunshine Valley region ..... 8 & 9
5. Structure contours of the top of the uppermost basalt flow and thickness contours of lake beds from Winograd 12
6. Maps of water-level elevations for the decades of the 1950s, 1980s, and 2010s 15–16
7. Map of sample sites for water chemistry analyses 18
8. Map showing the location of the TEM sites in Sunshine Valley 20

9. Maps of water-level elevation changes from the 1950s to the 1980s and the 1980s to the 2010s 22
10. Selected hydrographs for the Sunshine Valley region and location of wells on map 23
11. Map of Stiff diagrams of major ion-chemistry 26
12. Piper diagram illustrating major ion chemistry 27
13. Plot of anions bicarbonate, sulfate, and chloride against total dissolved solids 28
14. Plot of cations calcium, sodium, and magnesium against total dissolved solids 28
15. Maps of total dissolved solids and sulfate concentrations across the study area 29
16. Calculated saturation indices against total dissolved solids 30
17. Map of stable isotopic composition of hydrogen in water samples and locations of the three precipitation collection sites and samples defining the evaporation trend in Taos Ski valley 30
18. Map and plot of tritium and ^{14}C age-dating results 31
19. Tritium, ^{14}C, total dissolved solids, and temperature plotted against well depth 32
20. Temperature logs for the three wells measured in this study 32
21. Model resistivity curves from A-A' on Figure 8 33
22. Model resistivity curves from B-B' and C-C' on Figure 8 33
23. Plot comparing ion concentrations sourced from dissolution of calcite, dolomite, gypsum, anhydrite, and halite 35
24. Piper diagram of major ion chemistry after correction for ion exchange 36
25. Temperature logs measured by Reiter et al. and Edwards south of Sunshine Valley 39
26. Silica, lithium, fluorine, and boron plotted against temperature 40
27. Cross-section C-C' in Fig. 4 41
28. A conceptual model of hydrogeology of the Sunshine Valley region 43
29. Map showing samples used in CMB recharge analysis 47
30. Plot of Cl/Br molar ratio against chloride concentration 50
31. Recharge scenarios 51
32. Geometry of the Dupuit approximation for unconfined groundwater flow 53
33. Summary of the water budget for the Sunshine Valley aquifer 56

Tables

1. Chloride mass-balance calculations and streamflow corrections for water budget 46
2. Discharge from and recharge to Sunshine Valley 53
3. Estimation of groundwater flux into the Rio Grande from the northern Taos Plateau 54

Appendix

A. Water level data ..... 8 sheets
B. Water chemistry data ..... 5 sheets
C. Stream flow data ..... 8 sheets
D. Cl Br t-test results ..... 1 page
E. Conversion factors ..... 1 page

(Available in digital format, http://geoinfo.nmt.edu/publications/openfile/details.cfml?Volume=607)

EXECUTIVE SUMMARY

The regional hydrologic importance of the Sunshine Valley of northern Taos County, New Mexico, is belied by its remote location and sparse population. This is due to the large increase in flow of the Rio Grande in the reach adjacent to Sunshine Valley, and the transfer of 1,752 acre-feet per year of water rights downstream from the valley as part of the Aamodt Settlement Agreement. There has been no detailed hydrologic investigation of the region since the 1950s. This study integrates new physical and chemical hydrologic data, field geophysical investigations, and previous work and historical data to elucidate the hydrologic regime in the valley and document changes to the groundwater system since the 1950s. A hydrologic conceptual model and water budget for the aquifer system were prepared.

The aquifer underlying Sunshine Valley is laterally and vertically heterogeneous, with sand and gravel layers overlying and interbedded with fractured and highly transmissive basalt flows. A portion of this complex aquifer was investigated using a small-scale transient electromagnetic (TEM) survey in central Sunshine Valley; this survey identified a resistive layer at a depth of 210-215 ft across a 1.5 mi^2 area that is interpreted to be fresh water within a sand-and-gravel aquifer.

Groundwater recharge to the aquifer system occurs in the mountains to the east of the valley, and is dominated by high-elevation winter precipitation. Little direct recharge occurs across the valley floor. Recharge from surface water arrives in the valley aquifer as both infiltrating streamflow and irrigation water derived from streamflow. More than half of the total groundwater recharge to the Sunshine Valley aquifer occurs as groundwater migrating laterally from the mountains to the east. The steep topography and geologic features of the Questa caldera probably influence the amount of recharge by this mechanism. Elevated temperature-depth measurements and discharge temperatures in wells west and southwest of Costilla are associated with upwelling of warmer-than-average groundwater near Quaternary faults; the warm temperatures may be related to deep circulation and heating of groundwater within the mountain block. Discharge from the Sunshine Valley aquifer occurs in the Rio Grande Gorge and lower Red River Canyon as spring discharge and direct discharge though the stream beds.

An estimated 1,000 to 2,000 acre-feet per year of groundwater has been lost from storage since the 1980s, corresponding to water-level declines of few feet per year across the region. The water budget calculations are generally consistent with the storage change results, with estimated discharges falling between the estimated upper and lower bounds of recharge inputs. However, the water budget analysis is constrained by fundamental data limitations and is neither accurate nor precise enough to independently confirm or refute the independent estimates of groundwater storage losses.

Reduction of groundwater pumping due to the water-rights transfer can ultimately result in additional water flowing though the Sunshine Valley aquifer to discharge in the Rio Grande and Red River on a time scale of a few to several tens of years. Current levels of groundwater withdrawals for irrigation are unlikely to be the main cause of the groundwater storage changes since the 1980s. Trends in decreasing regional precipitation, increasing temperature, and increasing surface water-use are more likely factors affecting the amount of water in storage in the aquifer and the amount of discharge. Continued declines in annual precipitation and streamflow and increases in mean annual temperature will decrease the amount of recharge to and discharge from Sunshine Valley.

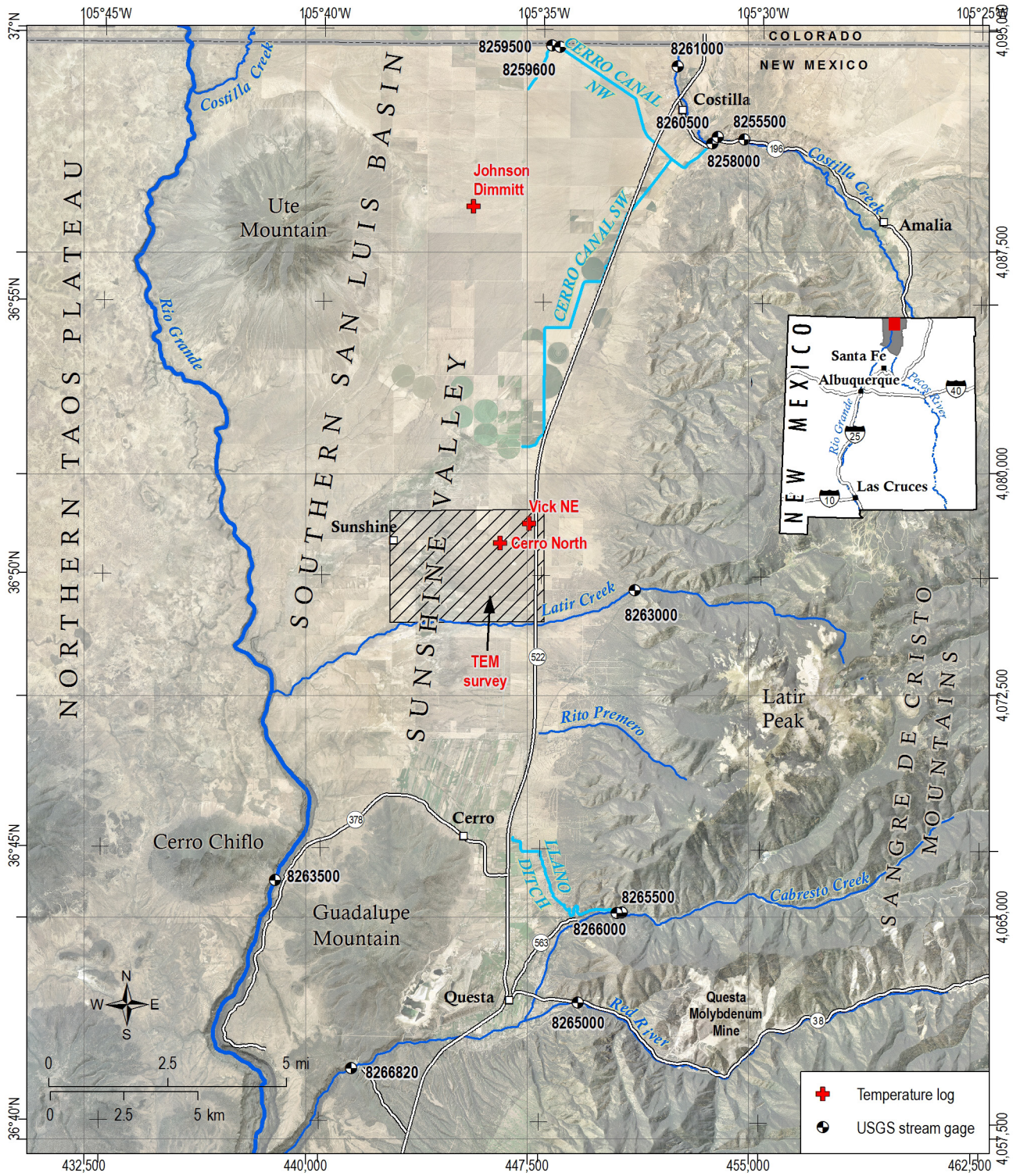

Figure 1. Map of the study area in northern Taos County, New Mexico, with regional location shown in inset. Stream gauges with USGS identification numbers are those used in water budget calculations. Wells with temperature logs are shown as red crosses. Irrigated areas appear as dark green regions northeast of Sunshine and north of Cerro. Llano Ditch and Cerro Canal are major irrigation diversions. Region of the TEM geophysical investigation (Fig. 8) is shown by the box in central Sunshine Valley.

I. INTRODUCTION

The Sunshine Valley of Taos County in northern New Mexico extends north from the towns of Questa and Cerro into southern Colorado, north of the town of Costilla. It is the southeastern portion of the larger San Luis Basin of the Rio Grande rift (Fig. 1). Although traditionally referred to as a valley, the topography of the region is more accurately described as a high mountain plateau bounded on the east by the steep range front of the southern Sangre de Cristo Mountains, with peaks over 12,000 feet, and on the west by the gorge of the Rio Grande. Guadalupe Mountain (8,761 feet) forms most of the southern boundary of Sunshine Valley. A low divide southeast of the town of Cerro between Guadalupe Mountain and the Sangre de Cristo Mountains divides the Sunshine Valley from the Cabresto Creek drainage, which flows east from the mountains and then south to the Red River. This divide forms the southern boundary of the study area. The dormant volcano, Ute Mountain, rises to 10,093 feet in the northwest corner of the valley. Elevations on the valley floor average about 7,500 feet. Costilla Creek and Latir Creek are the two main perennial drainages that enter the valley from the mountains to the east.

This study only considers the area of Sunshine Valley within New Mexico. The region is sparsely populated. Cerro has a population of 428 (2000 census) and Costilla has a population of 205 (2010 census). Much of the population lives in a rural setting. The economy is mostly based on ranching and agriculture; the latter is dependent on irrigation from both surface and groundwater (Fig. 2). The irrigated areas are concentrated around and north of Cerro and between Sunshine and Costilla (Fig. 1).

The remote and sparsely populated nature of the study area belies its significance to the hydrologic regime in northern New Mexico. It has been known since the 1920s (Winograd 1959, and references therein) that there is a significant influx, or accretion, of groundwater to the Rio Grande in the reach that bounds the Sunshine Valley to the west. This water is sourced from aquifers that underlie the Sunshine Valley to the east and the Taos Plateau to the west of the river and enters the Rio Grande as seepage and

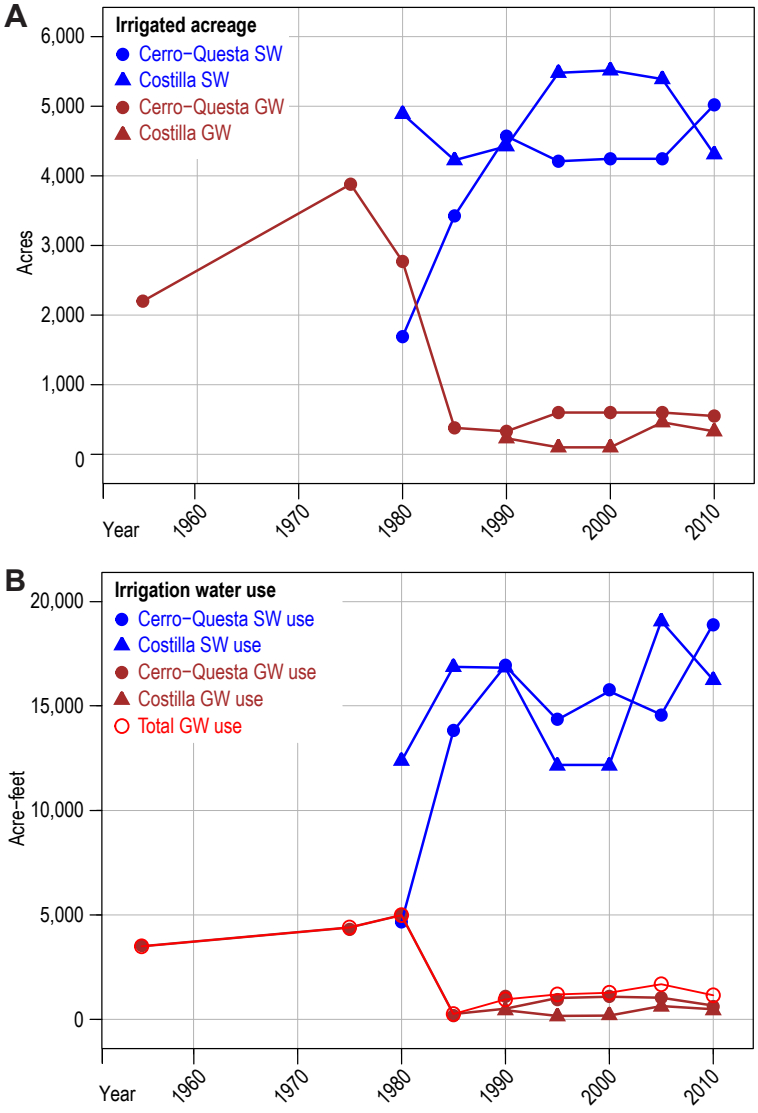

Figure 2. **A**—Plot of irrigated acreage in the Sunshine Valley region over time. **B**—Plot of water use for irrigation in Sunshine Valley region over time. Data from the NM Office of the State Engineer. SW = surface water, GW = groundwater

spring discharge. The recent Aamodt Settlement Agreement concerning pueblo and non-pueblo water rights in the Nambe–Pojoaque–Tesuque basin north of Santa Fe has an important clause concerning groundwater in the Sunshine Valley (Aamodt Settlement Agreement, 2018). This clause states that 1,752 acre-feet per year of groundwater rights used for irrigation in Sunshine Valley are to be transferred to the Nambe–Pojoaque–Tesuque basin as surface water for subsequent diversion from the Rio Grande. The hydrological reasoning behind this transfer is that groundwater not pumped for consumptive irrigation use in the Sunshine Valley will naturally discharge to the Rio Grande and be available downstream as surface water.

Given the regional significance of the hydrologic system, and the concern amongst local residents about the transfer of water rights out of the area, the New Mexico Bureau of Geology and Mineral Resources (NMBGMR) was tasked with completing an updated hydrogeologic study of the Sunshine Valley. This project is timely as the only comprehensive hydrogeologic study of this region is the work of Winograd (1959), which is now 60 years old. The goals of the present study are to characterize and assess any changes in the nature of the aquifer system and groundwater conditions in the Sunshine Valley since the work of Winograd (1959). Temporal trends in groundwater levels and spatial variation in water chemistry are described and interpreted in terms of groundwater recharge, discharge, flowpaths, relation to surface water, and use. The geophysical methods of temperature-depth measurements and transient electromagnetic surveying were used to investigate details of groundwater flow patterns and shallow subsurface geology, respectively. A hydrologic budget for the Sunshine Valley region is presented.

II. CLIMATE AND PRECIPITATION

Sunshine Valley lies within the northern mountain climatological division of New Mexico (Hacker and Carleton, 1982). The climate is semiarid, with mild summers, cold winters, and generally dry and sunny weather. The average daily maximum and minimum temperatures at Cerro are 60 and 28°F, respectively. Average total precipitation and snowfall at Cerro are 12.6 and 55 inches, respectively (Fig. 3). Precipitation is about 50% higher in the mountains (Hacker and Carleton, 1982; Garrabrandt, 1993). Most precipitation in the valley is from rainfall during summer thunderstorms, with less than 20% occurring as snow, but a third or more of the annual precipitation in the mountains is snow (Hacker and Carleton, 1982; Garrabrandt, 1993). Precipitation varies greatly from year to year. Estimates of evaporation in the valley range from 43–56 inches per year (Garrabrandt, 1993), much larger than the annual precipitation.

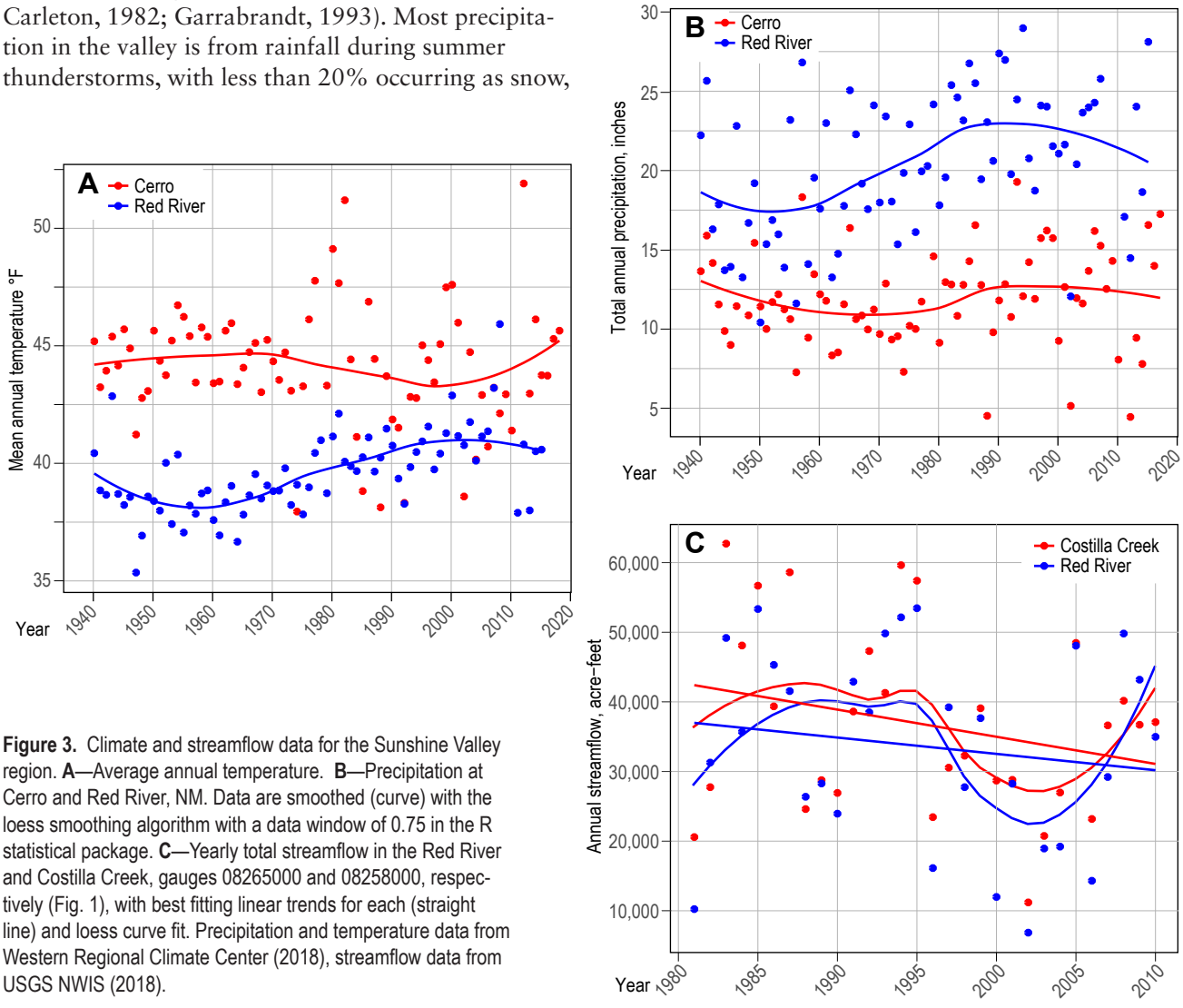

Figure 3. Climate and streamflow data for the Sunshine Valley region. **A**—Average annual temperature. **B**—Precipitation at Cerro and Red River, NM. Data are smoothed (curve) with the loess smoothing algorithm with a data window of 0.75 in the R statistical package. **C**—Yearly total streamflow in the Red River and Costilla Creek, gauges 08265000 and 08258000, respectively (Fig. 1), with best fitting linear trends for each (straight line) and loess curve fit. Precipitation and temperature data from Western Regional Climate Center (2018), streamflow data from USGS NWIS (2018).

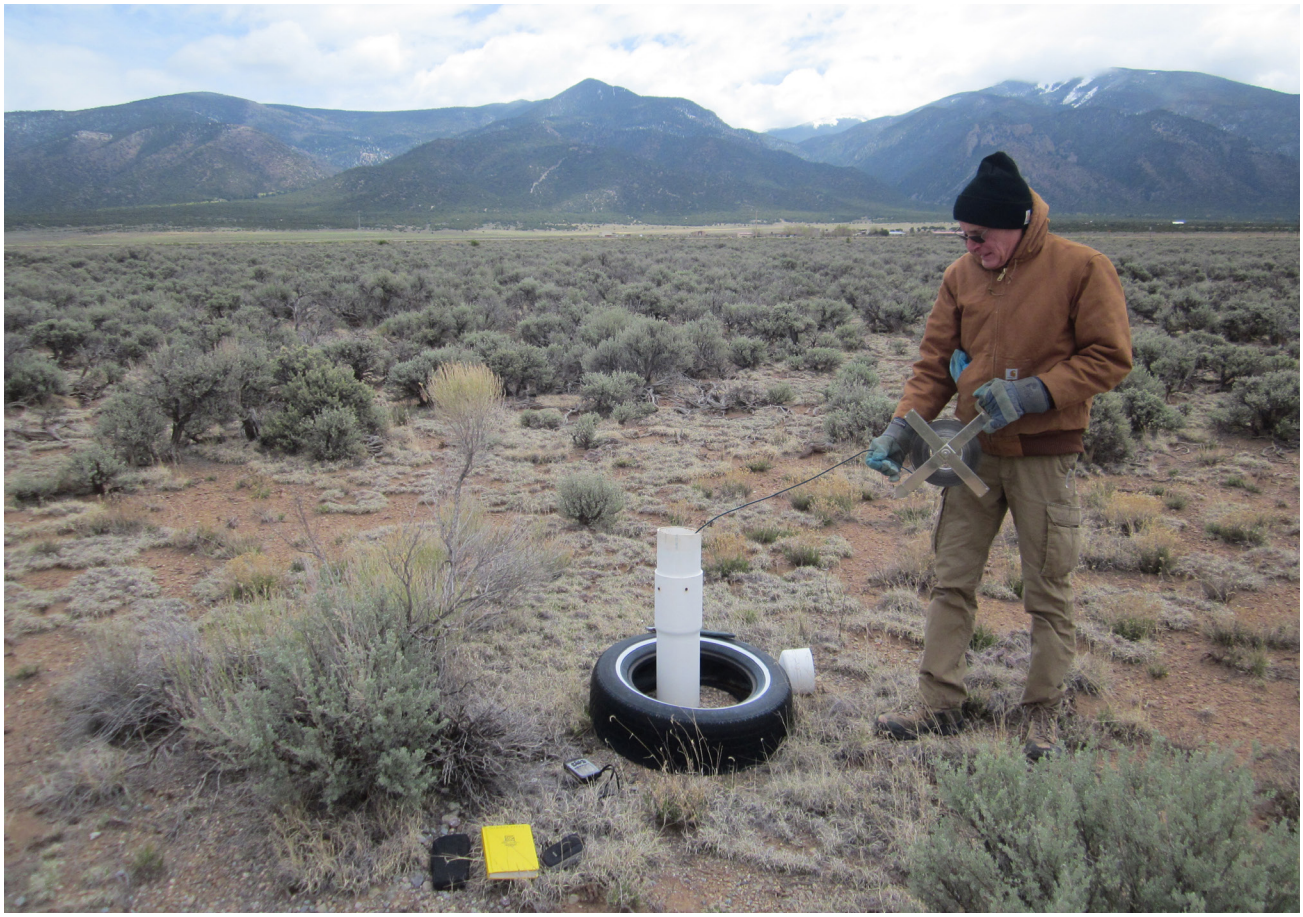

Measuring water levels with a steel tape in Sunshine Valley. The Sangre de Cristo Mountains rise in the background.

III. PREVIOUS WORK

Geology

As noted, the only previous comprehensive hydrogeologic study of the region is the work of Winograd (1959). Winograd characterized the basic geology and hydrology of the region, inventoried and measured wells, and presented a water table map, limited water chemistry data, and a semi-quantitative account of surface and groundwater inflows and outflows in the region. Several older studies are referenced by Winograd (1959), but the publications are no longer readily accessible. The most significant of these is Bliss and Osgood (1928), who conducted a seepage study along the Rio Grande in the reach adjacent to Sunshine Valley and first documented the gain in flow of the Rio Grande due to groundwater accretion.

Studies focused on the geology of the region include numerous recent 1:24,000- and 1:50,000-scale geological maps by the NMBGMR (Kelson et al., 2008; Kelson and Bauer, 2012) and U.S. Geological Survey (USGS) (Ruleman et al., 2013; Thompson et al., 2014a, 2014b). Lipman and Reed (1989) mapped the bedrock geology of the Sangre de Cristo Mountains to the east of Sunshine Valley. These maps cover the study area and address both the bedrock and surficial geology of Sunshine Valley and the adjacent Sangre de Cristo Mountains.

Machette et al. (2013) and Ruleman et al. (2013) described the Miocene to Pleistocene evolution of the Sunshine Valley region, including the formation of Pleistocene Lake Alamosa, integration of the Rio Grande as a through-flowing drainage, and the geomorphic development of the present-day landscape. Machette et al. (2007) referenced numerous papers about Quaternary geology and tectonics and the hydrology of the San Luis Valley region. Drenth et al. (2013) investigated the geologic structure of south-central San Luis Valley, including the northern part of the study area, using geologic maps and aeromagnetic and gravity techniques. Several guidebooks published by the New Mexico Geological Society contain information about many aspects of the geology and hydrology of the study area and surrounding region (e.g., Baldridge et al., 1984; Bauer at al., 1990; Brister at al., 2004).

Hydrogeology

There have been many previous studies addressing the hydrogeology of all or part of the San Luis Valley. The seminal study of Winograd (1959) has already been noted. Emery et al. (1971) described hydrogeologic conditions in the San Luis Valley north of the New Mexico–Colorado border. Summers and Hargis (1984) reinterpreted some of the hydrogeologic conditions in Sunshine Valley described by Winograd (1959), prompting a rebuttal by Winograd (1985). Hearne and Dewey (1988) performed a hydrologic analysis of the entire Rio Grande basin north of Embudo, NM (which is south of Sunshine Valley) that included calculating basin yields and simulating the aquifer system with a numerical groundwater flow model. Garrabrandt (1993) described groundwater and surface water resources in Taos County, and Johnson (1998) investigated surface water resources of the county in more detail. Recent NMBGMR reports have described the hydrogeology of the south Taos Valley (Johnson et al., 2016) and the northern Taos Plateau, across the Rio Grande from Sunshine Valley (Johnson and Bauer, 2012). Bauer et al. (2007) inventoried springs in the Rio Grande gorge and provided limited spring discharge and water chemistry data. Darr (2011) conducted a site-specific hydrology study in the farthest southeastern portion of Sunshine Valley, including aquifer test results and a local water table map. Kinzli et al. (2011) reinvestigated groundwater accretion to the Rio Grande in the reach adjacent to Sunshine Valley using an acoustic Doppler current profiler.

Numerous studies have investigated the hydrogeology of the Questa Molybdenum Mine and surrounding area, just southeast of Sunshine Valley, to understand the mine's impact on surface and groundwater quality. Natural hydrothermal alteration of mineralized areas is abundant in the Questa caldera, particularly in the Red River Canyon, which complicates determination of the anthropogenic impacts of mining on water quality (e.g., Ludington et al., 2004; Maest et al., 2004; Plumlee et al., 2006; Nordstrom, 2008). An unpublished report (Vail Engineering, 1993) contains a detailed analysis of the seepage from

A

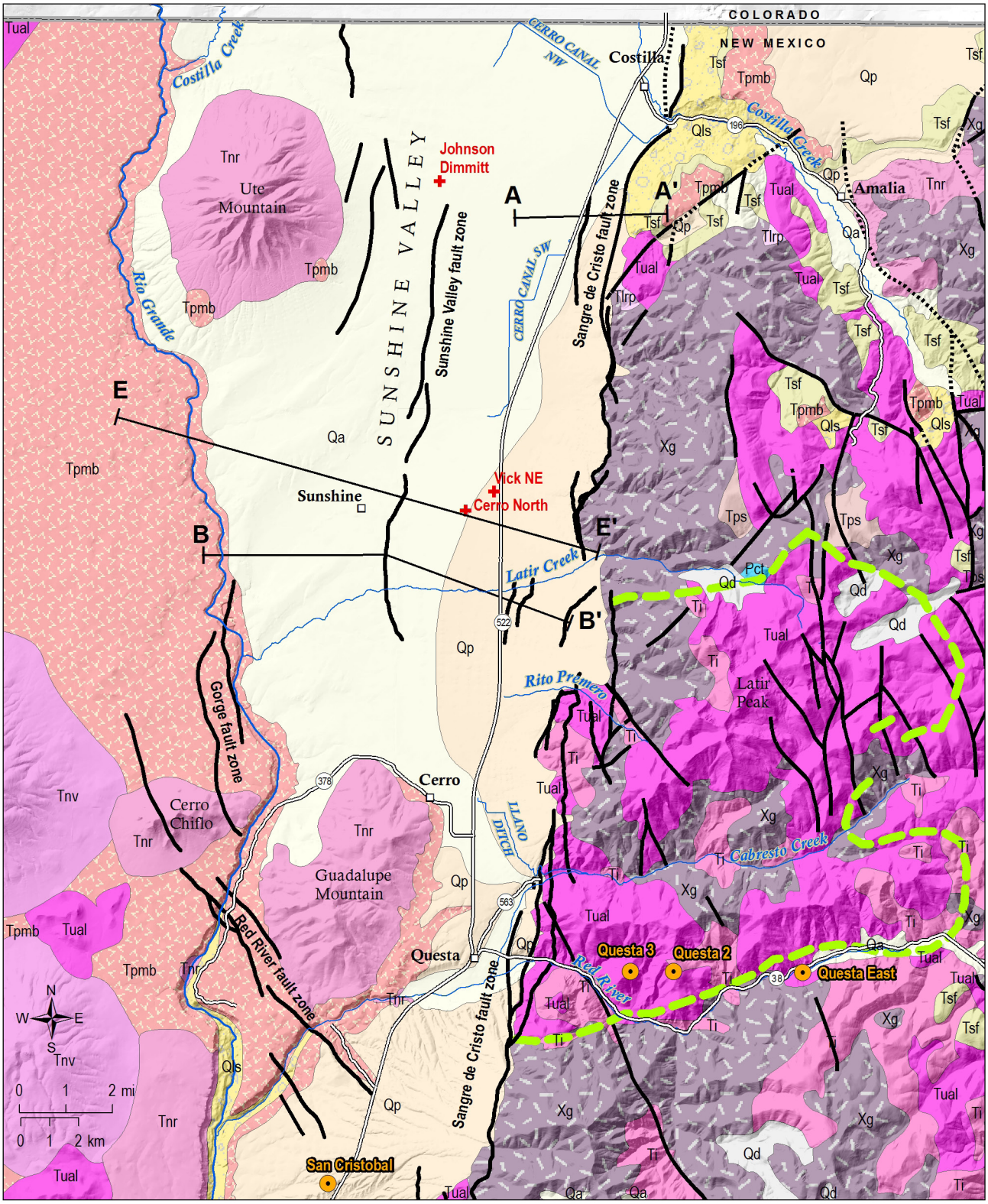
COLORADO
NEW MEXICO
Costilla
Costilla Creek
CERRO CANAL NW
CERRO CANAL SW
Amalia
Ute Mountain
Tnr
Tpmb
Tual
Tsf
Tps
Tlrp
Qp
Qa
Qls
Qd
Pct
Ti
Xg
SUNSHINE VALLEY
Sunshine Valley fault zone
Sangre de Cristo fault zone
Johnson Dimmitt
Vick NE
Cerro North
Sunshine
Latir Creek
Rito Primero
Latir Peak
Cabresto Creek
LLANO DITCH
Cerro
Gorge fault zone
Cerro Chiflo
Tnv
Guadalupe Mountain
Red River fault zone
Red River
Questa
Questa 3
Questa 2
Questa East
San Cristobal
Rio Grande
A
A'
B
B'
E
E'
196
522
378
563
38
N
W
E
S
0 1 2 mi
0 1 2 km
Fault (exposed)
Fault (concealed)
Caldera margin
Cross section
Temperature log (this study)
Temperature log (previous study)

B

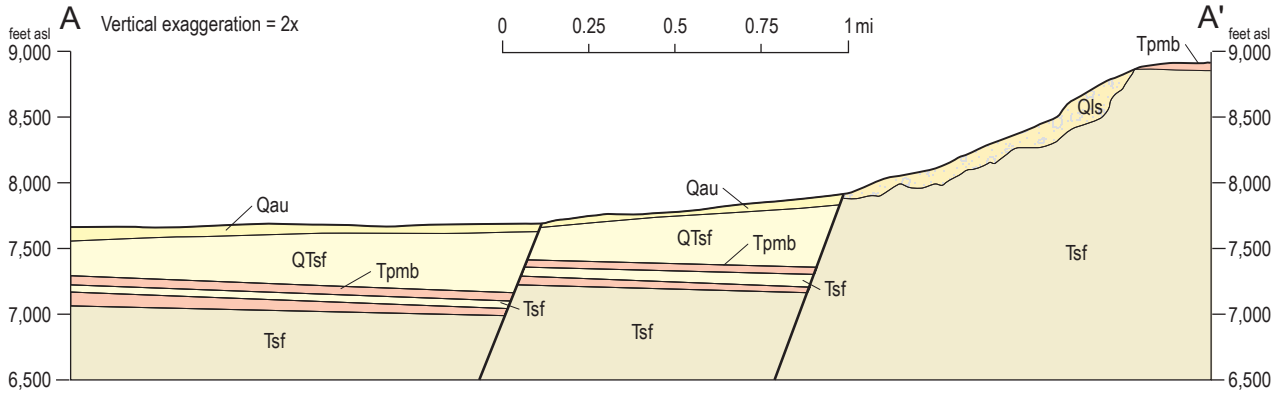

C

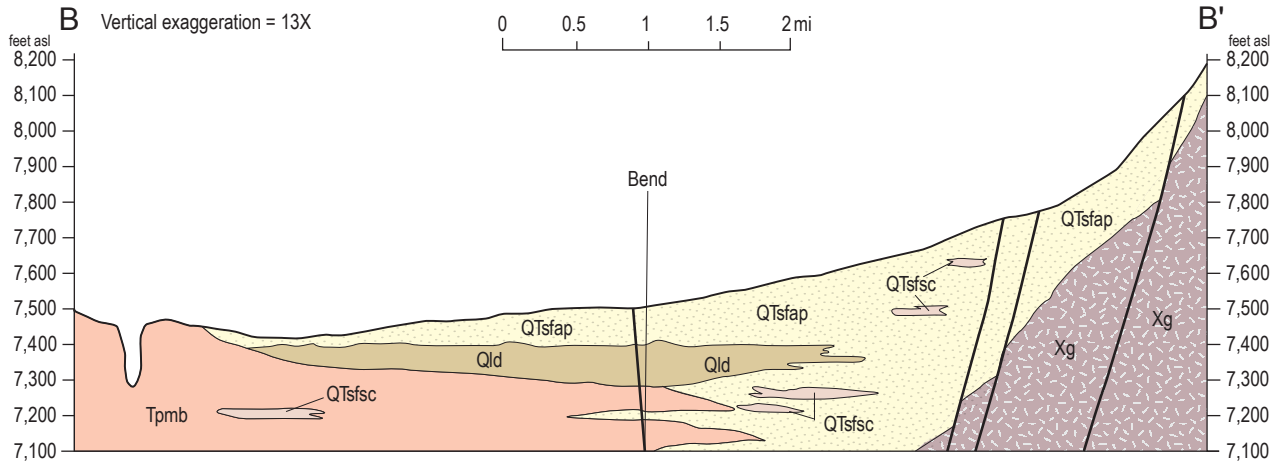

Geologic unit

- Qa—Alluvium (upper Pleistocene–Holocene)
- Qd—Glacial deposit (middle to upper Pleistocene)
- Qp—Piedmont alluvial deposit (lower Pleistocene–Holocene)
- Qls—Landslide deposit and colluvium (Pleistocene–Holocene)
- Tsf—Lower Santa Fe Group (upper Oligocene–upper Miocene)
- Ti—Intermediate to silicic intrusive rock (Eocene–Pliocene)
- Tlrp—Rhyolitic to dacitic pyroclastic rock and ash-flow tuff (upper Eocene–lower Oligocene)
- Tnr—Silicic to intermediate volcanic rock (Neogene)
- Tnv—Intermediate to silicic volcanic rock (Neogene)
- Tpmb—Basaltic to andesitic lava flows of the Servilleta Basalt (Miocene–Pliocene)
- Tps—Paleogene sedimentary rock
- Tual—Silicic andesite and dacite (upper Oligocene)
- Pct—Cutler Formation (upper Pennsylvanian–Wolfcampian)
- Xg—Paleoproterozoic metamorphic and plutonic rock

Figure 4. Geologic map and geologic cross sections of the Sunshine Valley region. **A**—Geologic map of the Sunshine Valley region, with locations of wells logged for temperature in this study (red crosses) and previously published temperature logs from Reiter et al. (1975) and Edwards et al. (1978) (orange circles). Geology simplified from New Mexico Bureau of Geology and Mineral Resources (2003). Quaternary faults along rangefront and in valley from Jochems et al. (2016). Cross-section C-C' shown in Fig. 27. **B**—Cross-section A–A', simplified from Ruleman et al. (2013); 2x vertical exaggeration. QTsf—Upper Santa Fe Group (middle Pleistocene to Pliocene); Unit Qau is equivalent to Qa and Qp, undivided, in 4a. **C**—Cross-section B–B', simplified from Winograd (1959); 13x vertical exaggeration. Offsets on faults are uncertain, units cut at surface are Holocene to middle Pleistocene. QTsfap: Tsf and Quaternary alluvial and piedmont deposits, undivided; Qtsfsc: silt and clay lenses; Qld – lake deposits. The Sunshine Valley fault zone mapped by Ruleman et al. (2013) does not appear on Winograd's original cross section.

tailing impoundments near Questa and natural spring flow to the Red River. Robinson (2018) described the hydrologic conditions and mixing of groundwater with different chemical compositions around Questa. Robinson (2018) showed that the chemistry of groundwater near and south of the divide separating Sunshine Valley from the Cabresto Creek drainage is affected by water sourced from areas of natural hydrothermal alteration in the Cabresto Creek and Red River drainages and potentially by seepage from the Questa Mine tailing impoundment west of Questa.

Geophysics

Measurements of temperature as a function of depth in wells are increasingly used to evaluate groundwater-flow systems (e.g., Saar, 2010; Kurylyk et al., 2018). Temperatures in shallow boreholes are commonly disturbed by fluid flow, and the shape of the temperature-depth profile can be used to characterize localized convection within and around the wellbore. Thermal profiles (logs) that are concave upward may indicate downward groundwater flow; as cool water infiltrates downward, the upper portion of a well is cooled relative to the bottom (Wade and Reiter, 1994). In contrast, convex-up logs suggest upward groundwater flow, as warm water from depth heats the shallower part of a well (Wade and Reiter, 1994). Lateral flow of relatively cold or warm water moving around a casing can produce isothermal or spiked profiles, depending on the thickness of the aquifer. Logs that show an isothermal trend (i.e., little change in temperature with depth) indicate high rates of vertical or lateral movement of groundwater. Temperature profiles with a steady linear increase of temperature with depth indicate conductive thermal conditions with little groundwater movement. Conductive logs commonly have a change in slope in geothermal gradient related to changes in rock type and associated changes in thermal conductivity. Temperature logs are also useful in identifying possible geothermal resources.

Prior to this study, few groundwater-discharge temperatures (e.g., Bauer et al., 2007; Johnson and Bauer, 2012) and no temperature-depth (thermal-profile) data from wells were available for Sunshine Valley. Reiter et al. (1975) and Edwards et al. (1978) measured thermal profiles, however, in four deep wells a few miles south and east of Sunshine Valley. Three of these drillholes were located in or near the Questa Molybdenum Mine within the Sangre de Cristo mountain block (Fig. 4).

Ruleman et al. (2013) presented both gravity and aeromagnetic data for Sunshine Valley. Gravity data were from the PACES (Pan-American Center for Earth and Environmental Studies) gravity database (https://research.utep.edu/default.aspx?tabid=37229), and additional data were collected along two east-west profiles (Ruleman et al., 2013; fig. 6). The gravity data were jointly inverted with two high-resolution aeromagnetic surveys published by Bankey et al. (2005, 2006) to develop a cross-sectional model across Sunshine Valley.

The transient electromagnetic (TEM) geophysical method can provide information about aquifers in areas between wells and was used in this study to estimate the depth to aquifer units in the subsurface of Sunshine Valley. TEM is a time-domain, surface-based geophysical imaging method that can be used to determine the distribution of conductive and resistant fluids and rocks to depths of 1,640–3,280 ft. The porosity of the rock and the composition of the saturating fluids are first-order controls on electrical resistivity in the subsurface. Dry alluvial sedimentary deposits with air-filled pore spaces are relatively poor electrical conductors and have high resistivity in the range of 120 to 400 ohm-m (Simpson and Bahr, 2005). Water is a much better conductor of current than solids, so an electrical current primarily moves through the fluid phase in water-saturated sand. Resistivity ranges between 80 and 120 ohm-m for rock units saturated with fresh water (20–50 mg/L total dissolved solids, TDS). This method has not been applied in this area and represents a new contribution to our understanding of this region.

IV. REGIONAL GEOLOGY

Sunshine Valley lies in the southeastern part of the San Luis Basin of the Rio Grande rift. Sunshine Valley is bounded on the east by the Sangre de Cristo Mountains and, west of the Rio Grande, by the northern Taos Plateau (Fig. 1). The Sangre de Cristo Mountains are composed of Precambrian igneous and metamorphic rocks intruded and overlain by Oligocene to Miocene plutonic and volcanic rocks of the Latir Volcanic Field (Lipman and Reed, 1989). The basin is filled with sediment of the middle Miocene to Pliocene Santa Fe Group. The upper part of the Santa Fe Group is interlayered with, and ultimately overlain by, lava flows of the upper Miocene to Pliocene Servilleta Basalt (Dungan et al., 1984; Ingersoll et al., 1990) (map unit Tpmb, Fig. 4). Within Sunshine Valley, the Santa Fe Group is dominantly fine-grained silty sand with minor lenses of pebble gravel (Winograd, 1959; Ruleman et al., 2013). The lava flows, together with numerous intermediate to felsic composition volcanic domes such as Ute Mountain and Guadalupe Mountain, comprise the Taos Plateau Volcanic Field (Lipman and Mehnert, 1979). West of the Rio Grande, much of the land surface is exposed basalt, but east of the river in Sunshine Valley, the lavas are largely buried by alluvial-fan, debris-flow, and piedmont deposits derived from the Sangre de Cristo Mountains and Ute Mountain (Fig. 4).

Sunshine Valley and the San Luis Basin lie on the western, downthrown side of the Sangre de Cristo fault zone, which is a steeply west-dipping normal fault zone that trends north-south at the foot of the mountains on the east side of the valley (Fig. 4). This fault zone and the east-side-down Sunshine Valley faults in the middle of the valley were active in the late middle Pleistocene to Holocene, as can be seen by prominent topographic scarps along much of their length and displacement of upper Pleistocene deposits (Ruleman et al., 2013) (Fig. 4). Recurrent movement on these faults likely influenced the eastward extent of both buried basalt flows and lacustrine beds (described below) in the central part of the valley (Fig. 5). The Gorge fault zone and Red River fault zone bound the western and southern sides, respectively, of the local structural basin that underlies Sunshine Valley (Kelson at al., 2008; Ruleman et al., 2013; Thompson et al., 2014a, 2015b). Both have discontinuous fault segments that do not cut middle Pleistocene piedmont-alluvium deposits, indicating less recent movement than along the Sangre de Cristo and Sunshine Valley faults. The Gorge fault zone consists of generally north-trending segments, with the east side down, and the Red River fault zone consists of northwest-trending segments with the northeast side down (Fig. 4). The Sunshine Valley fault zone and Sangre de Cristo fault zone are both prominent features on the aeromagnetic map of Ruleman et al. (2013), which also includes features they interpreted to be buried faults with no surface expression.

Ruleman et al. (2013) determined the maximum depth of bedrock, and thus the corresponding thickness of sedimentary and lava fill of the Sunshine Valley structural basin, to be 5,240 ±650 ft. The estimate was based on integration of information from geologic maps with interpretation and modeling of high-resolution gravity and aeromagnetic data across the region. The deepest part of the basin is between the Sunshine Valley and Sangre de Cristo fault zones. Using geophysical data, Drenth et al. (2013) estimated the total thickness of Santa Fe Group sediment and basalts under northern Sunshine Valley to be 3,600 ft at the New Mexico–Colorado state line.

The Sunshine Valley area was a closed basin prior to the middle Pleistocene (Ruleman et al., 2007). During this time a series of sedimentary units were deposited over the Santa Fe Group sediments and Servilleta basalts. These include lacustrine sediments deposited in Lake Sunshine, which most likely was an series of ephemeral playa, in west-central Sunshine Valley (Summers and Hargis, 1984; Ruleman et al., 2013) (Fig. 5). The lacustrine deposits consist of brown and red silt and sandy clay interstratified with sandy gravel that forms discontinuous layers and lenses, and are locally up to 160 ft thick (Winograd 1959; Ruleman et al., 2013).

In Sunshine Valley, sediment of the Santa Fe Group, flows of Servilleta Basalt, and lacustrine beds are overlain by a succession of surficial deposits (Ruleman et al., 2013) (Fig. 4). The oldest are piedmont-alluvial deposits of pebbly sand and

sandy pebble gravel that form broad dissected fans. Deposition of the fans predated the incision of the Rio Grande Gorge because the youngest alluvial deposit in this succession is preserved on both sides of the river. Inset into the alluvial fans are finer-grained units that postdate incision of the gorge and are interpreted as glacial outwash. The youngest units in Sunshine Valley were deposited by the modern stream system after the valley reached its modern geomorphic configuration.

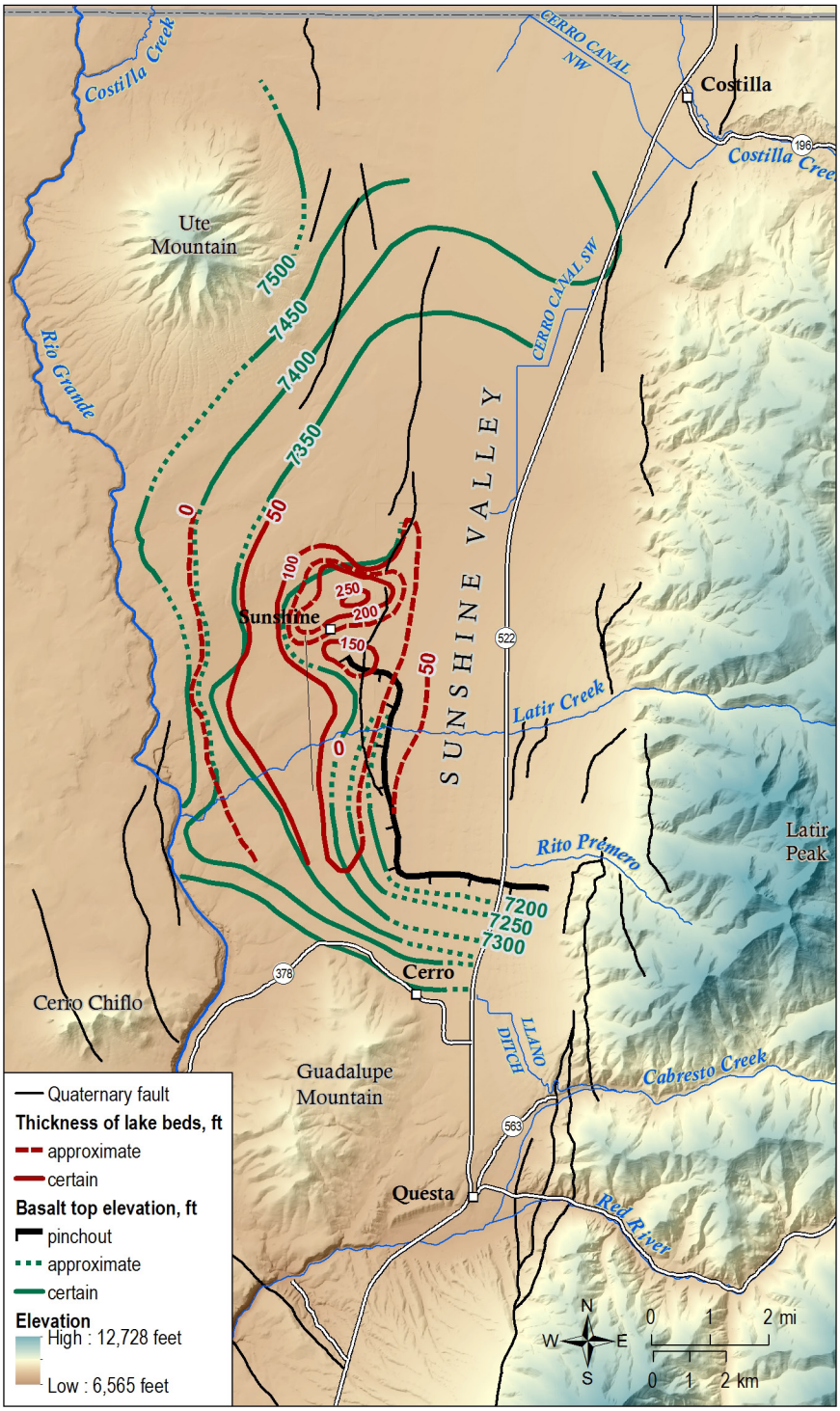

Figure 5. Structure contours of the top in the uppermost basalt flow and thickness contours of lake beds from Winograd (1959). Structure contours are modified and extended from Winograd (1959) as described in the text. The eastern pinchout of basalt flows is from Summers and Hargis (1984).

V. REGIONAL HYDROGEOLOGY

The study of Winograd (1959) described the physical hydrology of the Sunshine Valley aquifer in detail. His work was based on an inventory of stock, irrigation, and domestic wells, numerous water-level measurements, and interpretation of subsurface geology from examination of 55 well logs. Although Summers and Hargis (1984) reinterpreted some aspects of the groundwater flow regime in the central part of Sunshine Valley, their subsurface interpretations and Darr (2011) are in agreement on the basic nature of the subsurface geology and the hydrologic system.

Groundwater in the study area dominantly occurs under water-table (unconfined) conditions at depths from a few tens to many hundreds of feet within the sediments and basalts of the Santa Fe Group and the overlying deposits. The aforementioned lacustrine beds have relatively low permeability, especially compared to the basalt flows, which are highly transmissive due to abundant fractures and brecciated and vesicular zones between flows. Where low-permeability alluvial and/or lacustrine beds overlie basalts, "semiperched" conditions occur. This is common especially in the central portion of Sunshine Valley. Winograd (1959) described this scenario as "semiperched" because there is complete saturation below the water table, yet heads are lower in the transmissive basalts, wherein water flows east to west under very low gradients. True perched conditions, where the saturated zones are separated by unsaturated regions wherein hydraulic heads are negative, probably only occur locally and/or seasonally beneath major drainages entering the valley from the east. Where wells penetrate through the sediments into the basalts, water has been observed to cascade downward from the overlying sediments into the basalts, or between basalt layers, if there are multiple screens and/or the well is not cased properly (Winograd, 1959, and this study). Such cascading wells may act as drains, potentially lowering water levels in the sediments or even causing dewatering. Robinson (2018) noted how well drillers in the Cerro area take care to not penetrate the basalt layers beneath the upper sedimentary deposits for this reason.

Winograd (1959) also described "sub-artesian" conditions, where the lacustrine and/or other low-permeability layers in the valley are surrounded by or embedded in coarser, more permeable sediments. In this case, wells drilled through the low-permeability bed into the coarser sediments below often have water levels that rise above the base of the low-permeability bed. This is because the lacustrine beds are acting as partial confining units, although they remain saturated. The term "sub-artesian" is used because, although the water level rises above the base of the lacustrine beds, the wells do not flow to the surface.

Analogous to the cascading wells, the volcanic edifices of Ute Mountain and Guadalupe Mountain act as regional groundwater drains. Sedimentary basin fill of Sunshine Valley abuts these mountains and overlies basalt flows. Water levels in the sediments are much higher (the "semi-perched"conditions described above) than in the fractured and transmissive igneous rocks of the two mountains (Winograd, 1959). Anecdotally, local residents reported that attempts to drill wells south of state highway NM 378 in Cerro proved fruitless due to the great depth to water in the igneous rocks of Guadalupe Mountain. Yet many productive wells exist just north of the road with depths of less than 200 feet in the basin fill sediments.

Latir Creek and Costilla Creek, the two main perennial drainages entering the study area (Fig. 1), rarely flow to the Rio Grande. Both drainages are diverted in part into irrigation canals, but the surface water of both streams ultimately infiltrates into the Sunshine Valley aquifer or is consumed by evapotranspiration. This illustrates the highly permeable nature of the surficial deposits and that much of the recharge to the aquifer system is derived from precipitation in the Sangre de Cristo Mountains to the east.

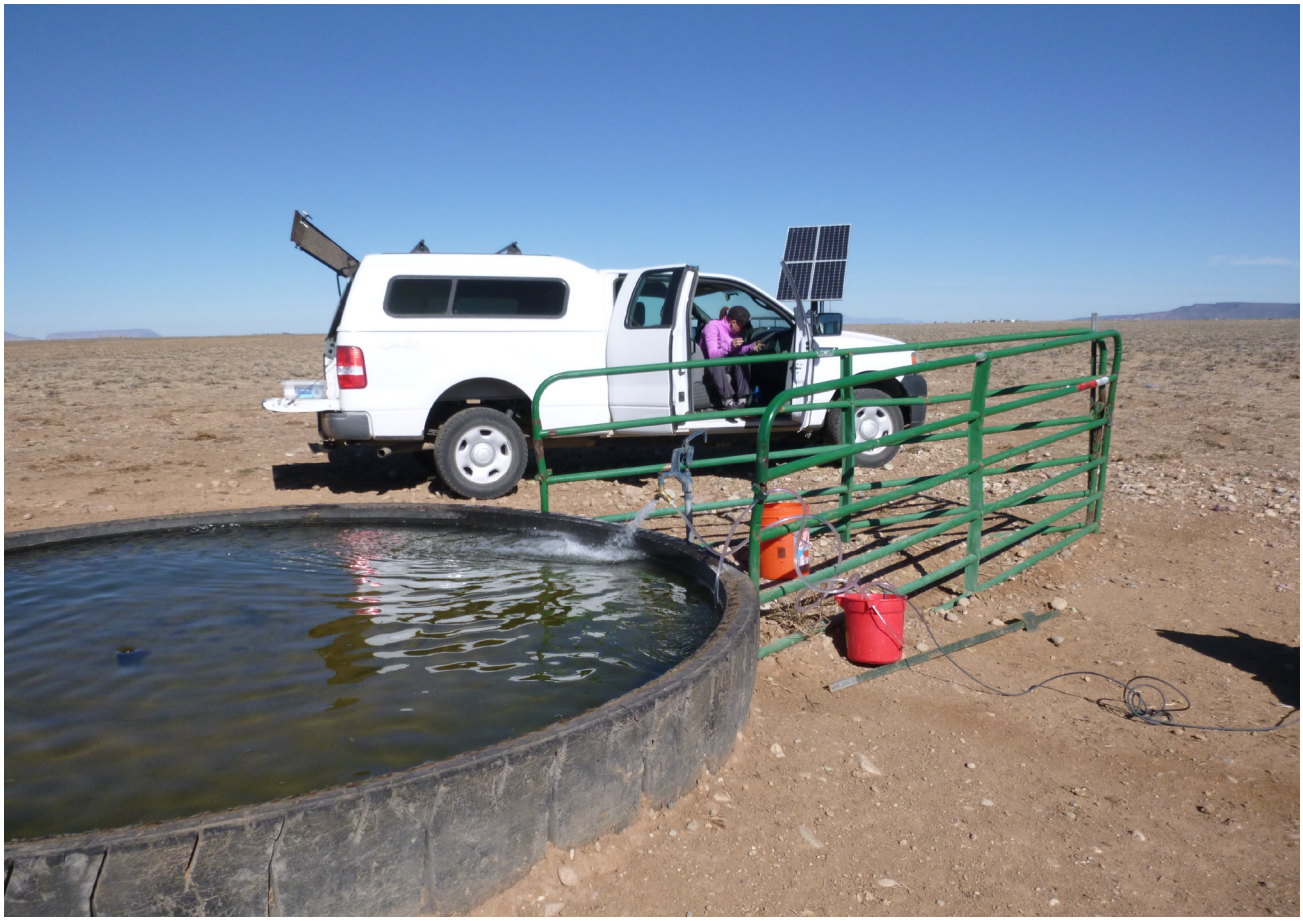

Collecting a water sample from a solar-powered stock well in Sunshine Valley.

VII. METHODS

A. Physical and Chemical Hydrologic Data Collection

Water-level measurements

Thirty wells in Sunshine Valley were visited in November 2017 (Figure 6, Appendix A). Depth to water was successfully measured in twenty of these; measurements were not possible in the other ten. Wells suitable for collection of water samples were also identified at this time. Water levels were measured with a steel tape. At least two depth-to-water measurements were made at each well to ensure repeatability within 0.02 feet.

Water samples

Samples were collected from 12 wells and one stream (Fig. 7, Appendix B). For the wells, a sampling manifold system was attached to the water spigot or discharge pipe, and field parameters were monitored with a YSI Model 556 Multiprobe in a flow-through cell. Sampling was initiated when several well volumes had been purged and/or the field parameters had stabilized. The field parameters measured were temperature, specific conductance, pH, oxidation-reduction potential (ORP), and dissolved oxygen (DO). The DO probe was calibrated onsite before sampling. The pH electrode was calibrated at the beginning of the sampling week against pH 4, 7, and 10 buffers. A separate sampling manifold was used for each well, and the sampling equipment was rinsed with deionized water before sampling and cleaned at the end of each session. The stream sample was directly collected from Costilla Creek at the stream gauge (USGS ID 08255500) east of Costilla.

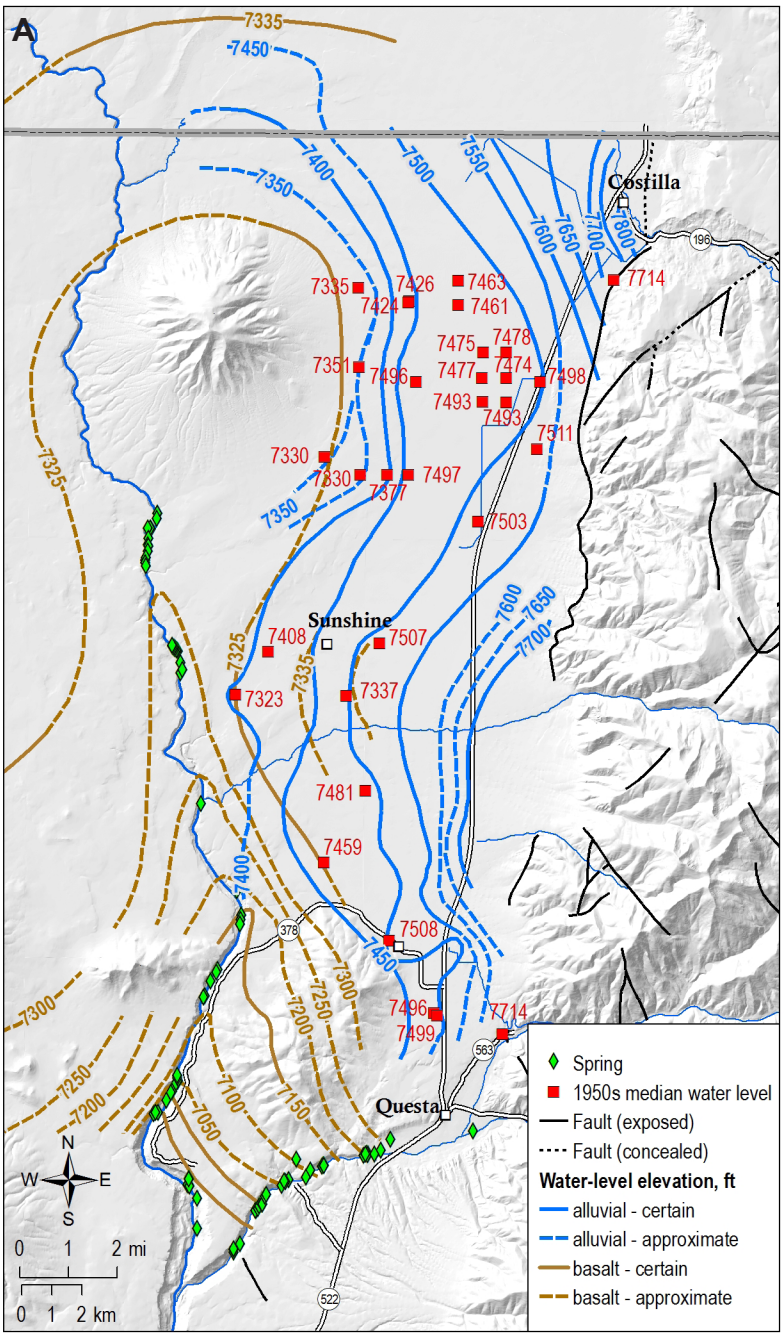

Figure 6. A—Map of water level elevations for the 1950s decade. Contours are those of Winograd (1959), modified in Sunshine Valley where appropriate with additional median water levels from the 1950s decade in the labelled wells. Wells used by Winograd (1959) are not shown. Distinction between alluvial and basalt contours here and in 6.C is discussed in the text.

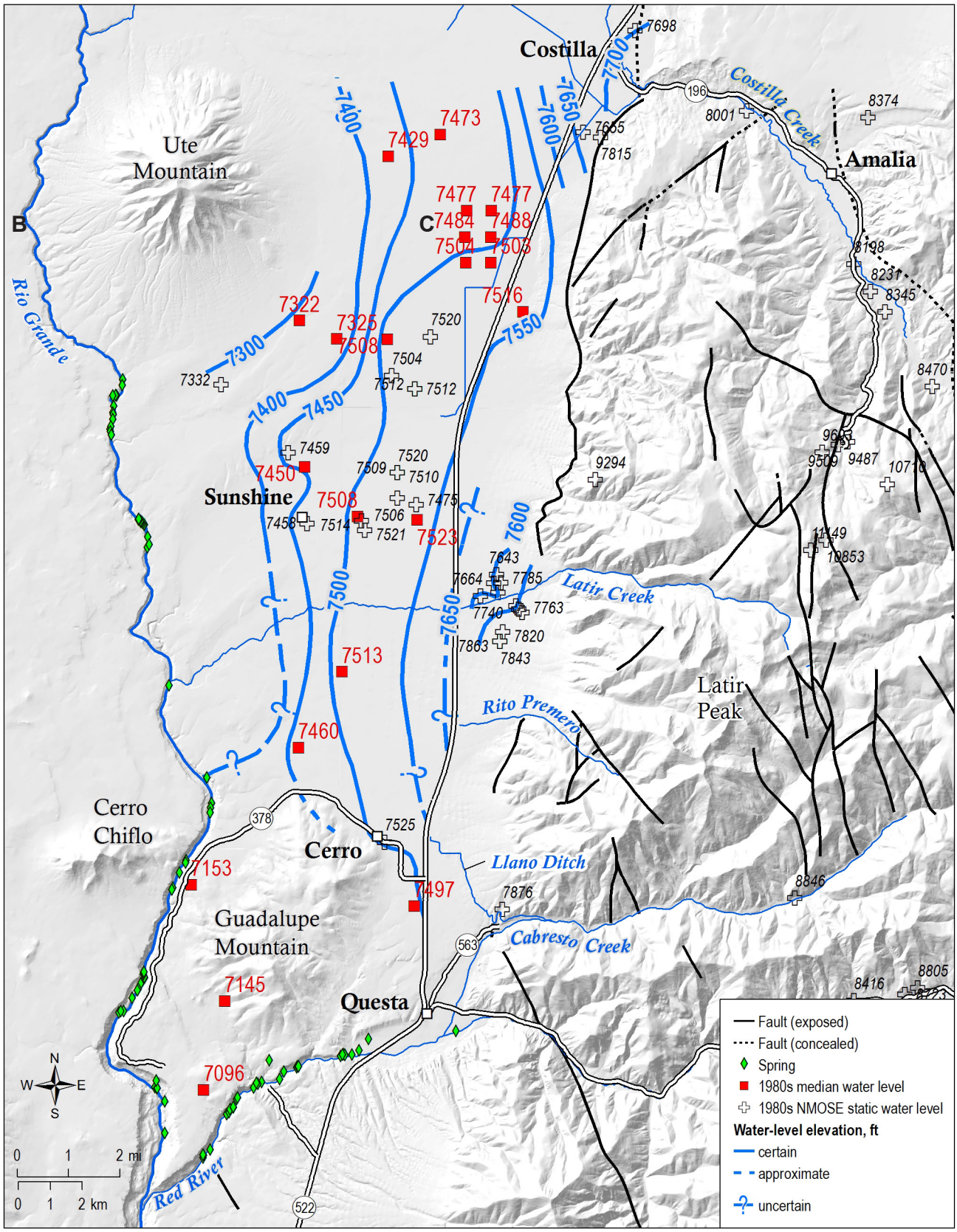

Figure 6. B—Map of water level elevations for the 1980s decade. Contours based on decadal median water levels (squares) and static water levels from NMOSE records (crosses).

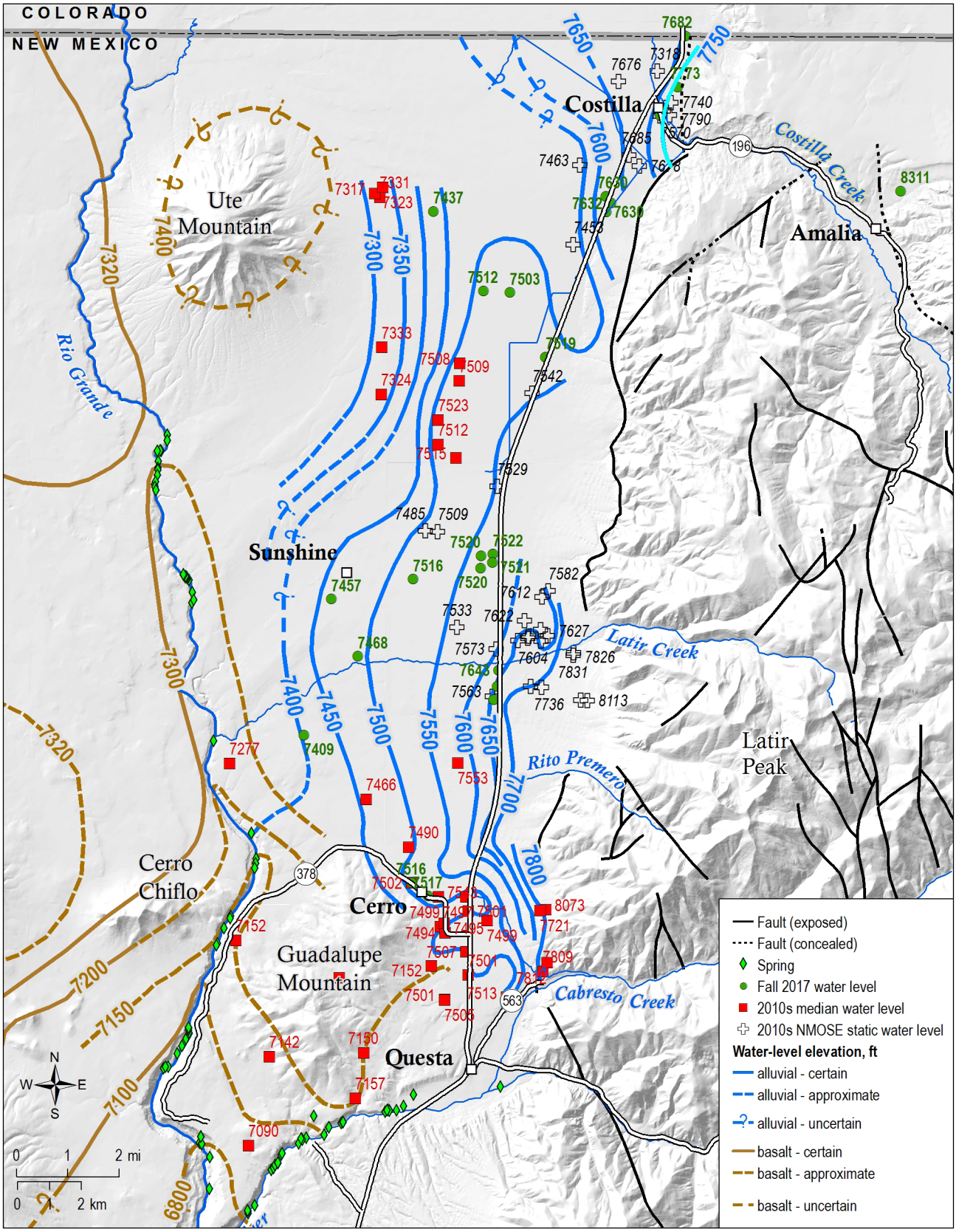

Figure 6. C—Map of water level elevations for the 2010s decade. Contours based on water levels measured in this study (green circles), decadal median water levels (red squares), and static water levels from NMOSE records (crosses). Basalt contours are from Johnson and Bauer (2012); wells used by Johnson and Bauer (2012) are not shown.

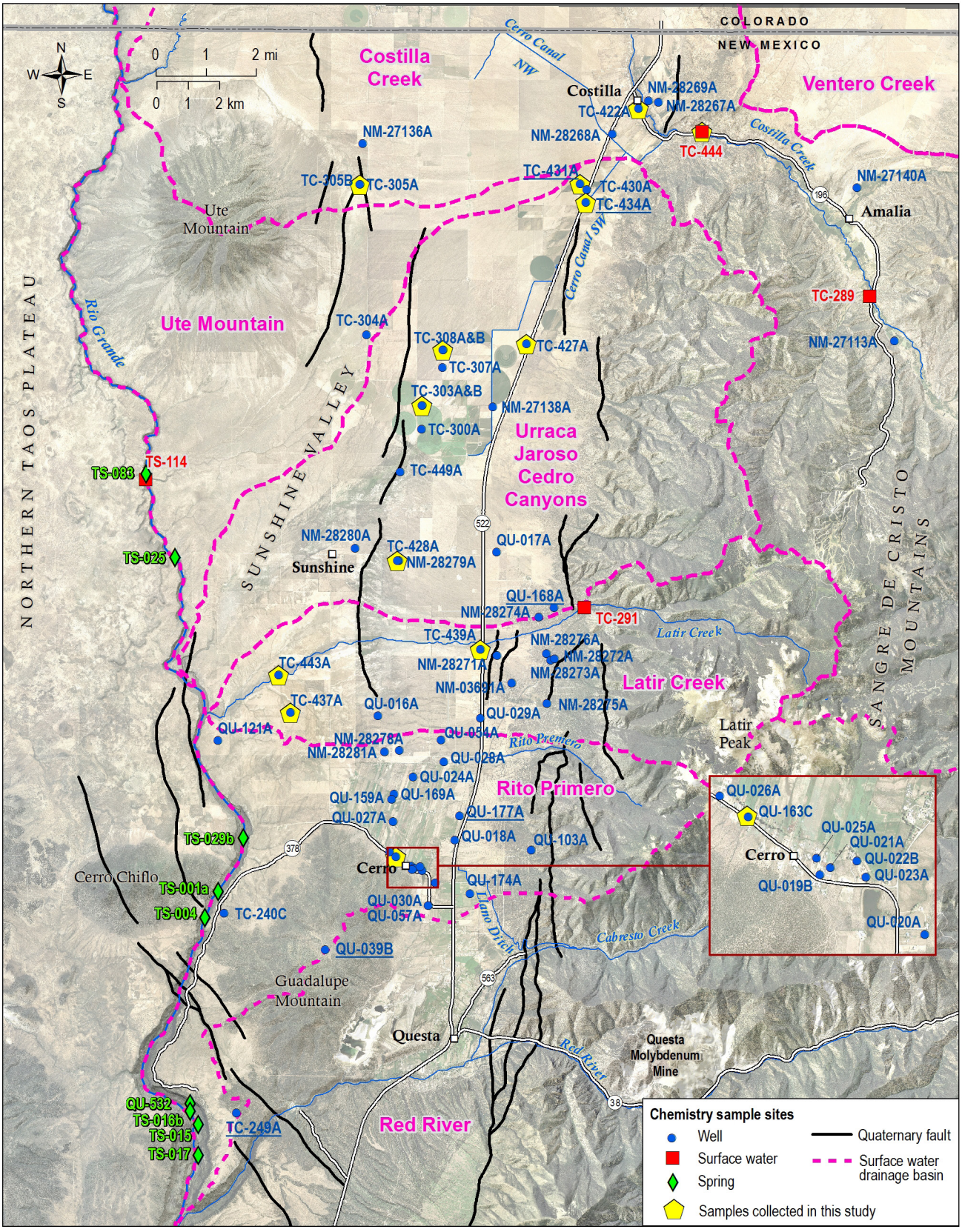

Figure 7. Map of sample sites for water chemistry analyses. The pink dashed lines are drainage basin boundaries. The south boundary of the Rito Primero drainage was chosen as the southern edge of the study area for water chemistry interpretation. Samples at sites highlighted in yellow were collected in spring 2018 during this study. Sites with underlined labels comprise the warmer "upper" temperature depth trend in Fig. 19D.

General ion and trace metal chemistry

Water samples from wells and streams were collected using new, certified-clean polypropylene containers after three repeated rinses. Samples for general ion chemistry analyses were collected using 250-mL polypropylene bottles. Water samples for trace metal chemistry were filtered onsite through an inline 0.45 µm filter into 125-mL polypropylene bottles and acidified to pH<2 using ultra-pure nitric acid. Alkalinity (as mg/L) and pH were determined in the NMBGMR chemistry laboratory using a Metrohm titrator. Specific conductivity was measured using a YSI 3200 meter. Chemical analyses for chloride, sulfate, nitrate, nitrite, phosphate, bromide, and fluoride were performed using a Dionex DX-600 ion chromatograph. Cations (Na, K, Ca, and Mg) and iron were analyzed using a Perkin Elmer OPTIMA 5300 DV Inductively Coupled Plasma Optical Emission Spectrometer (ICP-OES). Trace metals were analyzed by Inductively Coupled Plasma Mass Spectroscopy (ICPMS) using an Agilent 7500 IS. The quality of the chemical analyses was inspected by analyzing blanks, standards, duplicate samples, and checking ion balance. The ion balance errors for the analyses were generally within ±5%.

Saturation indices for calcite, gypsum, quartz, Ca-montmorillonite, albite, kaolinite, and potassium feldspar were calculated for each water sample using the program PHREEQC Interactive version 3.3.2 (Parkhurst and Appelo, 1999). Calculations were performed with both the default electron-potential-in-solution value of 4 and values derived from field ORP measurements (if available). No significant difference was noted between the two sets of calculations.

Stable isotopes

Waters were also analyzed for stable isotopes of oxygen-18 (^{18}O) and hydrogen-2 (^{2}H, deuterium or D). Samples were collected in 25-mL amber glass bottles after three repeated rinses. Samples were analyzed at the New Mexico Institute of Mining and Technology stable isotope laboratory on a Picarro L1102-i Cavity Ringdown Spectrometer isotopic water liquid analyzer. Analytical uncertainties for $\delta^{18}O$ and $\delta^{2}H$ typically were less than 0.1 per mil (‰) and 1‰, respectively.

Carbon isotopes and tritium

A subset of water samples from wells was analyzed for tritium (^{3}H) and carbon-14 (^{14}C) activity to determine groundwater age. Tritium samples were collected in two 500-mL polypropylene bottles and analyzed by internal gas proportional counting with electrolytic enrichment at the University of Miami Tritium Laboratory, following the sampling protocol described on the Rosenstiel School of Marine and Atmospheric Science website (refer to https://rsmas.miami.edu/groups/tritium/advice-sampling-tritium.html). The enrichment step increases tritium concentrations in a sample about 60-fold through volume reduction, yielding lower detection limits. Accuracy of this low-level measurement is 0.10 tritium unit (TU) (0.3 picoCuries per liter, pCi/L, of water), or 3.0%, whichever is greater. The stated errors, typically 0.09 TU, are one standard deviation.

Water samples for carbon-dating were collected in one 1-L polypropylene bottle, after rinsing three times, and analyzed by International Chemical Analysis, Inc. The ^{14}C activity of each water sample was derived from the dissolved inorganic carbon by accelerator mass spectrometry. Results are reported as ^{14}C activity (in percent modern carbon, pMC) and as radiocarbon years before present, where "present" is considered as the year 1950. No corrections for geochemical effects, such as water-rock interactions, were completed. The reported apparent ^{14}C ages do not precisely represent the residence time of the water within the aquifer; the ^{14}C activity and apparent ^{14}C age are used as relational tools to interpret hydrologic differences among water samples.

B. Geophysical Methods

Temperature logging

Temperature was measured as a function of depth in open, unequipped wells in Sunshine Valley to identify patterns of groundwater movement in the subsurface (Fig. 4). Temperature was logged at 1-m intervals using a Fenwall thermistor attached to a 1-km-long wireline cable that was lowered down the wellbores at a rate of 2 m/min. This particular thermistor works best in water. A digital multimeter attached to a computer recorded resistance in the thermistor and cable, which was converted to temperature by calibrating the truck-based system against a laboratory-calibrated platinum resistance thermometer. Vertical geothermal gradients (dT/dz) were calculated by linear regression using least squares estimation. Reproducibility of the measurements is ±0.02°C.

TEM surveys

The TEM method uses a transmitter box attached to two 24-volt batteries to send a current into a transmitter loop of copper wire laid on the ground surface. The current is rapidly shut off, which induces a set of downwardly diffusing eddy currents into the subsurface. These currents produce small secondary magnetic fields of opposite polarity that induce decaying voltages in a receiver coil antenna located in the center of the transmitter loop. Decaying voltages recorded at early times contain information about the shallow subsurface, whereas decaying voltages recorded at later times measure resistivity at greater depths. The magnitude of the induced currents is larger for conductive material than for resistive material. Thus, induced-current magnitudes can be used to estimate resistivity, and depth is estimated from the time after turnoff for a given sounding. In practice, this process is done rapidly and repeatedly, via a transmitted square wave. The frequency of the square wave is adjusted to determine the optimal recording characteristics for a given setting. The total depth of investigation of each TEM sounding is a function of the transmitter voltage and loop size. Equipment used in this study was optimized for depths of about 1640 ft (500 m) and a loop size of 328 x 328 ft (100 m x 100 m), with an input voltage of 48 volts.

TEM data in Sunshine Valley were collected during two field outings. The five stations measured during a trip in May 2018 were collected across a broad area, whereas the twelve stations deployed during a second trip in May 2019 were sampled using a grid with a 328 ft (100 m) spacing and a 328 x 328 ft (100 x 100 m) loop size; in other words, the loops were contiguous (Fig. 8). A powerline, fencing, and an electrical substation in the area were avoided.

Noise in the raw data was removed using TEMAVGW software from Zonge, the manufacturer of the TEM equipment. One-dimensional, resistivity-depth models were derived from the data with the program Zonge steminv using the stack option and a vertical smoothing factor of 2.

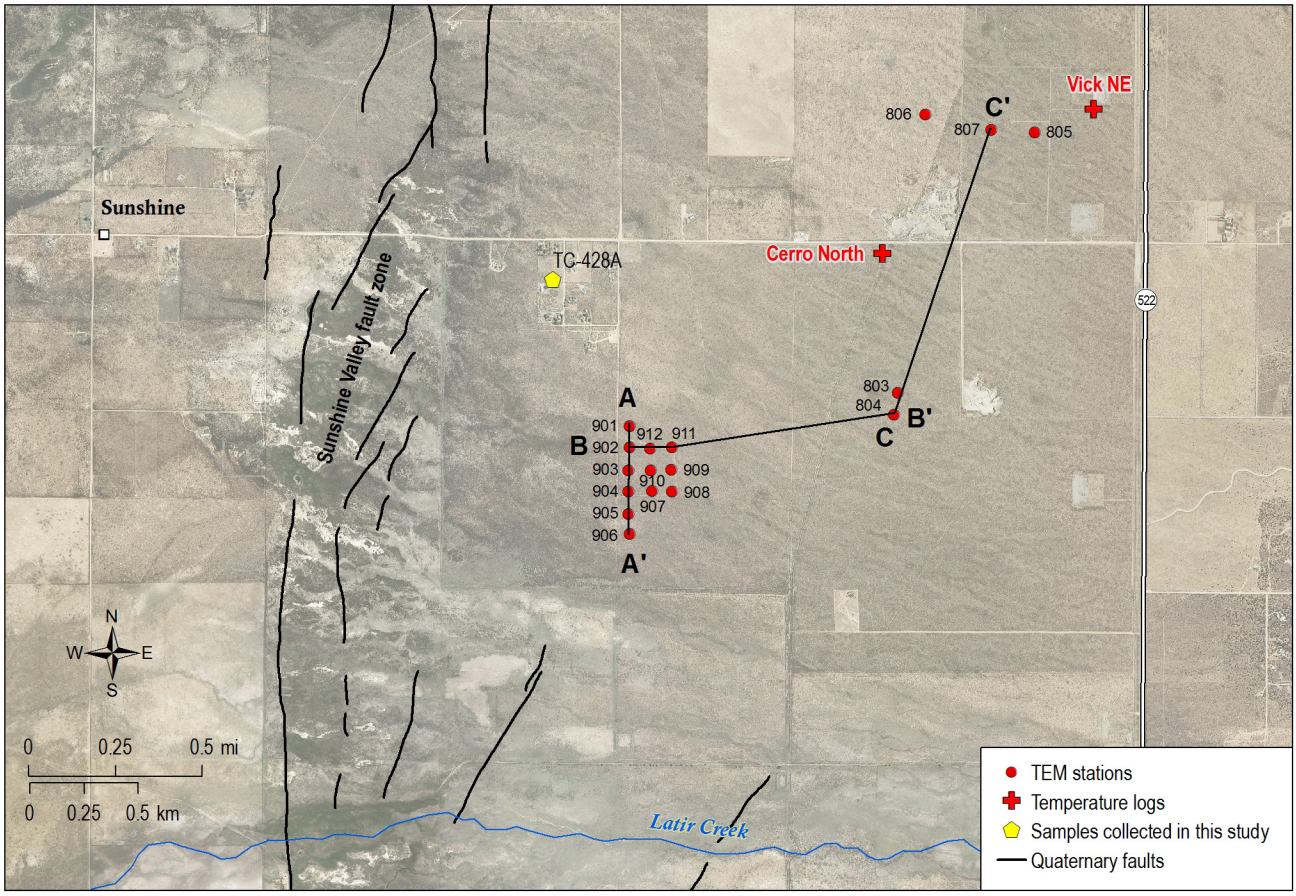

Figure 8. Map showing the location of the TEM sites in Sunshine Valley (see Fig. 1). Wells with thermal profiles measured in this study are shown. The Sunshine Valley fault zone as mapped by Ruleman et al. (2013) and the locations of the profiles in Figs. 21 and 22 are also shown.

C. Historical Data Evaluation

Water-level data

The database of water levels measured in wells maintained at the New Mexico Bureau of Geology and Mineral Resources (NMBGMR) was queried for water-level data in Sunshine Valley since the 1950s. These data have been collected by the United States Geological Survey (USGS), Taos Soil and Water Conservation District (TSWCD), and the NMBGMR. This historical dataset of well location and water-level data was filtered to remove wells with clearly erroneous locations and wells without a recorded total depth. Measurements with USGS data quality flags (which indicate low-quality measurements) were removed and all measurements taken during the nominal irrigation season (March through October, inclusive) were removed.

The median water-level elevation for each decade from the 1950s through the 2010s was calculated for each well in the filtered dataset. Additional static water-level measurements for wells drilled in the 1980s and 2010s with reported total depths were plotted using well records from the New Mexico Office of the State Engineer (NMOSE). These are considered lower-quality data and are used to supplement the previous dataset. The shallow "alluvial" and deeper "andesite-basalt" water-level surfaces of Winograd (1959, Plate 2) were digitized and modified with additional median water-level data for the 1950s decade where appropriate (Fig. 6). Water-level surfaces for the 1980s and 2010s decades were contoured by hand from the filtered data and the NMOSE data. Water levels measured during the present study were also incorporated into the 2010s water-level surface. The configuration of the water level surfaces of Winograd (1959) were used as a general guide in the preparation of the more recent surfaces, especially in areas with sparse data. Water-level changes between the 1950s–1980s and 1980s–2010s were calculated (Figs. 6, 9). Hydrographs were inspected for long-term trends in water level (Fig. 10).

Geochemistry data

In addition to the samples collected for this study, the NMBGMR database was queried for existing water chemistry data in Sunshine Valley. Data sources included the NMBGMR, the USGS, and the TSWCD. Some of the older analyses are not as complete as the data collected for this study (Appendix B). For example, many of the older data do not have field parameter, stable isotope, or environmental tracer measurements. The addition of this older data resulted in a water chemistry dataset of 78 samples from wells, springs, and streams. Samples selected were limited to the region north of the southern boundary of the Rito Primero drainage basin (Figure 7). This boundary was chosen to eliminate samples in the Questa area that may be anthropogenically affected by seepage of water from tailing impoundments and naturally affected by water draining from hydrothermal alteration scars in the Cabresto Creek and Red River drainages. Stable isotopic compositions of precipitation collected from 2013 to 2015, some groundwater geochemistry data, and interpretations from the recent work of Robinson (2018) on groundwater geochemistry in the Questa area were incorporated into the study.

Streamflow data

The USGS National Water Information System (https://waterdata.usgs.gov/nm/nwis/sw) was queried for streamflow data for all gauges in the Sunshine Valley area. These data were reviewed and processed to develop the water budget model. Streamflow data used in the study are presented in Appendix C.

Subsurface geology

Drillers' logs of water wells in Sunshine Valley were obtained from the NMOSE and examined to confirm the depth and extent of the fine-grained, clay-rich lake bed sediments and top of the basalt flows identified and mapped by Winograd (1959). While the basalts are easily identified by drillers and are readily noted in the logs, the descriptions of sediments were considered too inconclusive to justify making any changes to Winograd's (1959) contours of lake bed thickness (Figure 5). Winograd's (1959) contours of the top surface of the basalt flows were modified and extended based on identification of this unit in the well logs, where it can be reliably identified even in low-quality lithologic logs (Figure 5).

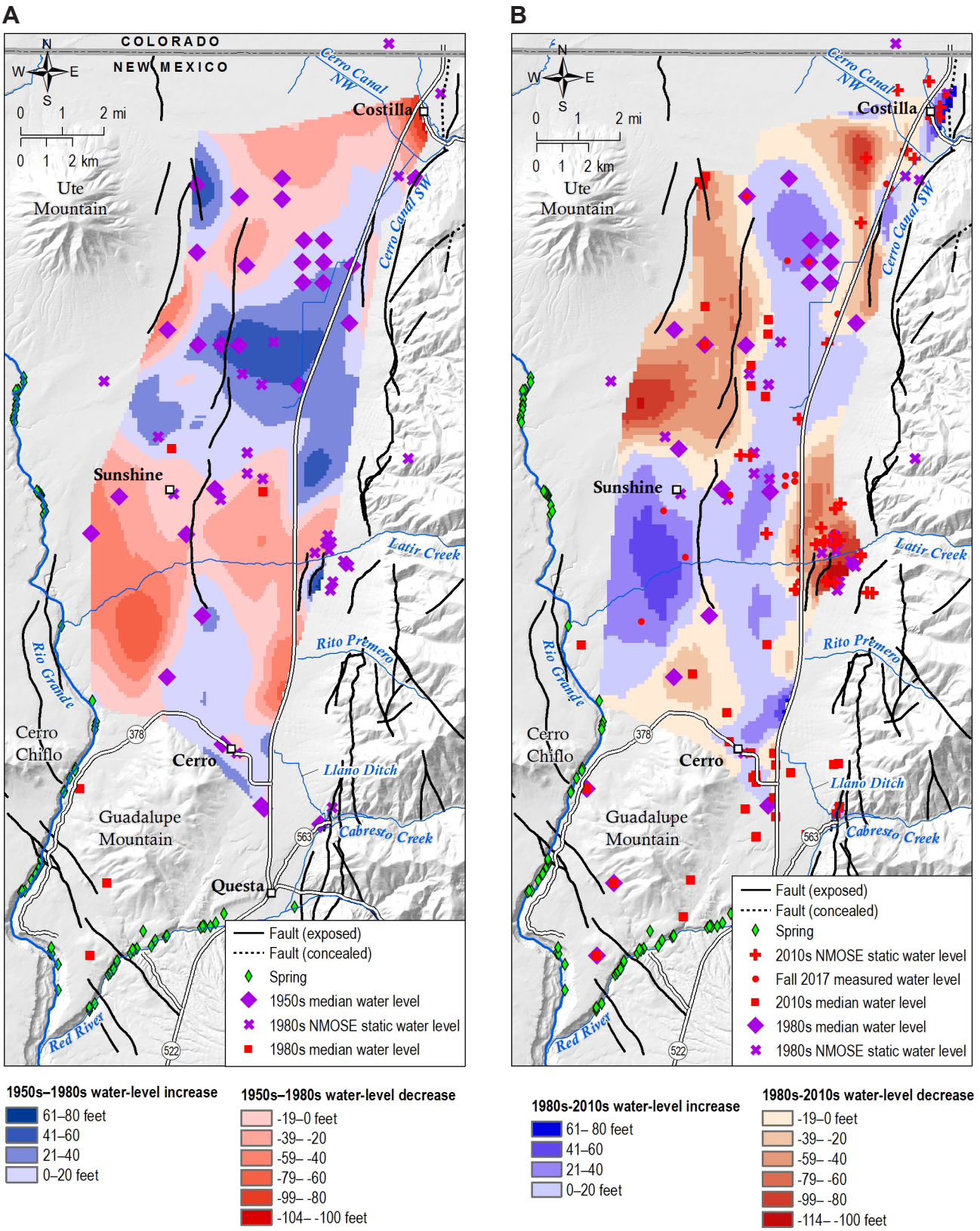

Figure 9. **A**—Map of water-level elevation changes from the 1950s to the 1980s. Wells shown are the same as those in Figure 6. Wells used by Winograd (1959) are not shown. Water-level declines are negative and areas of mapped water-level change are within the extent of the spatial correlation of water levels (~6 km radius around each well) identified by Rinehart et al. (2016). **B**—Map of water-level elevation changes from the 1980s to the 2010s. Wells shown are the same as those in Figure 6. Water-level declines are negative and areas of mapped water-level change are within the extent of the spatial correlation of water levels (~6 km radius around each well) identified by Rinehart et al. (2016).

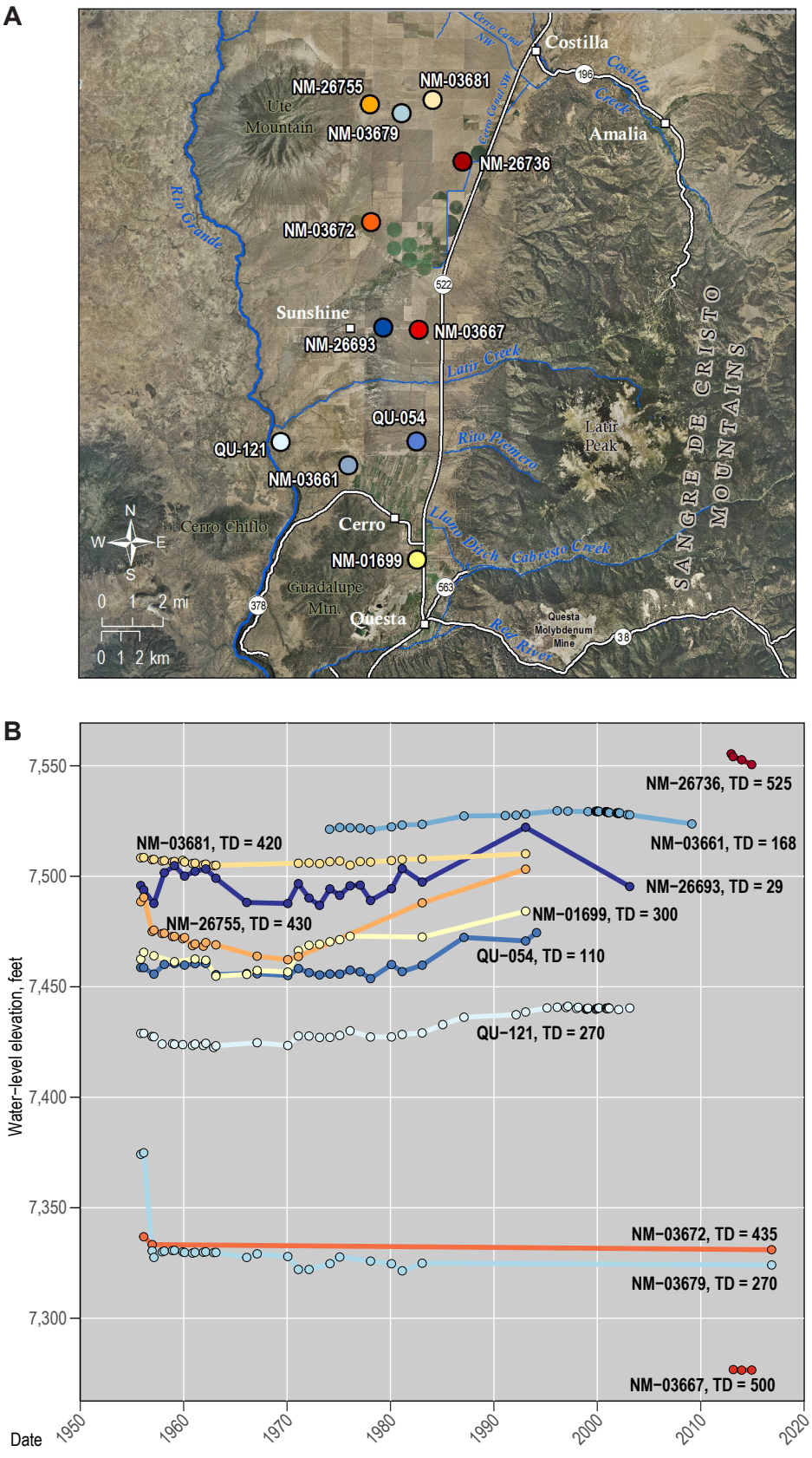

Figure 10. **A**—Locations of wells of selected hydrographs shown in the Sunshine Valley region. **B**—Selected hydrographs for the Sunshine Valley region. TD = total depth in feet

View north along the Rio Grande near Little Arsenic Spring.

VIII. RESULTS

Water-Level Elevations

The complete data set and a brief statistical summary of well information and water level data used in this study are presented in Appendix A. Well depths range from 29 to 890 feet; depths to water range from 5 to 791 feet. Median water-level elevation surfaces for the 1950s, 1980s and 2010s are shown in Figure 6. For the 1950s and 2010s time periods, well construction details in driller's logs and water-level data were sufficient to differentiate the shallower "alluvial" portion of the aquifer (contoured in blue) and the deeper "basalt" portion of the aquifer (contoured in brown), as was first done by Winograd (1959). Data from the 1980s were insufficient to map this distinction. The deeper basalt aquifer is dominated by basalt flows but includes minor intervals of gravelly sediments, whereas the shallower alluvial aquifer is the converse and also includes surficial deposits above the top of the Santa Fe Group (Fig.4; Winograd, 1959). There is no unequivocal evidence for a complete hydrologic distinction between the two portions of the aquifers such as a pervasive confining bed separating them; rather the differentiation is largely a reflection of the western and southern pinchouts of abundant Santa Fe Group sediments. Immediately northwest of Guadalupe Mountain this results in a large drop in water levels where only fractured (and thus highly transmissive) volcanic rocks are present (Winograd, 1959) (Figs. 6a, 6c). Conversely, immediately east and southeast of Ute Mountain the "alluvial" aquifer water levels are within a few tens of feet of the "basalt" aquifer, suggesting that the two divisions are poorly developed there (Fig. 6a). Changes in the water-level surfaces from the 1950s to the 1980s and the 1980s to the 2010s are shown in Figure 9. Eleven hydrographs are shown together in Figure 10, illustrating the variety of water-level trends throughout the area since the 1950s.

The closest well to the Rio Grande, QU-121, has recent water levels that are about 40 feet above the level of the river, which is about 2,300 feet due west (Fig. 10). The deepest water levels are wells NM-26755 and NM-03672, east and southeast of Ute Mountain, respectively. Both wells are completed in basalt flows. Water levels in NM-03672 are even with the top of the basalt, whereas water in NM-26755 is well below the top of the basalt. Both have not changed greatly since the mid-1950s.

Regional groundwater flow is from east to west, from recharge areas in the Sangre de Cristo Mountains to discharge sites in the Rio Grande Gorge and lower Red River Canyon. Groundwater contours curve noticeably around Guadalupe and Ute mountains, supporting the contention that these volcanic edifices act as drains from the shallower to deeper parts of the aquifer (Winograd, 1959). East of Ute Mountain, head gradients increase across the Sunshine Valley faults from 0.0035 (18 ft/mi) on the east to 0.017 (88 ft/mi) on the west (Figs. 4, 6). In the central area of the valley, gradients are low and not appreciably affected by the faults. The patterns of water-level change show association with the Sunshine Valley faults, especially in the 1980s–2010s time period, where the faults separate the linear region of water-level rise in the eastern valley from the region of water-level decline in the northwestern part of the valley (Fig. 9).

Water level declines in the late-1950s and early-1960s are noticeable regardless of well depth and ranged from a few feet to a few tens of feet. In the mid- to late-1970s and into the 1980s water levels tended to rise, again a few feet to a few tens of feet. Unfortunately, the frequency of repeat measurements has decreased greatly in the past 15 years, making delineation of recent water-level trends uncertain. The most recent measurements in wells QU-054, NM-03667, and NM-01699 suggest a declining trend. Figure 9 shows estimated regions of water level increase and decrease between the time periods represented by the contour maps shown in Figure 6. The variable quality, general sparseness of the water-level data, and interpolated nature of the water-level contours from which these changes were determined must be emphasized; nevertheless, there is spatial variability in the areas where water-levels have risen and fallen over the Sunshine Valley region from the 1950s to the 1980s, and again from the 1980s to the present decade.

Areas around the alluvial fans at the mouths of Costilla Creek and Latir Creek both show evidence

for downward flow and/or multiple water-bearing zones, as deeper wells tend to have deeper water levels. Water-level variations with depth become less obvious moving west from the Latir Creek fan and groundwater flow appears to be more horizontal or subparallel to the ground surface. Water-levels appear to have dropped about 100 feet near Costilla since the 1950s. The 7,700-foot water-level elevation contour in the 2010s is about where the 7,800-foot water-level elevation contour was in the 1950s. Local residents commented that many shallow wells have gone dry around Costilla, although some of these do so every year when streamflow is low and/or the irrigation ditches are dry.

Groundwater Chemistry

The locations and major ion chemistry of samples collected in this and previous studies are shown in Figures 7 and 11–12. The waters have total dissolved solids (TDS) ranging from 73 to 370 mg/L. Most samples are simple calcium-bicarbonate water types (Fetter, 2001) (Fig. 11). Eight of the nine springs are

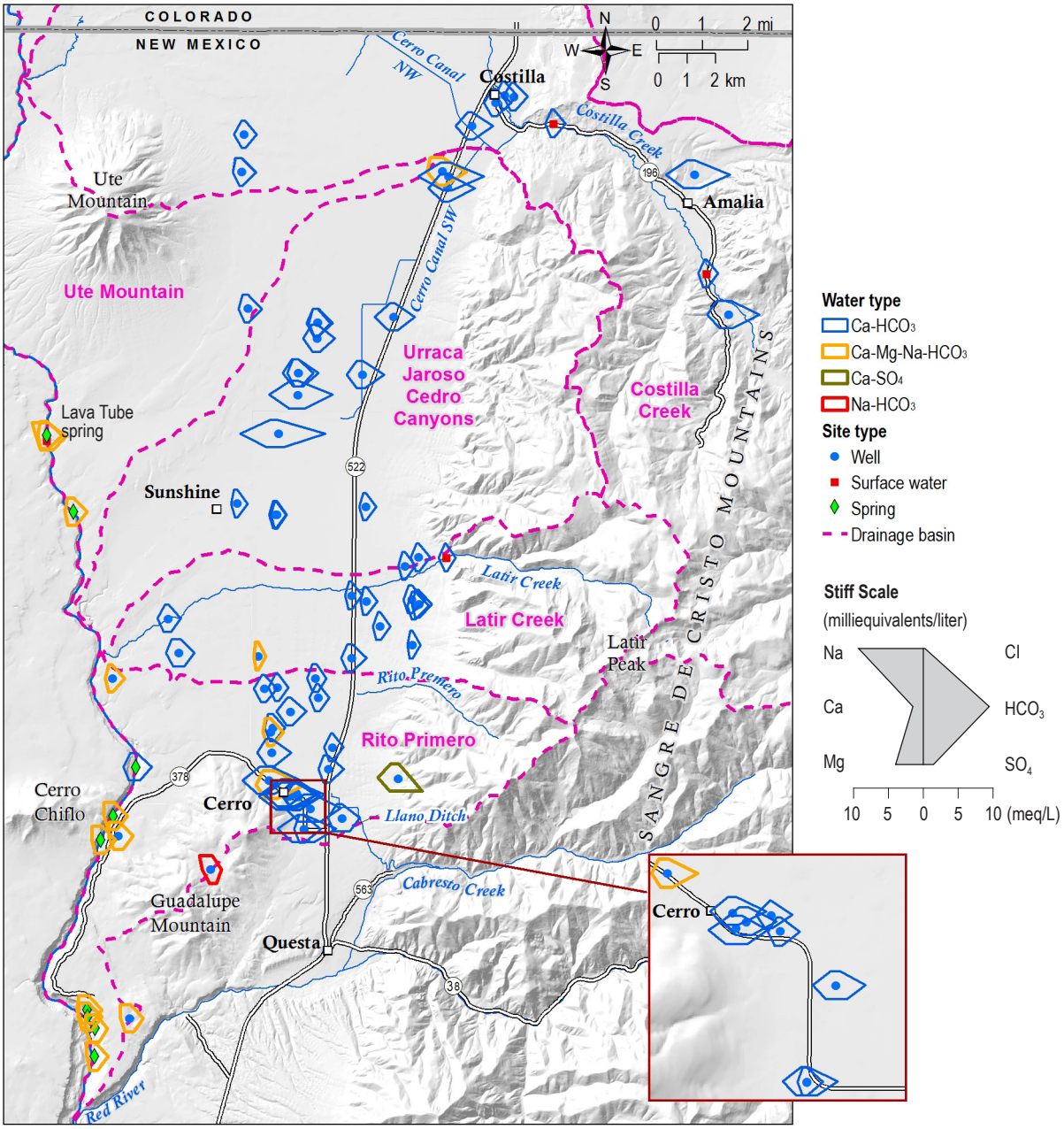

Figure 11. Map of Stiff diagrams of major ion-chemistry. Diagram size is proportional to TDS as indicated.

mixed-cation bicarbonate water types (TS-029bA is the exception). Well sample QU-039B on Guadalupe Mountain is a sodium-bicarbonate water. The Rio Grande water near Lava Tube spring (sample TS-114A) has a TDS of 213 mg/L and notably more sodium and less calcium and magnesium than water discharging from the spring (sample TS-083A). The Rio Grande water has much higher TDS than stream samples from Latir and Costilla creeks. In the cation triangle of Figure 12, samples show a diffuse trend towards increasing sodium at the expense of calcium, and magnesium to a lesser extent, indicative of ion exchange (Hounslow, 1995). In the anion triangle, samples show a linear trend of increasing sulfate at a relatively constant chloride content.

Bicarbonate, sulfate, and chloride increase linearly with TDS (Fig.13); QU-103A, the lone Ca-SO_4 water type has notably higher sulfate and lower bicarbonate. Calcium, magnesium, and sodium increase linearly versus TDS, with the most scatter in the sodium trend (Figure 14). QU-039B and TC-430A are outliers on the magnesium versus TDS trend. TDS, and thus the constituents correlated with it, such as sulfate, varies across the study area. Values of TDS and sulfate are highest around Cerro and in north-central Sunshine Valley, and intermediate in the gorge springs (Fig.15).

Saturation indices (SI) for calcite, gypsum, and quartz (Fig. 16A), and albite, potassium feldspar, kaolinite, and Ca-montmorillonite (Fig.16B) were

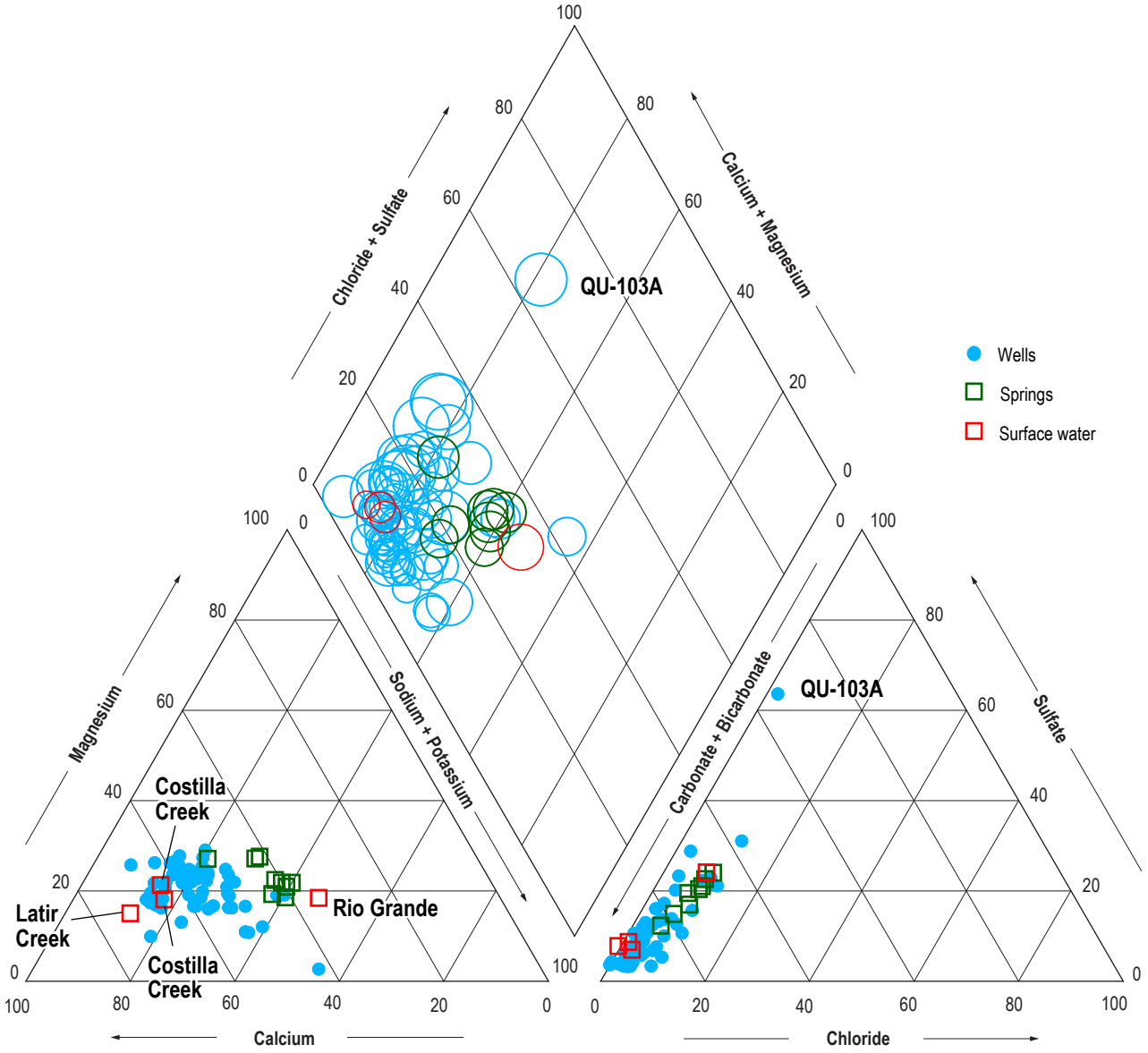

Figure 12. Piper diagram illustrating major ion chemistry. Well samples are blue, springs are green, surface water is red. Circle size in the diamond is proportional to TDS.

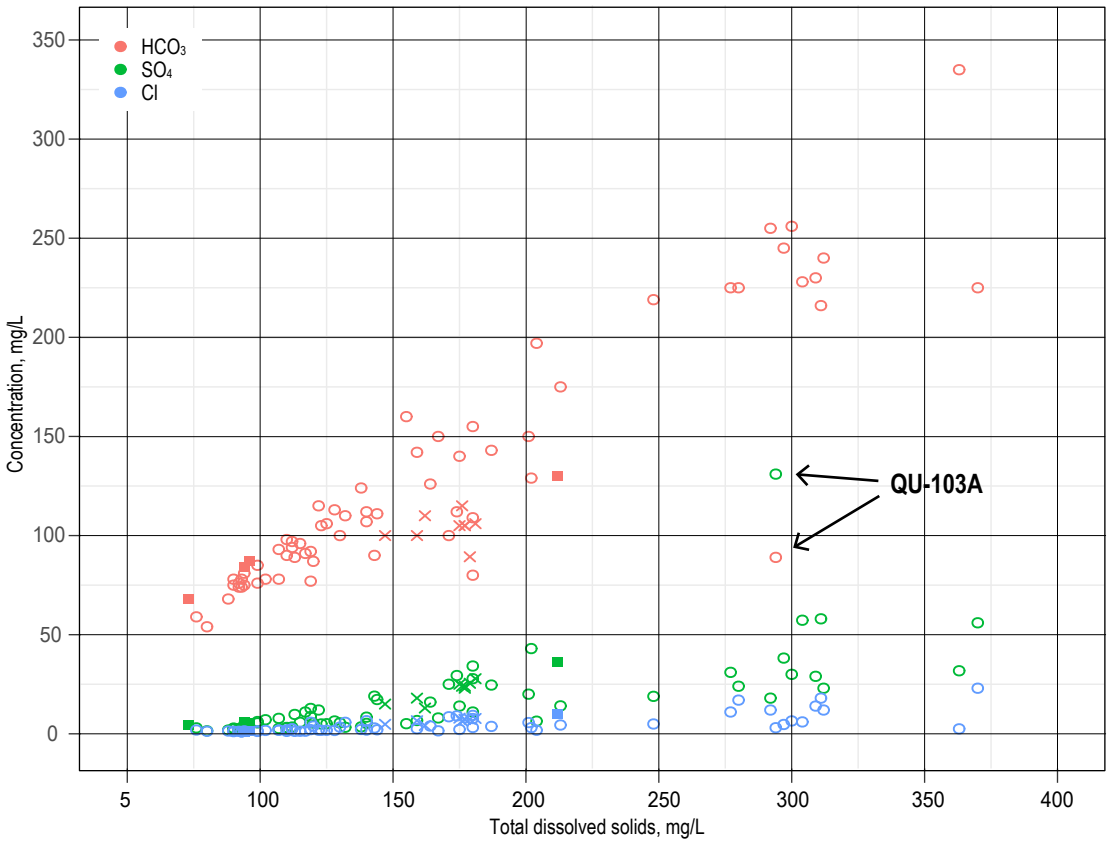

Figure 13. Plot of anions bicarbonate, sulfate, and chloride against total dissolved solids. Groundwater samples are circles, spring samples denoted with x, surface water samples are filled squares.

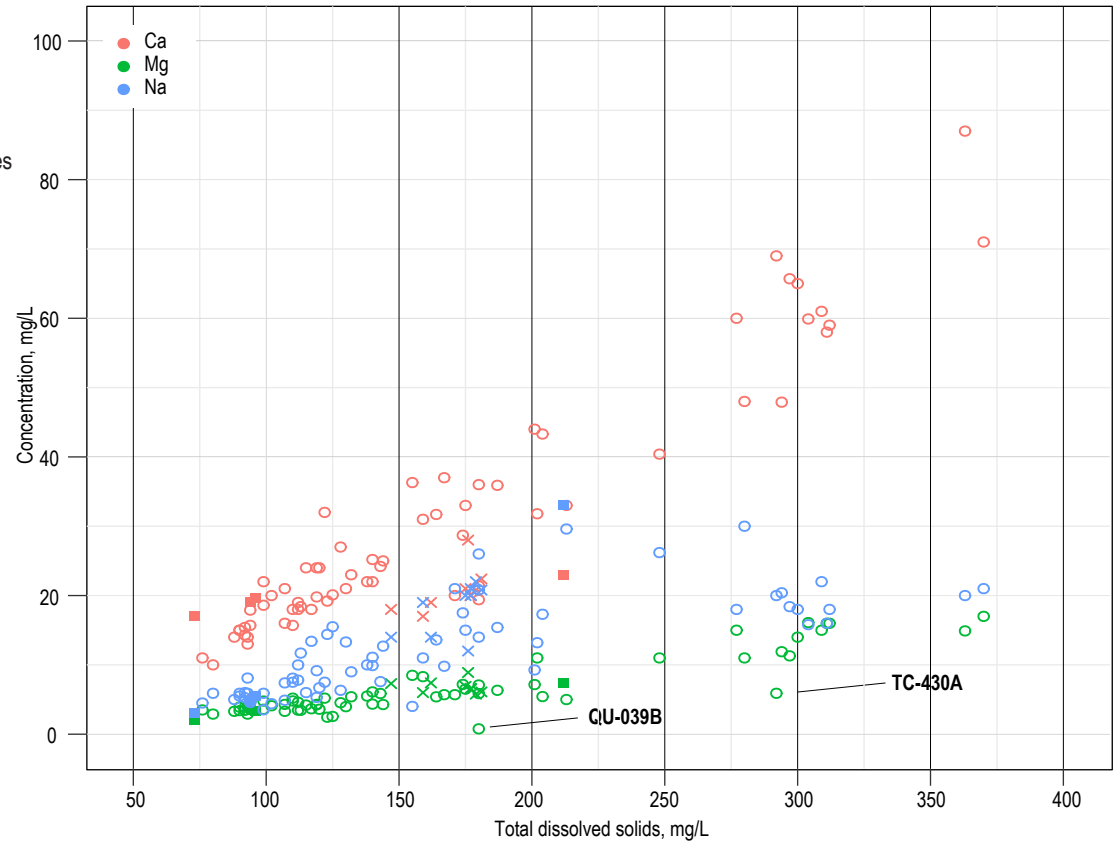

Figure 14. Plot of cations calcium, magnesium, and sodium against total dissolved solids. Groundwater samples are circles, spring samples denoted with x, surface water samples are filled squares.

calculated using PHREECQ Interactive version 3.3.2 (Parkhurst and Appelo, 1999). Gypsum and calcite show a tendency for increasing SI with increasing TDS, although gypsum does not achieve saturation even at the highest measured TDS (and thus Ca and SO_4 concentration). Several samples achieve calcite saturation. All but the lowest TDS sample are saturated with quartz. Albite is not saturated in any sample and potassium feldspar is not saturated in most samples, whereas kaolinite is saturated in all samples, and the Ca-montmorillonite is quite varied and shows no trend with TDS.

Stable isotopic compositions of water samples are shown in Figure 17 along with the global meteoric water line (GMWL, Craig, 1961) and a local meteoric water line for Questa (LMWL, data from Robinson, 2018). The LMWL is based on data from the three precipitation collectors shown in Figure 17. They are located at elevations of 7,523, 8,111, and 8,930 feet. The lowest elevation is similar to the central part of Sunshine Valley. The data defining the LMWL were separated into winter or cold season (defined as December–March) and summer or warm season (defined as June–September). Apart from the Rio Grande sample, the waters span a very small range of compositions, just 1.5‰ in $\delta^{18}O$ and 13‰ in δD. The Rio Grande water is much less depleted, does not resemble any of the local waters, and shows the effects of evaporation. QU-174A is more depleted than the other samples and is the only sample to not occur with the region of overlap between the summer and winter fields of the LMWL

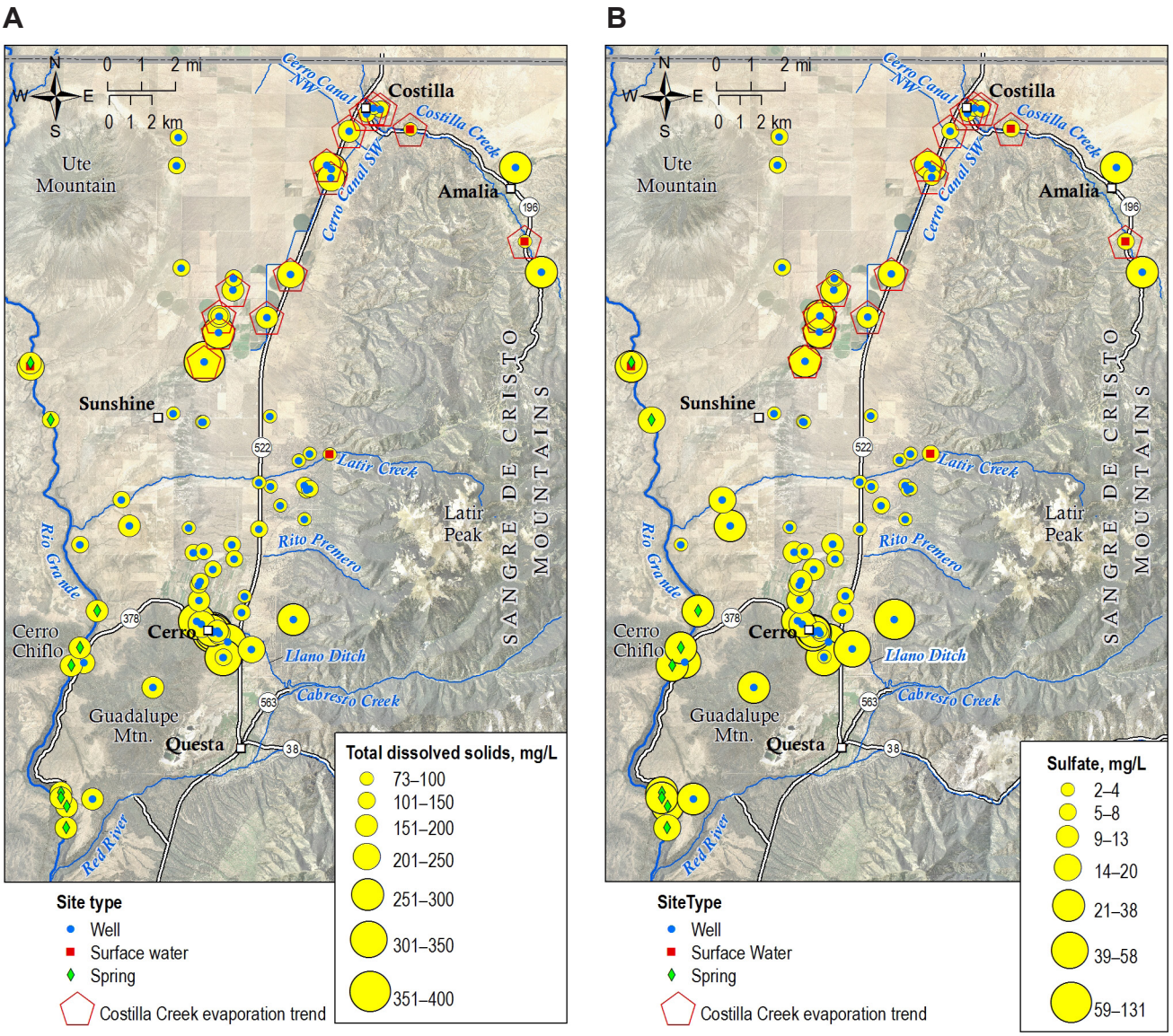

Figure 15. Maps of **A**—total dissolved solids and **B**—sulfate concentrations across the study area. Samples defining the Costilla Creek evaporation trend based on stable isotope data are shown with red pentagons. Note the association of these sample sites with irrigated areas northeast of Sunshine.

in Figure 17. The Costilla Creek samples and nine well samples west and southwest of the town of Costilla define a linear evaporation trend (shown with pentagons in Figs. 15, 17A).

Figure 18 shows results of tritium and ^{14}C age-dating analyses. Figure 19 shows these data plotted against well depth, along with TDS and temperature. For springs, the "depth" is the distance below the rim of the Rio Grande Gorge immediately east of the spring. Both tritium content and ^{14}C pMC (% percent modern carbon) vary widely, indicating both modern and old waters, and mixes of these. Neither tracer varies systematically with depth.

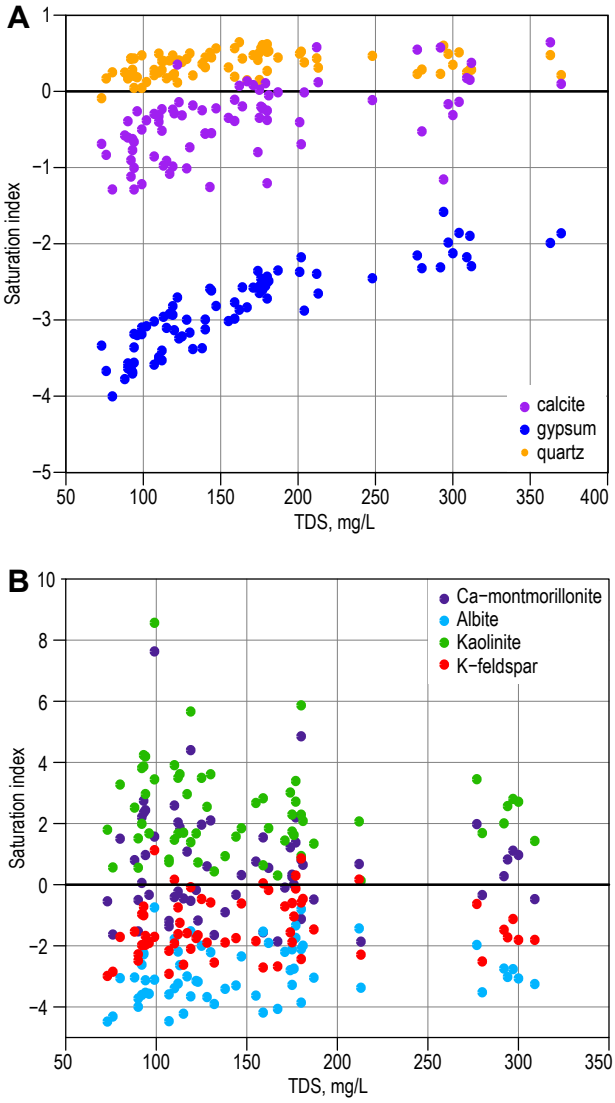

Figure 16. Calculated saturation indices (SI) against TDS. SI = 0 indicates the water is saturated with respect to the mineral. SI <0 indicates undersaturation. **A**—Calcite, gypsum, and quartz. **B**—Albite, potassium feldspar, kaolinite, and calcium-montmorillonite. SI >0 indicates supersaturation.

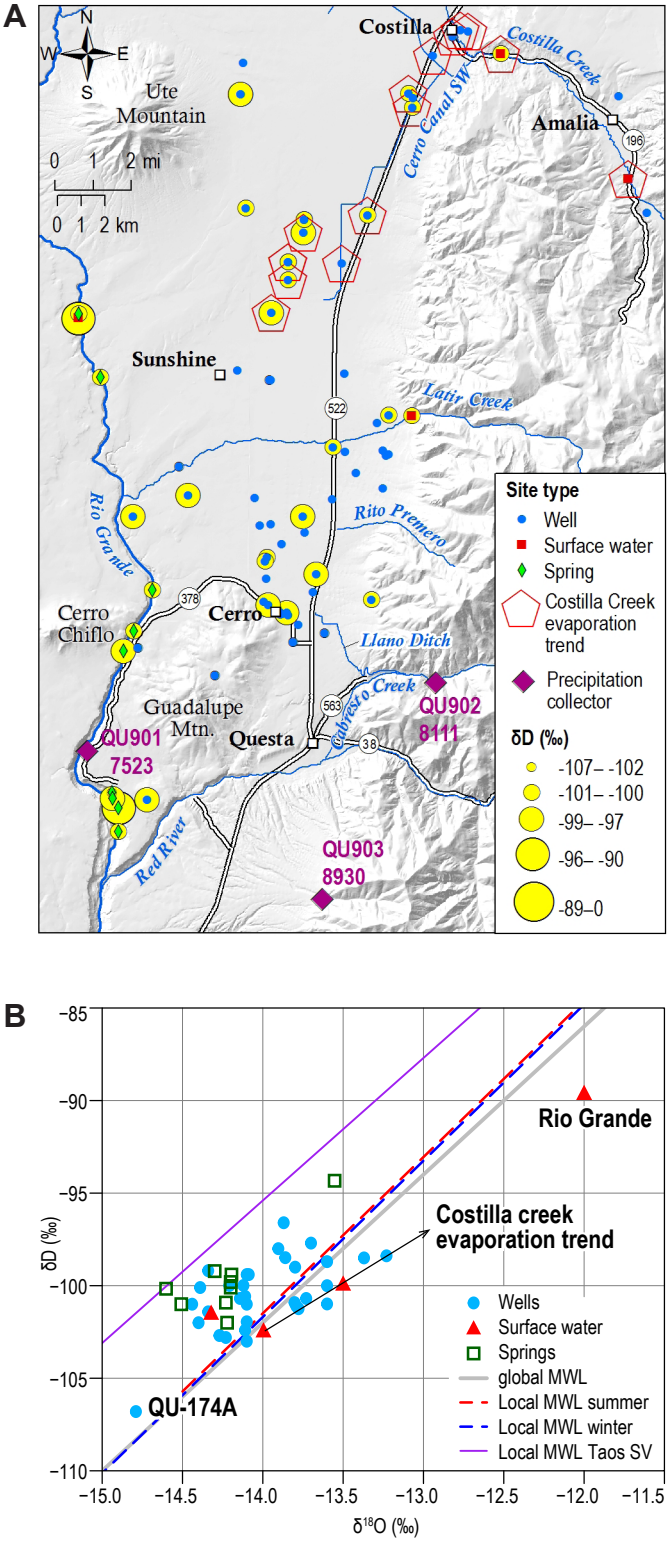

Figure 17. **A**—Map of stable isotopic composition of hydrogen in water samples and locations of the three precipitation collection sites (with elevations in feet) of Robinson (2018). Samples defining the evaporation trends are outlined with pentagons. **B**—Plot of stable isotopic compositions of water samples. Purple line is range of compositions for precipitation in Taos Ski valley (SV) (Drakos et al., 2018). MWL = meteoric water line. Global is from Craig (1961); local is from Robinson (2018).

Temperature-Depth Measurements

Figure 20 shows the three temperature logs measured in this study. The deepest well logged during this investigation, at 482 ft deep, is the Cerro North monitoring well (Figs. 4, 20). This well has three screened intervals at 134–239, 276–328, and 459–469 ft. The water table is at about 75 ft. The concave-up shape of the temperature-depth curve is characteristic of downward groundwater flow. The geothermal gradient in the upper part of the well is low, ranging from 0.3–4.2°F/1,000 ft. There is a small jump in gradient between 223 and 226 ft, suggesting the influx of slightly warmer water near the base of the upper screen. The gradient in the bottom 36 ft of the well below a depth of 446 ft increases dramatically to an average of 47°F/1,000 ft. Slightly warmer water (1.73°F higher than the temperatures above this point) appears to enter the well through the bottom screen. Detailed information about the rock types encountered in the well is not available, but nearby RG-32284, which is only 160 ft deep, encountered sand, gravel, and gravelly yellow clay.

The shallowest well is the Vick NE well located about 0.75 mi northeast of the Cerro North well (Fig. 4). This well is 138 ft deep, and the water table is at about 108 ft. The driller's log indicates the well is in sand and gravel. Water is about 0.4°F cooler than the same interval in Cerro North well (although the surface elevations are similar). The isothermal

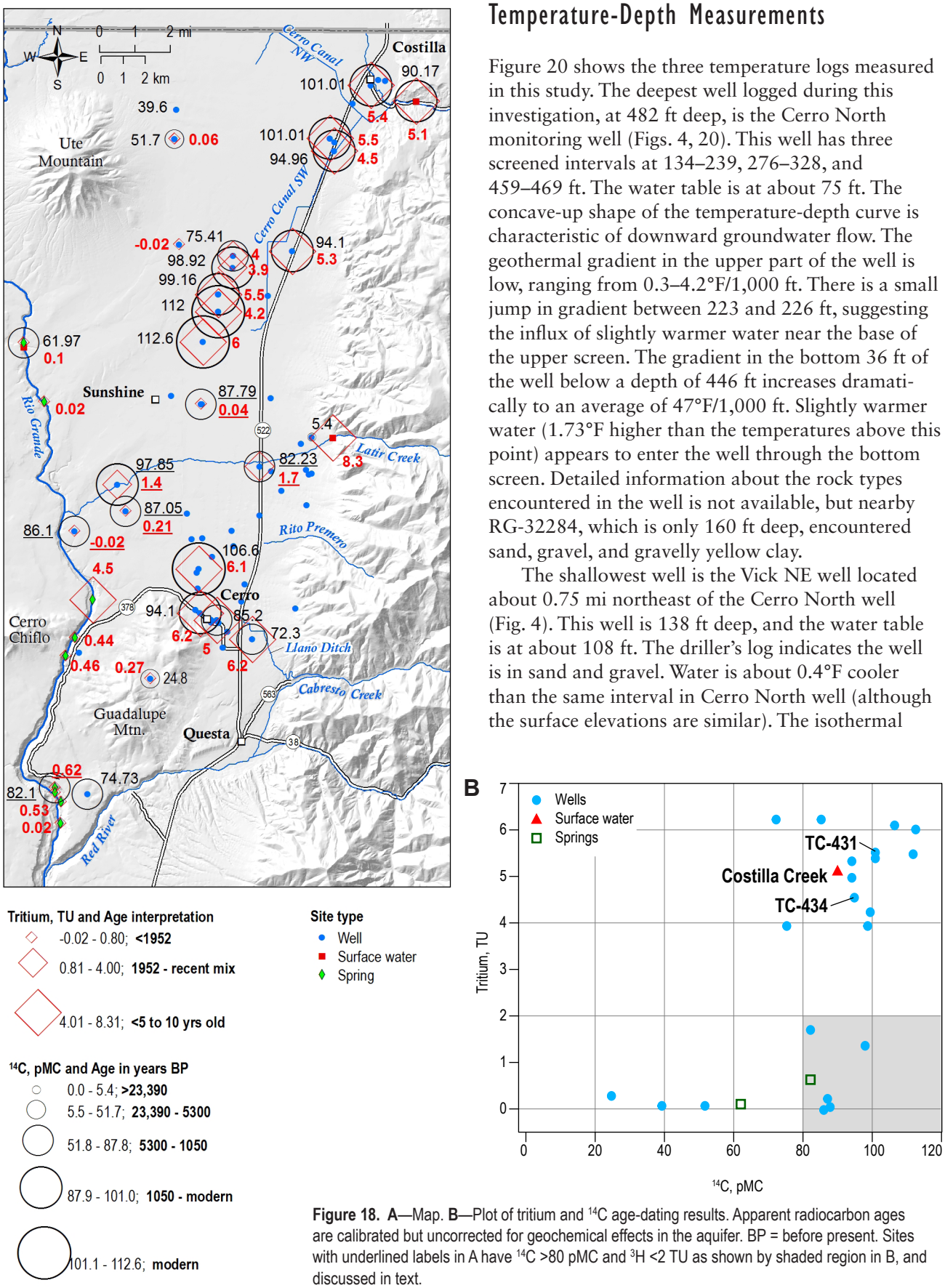

Figure 18. **A**—Map. **B**—Plot of tritium and ^{14}C age-dating results. Apparent radiocarbon ages are calibrated but uncorrected for geochemical effects in the aquifer. BP = before present. Sites with underlined labels in A have ^{14}C >80 pMC and ^{3}H <2 TU as shown by shaded region in B, and discussed in text.

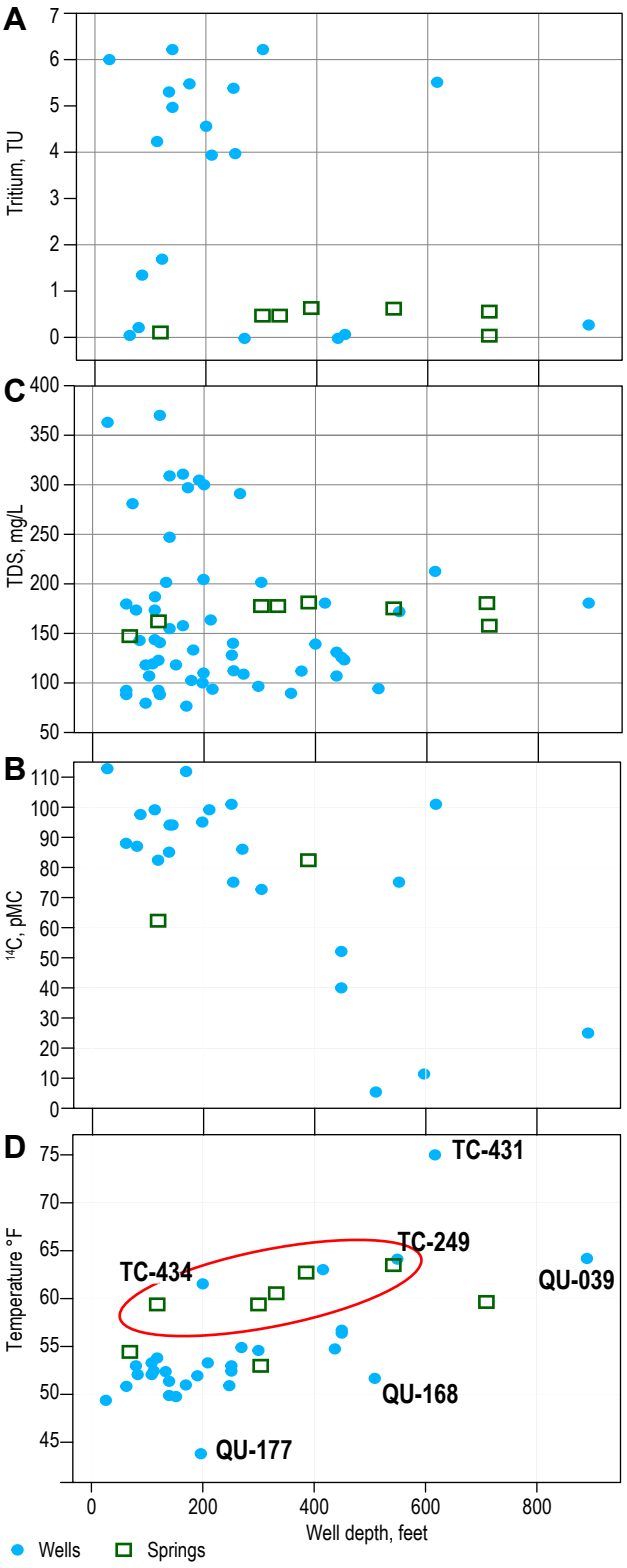

Figure 19. Parameters plotted against well depth. For springs, the "depth" is the distance below the gorge rim immediately east of the springs. Well samples are blue and springs are green. **A**—Tritium, **B**—^{14}C, **C**—Total dissolved solids, and **D**—Temperature. Circled samples in (D) and TC-431 define the "upper trend" described in the text and shown as samples with underlined labels on Figure 7.

character of the temperature-depth curve is indicative of groundwater flow, but the shortness of the measured interval precludes distinction between downward flow or lateral flow of colder water around the casing. Similarly, the Johnson-Dimmett well in the northern part of Sunshine Valley is isothermal and is not straightforward to interpret, but overall this well is warmer than the wells to the south by 12.5°F (Fig. 20). Detailed information about rock types encountered in the well is not available.

TEM Survey

Figures 21 and 22 show resistivity curves from the TEM measurements at the locations shown in Figure 8. TEM data from all 17 soundings processed during this study indicate the presence of a resistive layer at a depth of about 213 ft (65 m) (Figs. 8, 21–22). The top of the layer is relatively flat across an area of about 1.5 mi^2 in the middle of Sunshine Valley. The smooth inversion model used by Zonge does not fit the early-time data well, so a smoothing factor of 0.01 was applied to attempt a fit the early-time data. These models yielded resistivity values of 100 to 200 ohm-m. The slope of the dB/dt versus time curve below the resistive layer has a slope of 2.1, suggestive of an Earth response as opposed to noise. More conductive material below the resistive layer has resistivities on the order of 7 to 25 ohm-m.

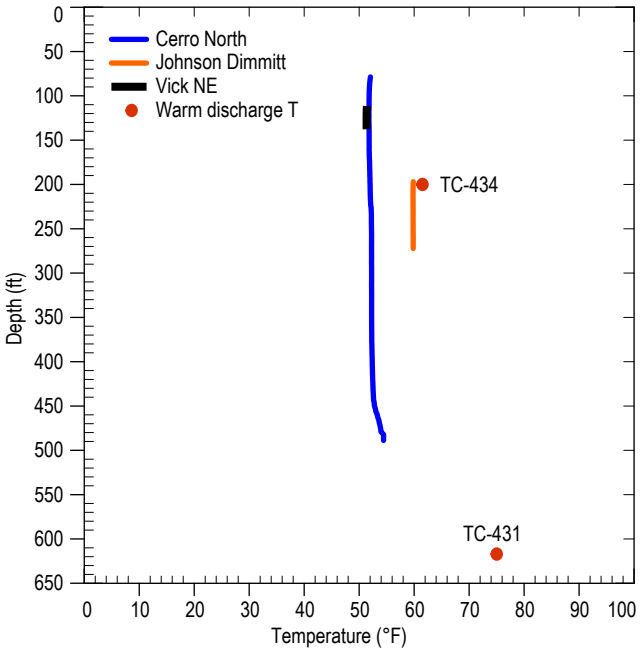

Figure 20. Temperature logs for the three wells measured in this study, with warm discharge temperatures of wells TC-434 (61.56 °F) and TC-431 (74.91 °F).

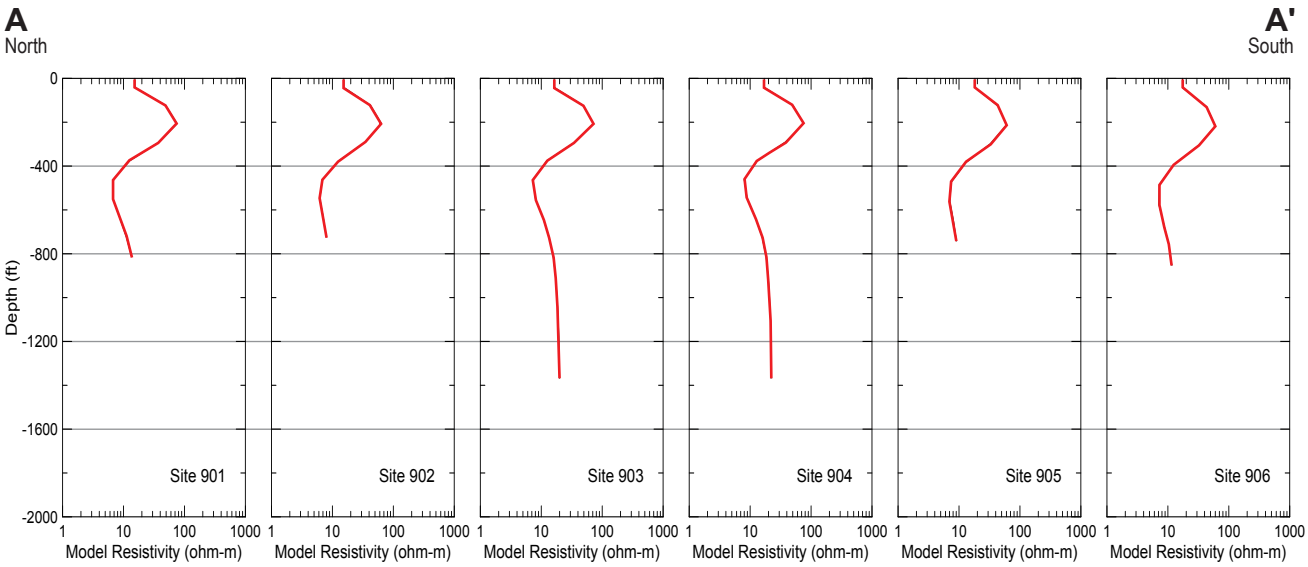

Figure 21. Model resistivity curves from 6 closely spaced contiguous sites located along a north-south line (A-A' on Fig. 8).

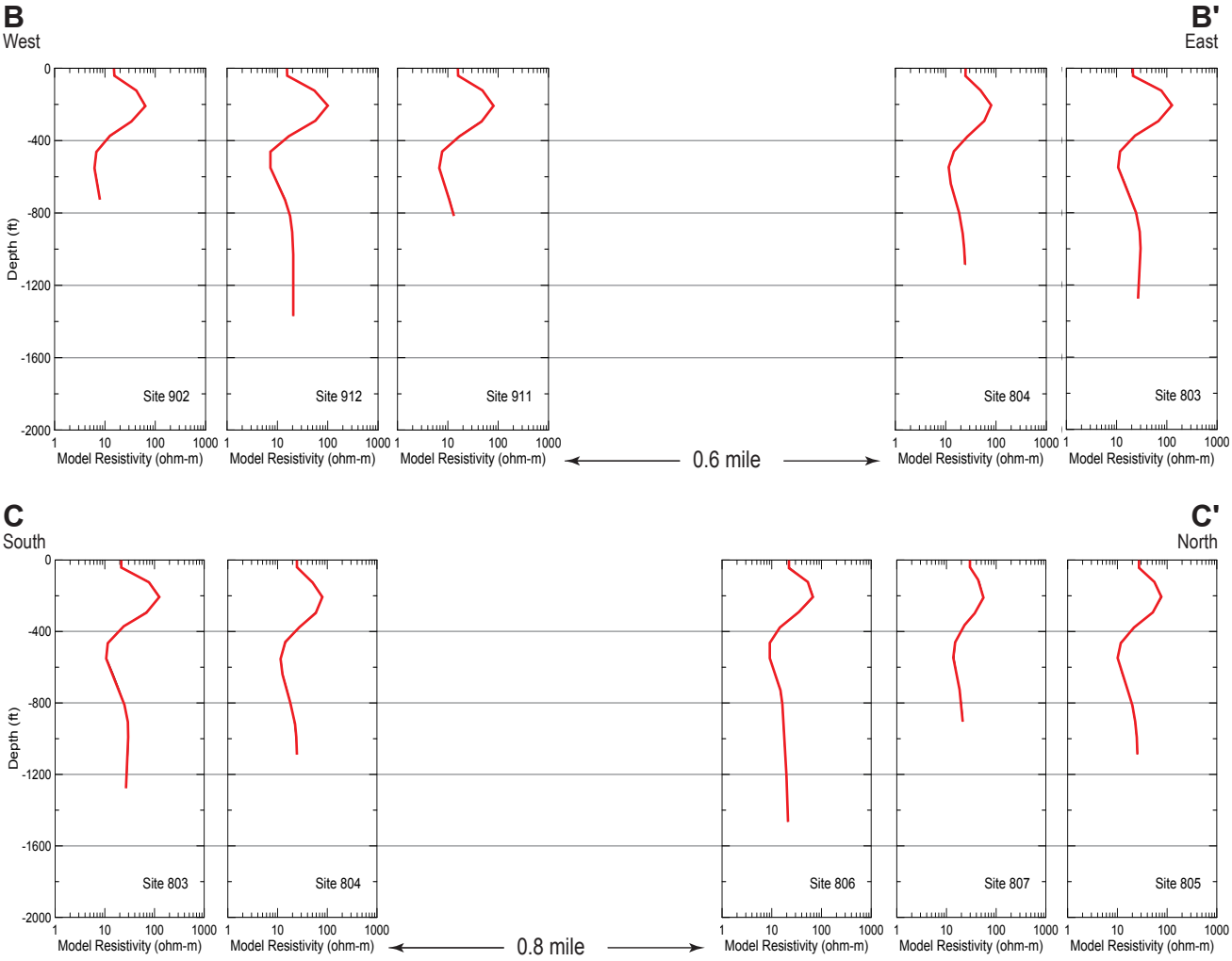

Figure 22. Model resistivity curves from a broader region of Sunshine Valley. The top profile B-B' is oriented E-W connecting two groups of TEM sites as shown on Fig. 8. The spacing between the groups is about 0.6 mile. The lower profile C-C' connects two groups along a NNE-SSW line. The spacing between these groups is approximately 0.8 mile. Note the similarity of the curves across the area.

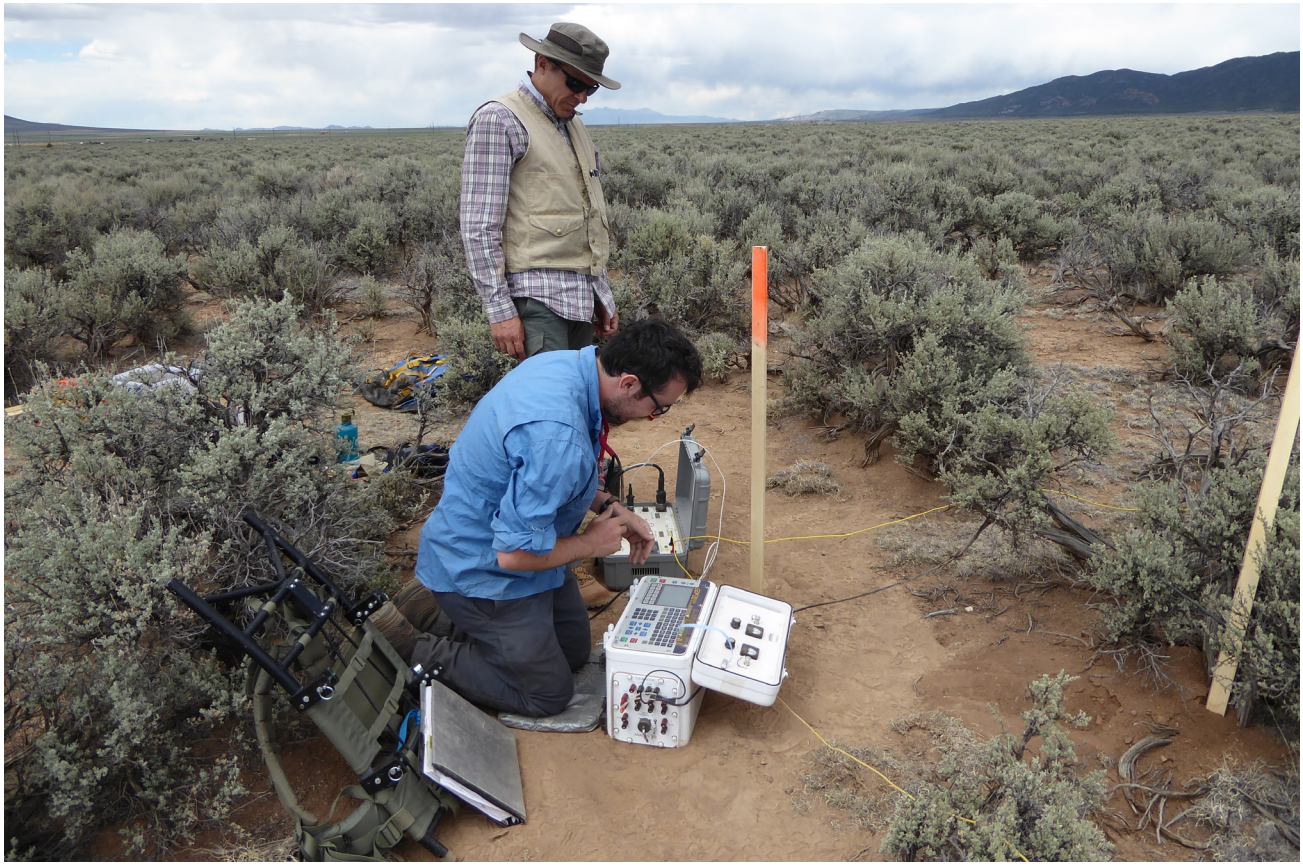

The senior author supervises the TEM survey. NMBGMR colleague Ethan Mamer collects the data.

IX. DISCUSSION

Processes Controlling Water Chemistry

Two trends are evident in Figure 12 that suggest geochemical processes affecting the water chemistry. First, in the cation triangle, the increase of sodium at the expense of calcium plus magnesium indicates ion exchange. In this process, sodium is released from clay-mineral interlayers and replaced by calcium plus magnesium (Hem, 1985). Figure 23 plots calcium plus magnesium in excess of that contributed by dissolution of calcite, dolomite, gypsum, and anhydrite against sodium in excess of that which could be contributed by the dissolution of halite. A slope of -1 on this plot indicates ion exchange is occurring and that reductions in the sum of calcium and magnesium are compensated by an increase in sodium.

Note in Figures 12 and 23 that the stream samples from Costilla and Latir creeks are among the most calcium-rich and sodium-poor of the water samples, whereas the Rio Grande is just the opposite. The Rio Grande water is a mix of many sources of overland runoff, surface water from tributaries, groundwater influx, and surface runoff from irrigated areas in the San Luis Valley. Its high sodium content is likely due both to ion exchange and evapotranspiration. Costilla and Latir creeks entering Sunshine Valley are low-TDS waters that are a mix of direct runoff and groundwater from shallow alluvium and/or fractured bedrock in their steep drainages. They have high tritium contents (5.1 and 8.3 TU, respectively, Fig. 18). The shallow groundwater component of these stream waters probably underwent some degree of ion exchange when in the soil and subsurface prior to discharging into the streams but less than the well and spring waters sampled to the west.

A simple correction calculation can semi-quantitatively "reverse" the effect of the ion exchange. For each sample, the equivalent quantity of "non-halite sodium" is apportioned to calcium and magnesium in the molar ratio in which these two constituents are present in the water analysis. The non-halite sodium is the sodium in excess of that which could be contributed by the dissolution of halite (the quantity plotted on the x-axis in Fig. 23). The effect is to remove sodium from the water and add calcium and magnesium, with the assumption that the ratio of the latter did not change during ion exchange. This is a semi-quantitative approach because other

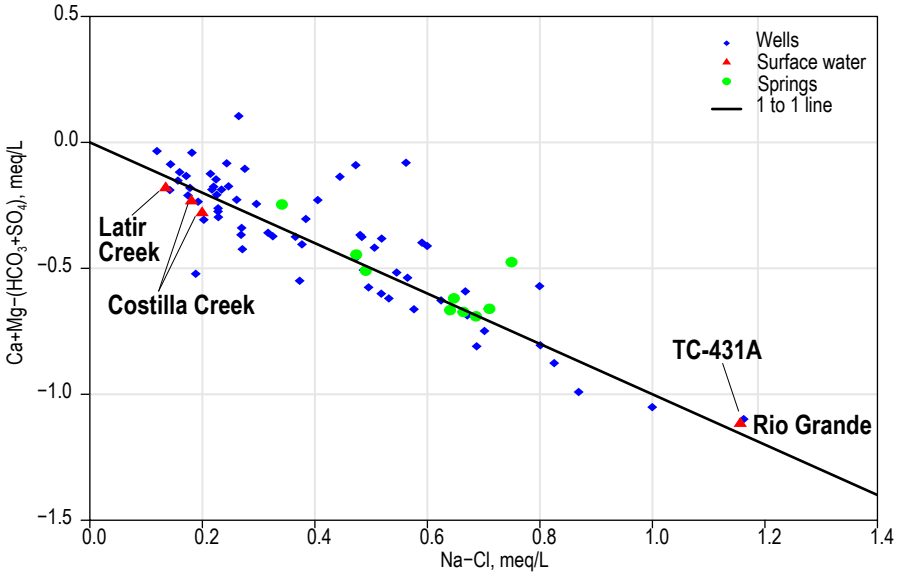

Figure 23. Plot comparing ion concentrations sourced from dissolution of calcite, dolomite, gypsum, anhydrite, and halite. Line with slope of ~1 illustrates the effect of ion exchange.

processes, such as silicate hydrolysis (see below), may affect water composition, but it serves to illustrate the dominant effect of ion exchange.

Results of this calculation are shown in Figure 24 and Appendix B. In Figure 24, the cation compositions corrected for ion exchange plot in a linear cluster centered on a region with a calcium to magnesium ratio of about 2.3 (70% calcium to 30% magnesium). Local Servilleta basalts have a calcium to magnesium ratio of 0.84 (Lipman and Mehnert, 1979), whereas typical compositions of the felsic to intermediate igneous and metamorphic rocks in the Sangre de Cristo range have molar calcium to magnesium ratios of about 1.5 to 2 or more (Best, 1982). These results are consistent with the "corrected" cation compositions reflecting weathering of these intermediate to felsic rocks, most likely in the form of sedimentary detritus comprising the basin fill underlying Sunshine Valley.

Weathering of primary silicate minerals by hydrolysis produces clay minerals, consuming water and carbon dioxide and releasing bicarbonate, silica, and free cations such as sodium and calcium. Examples of these reactions are potassium feldspar (e.g., orthoclase or sanidine) and albite weathering to kaolinite and/or montmorillonite. These feldspars are common constituents of the rocks in the Sangre de Cristo range and in the sediments of the basin fill. Figure 16 shows that samples are saturated with quartz and kaolinite, and many are saturated with Ca-montmorillonite. Calcite is only saturated at high TDS values and few samples are saturated with albite and potassium feldspar. These last two minerals should be unstable and break down to yield clay minerals within the aquifer.

A second process is evident in the anion triangle of Figure 12, where the sulfate proportion increases at relatively constant chloride proportion. This trend, and the increase of sulfate with TDS (Fig. 13), indicates the addition of sulfate to originally calcium-bicarbonate waters otherwise only affected by ion exchange. The five samples with the highest sulfate content are located in a small area between

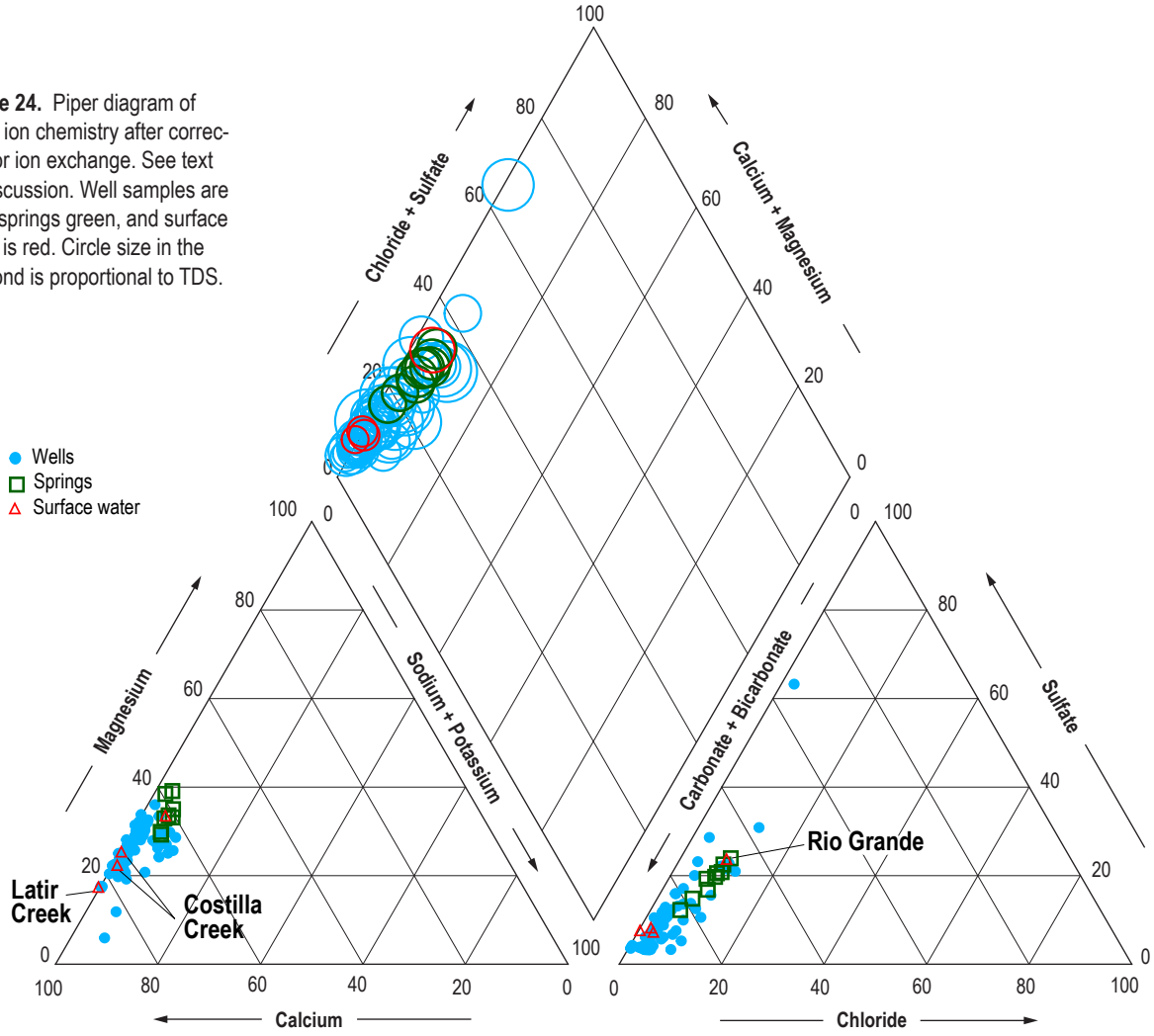

Figure 24. Piper diagram of major ion chemistry after correction for ion exchange. See text for discussion. Well samples are blue, springs green, and surface water is red. Circle size in the diamond is proportional to TDS.

Cerro and the mountain front (Fig. 15). Sample QU-103A is a clear outlier on Figures 12–13.

It is likely that sample QU-103A and the other high-sulfate samples near Cerro are due to mixing of some proportion of high-sulfate water ultimately derived from hydrothermally altered volcanic rocks in the Questa caldera to the east (Fig. 4). The hydrothermally altered zones have abundant pyrite, which oxidizes readily when the altered zones weather under the influence of oxygenated groundwater. Oxidation of pyrite releases a large amount of sulfuric acid. The acid reacts with available calcite, which consumes the acid and releases calcium. If enough carbonate is available to neutralize the acid, the pH of resulting waters will be near neutral. Gypsum formed as a result of this acid-sulfate weathering is abundant in the Questa caldera, and because it is highly soluble, calcium and sulfate are the dominant ions in surface water and groundwater in the Red River valley (Nordstorm, 2008). Such waters in the Sangre de Cristo Mountain block migrate down gradient to the west, mixing with water in the Sunshine Valley aquifer. This can cause local increases in TDS and sulfate concentration. Subsequent to mixing, calcium concentrations may be altered by ion exchange.

Stable Isotopic Compositions, Location, and Seasonality of Recharge

The stable isotope values of all samples plot near or beyond the depleted end of the range of summer precipitation and within the range of winter precipitation when compared to the LMWL for the Questa area (Fig. 17). The LMWL is based on precipitation at the level of the valley floor (Wild Rivers site, QU-901) to about 1,400 ft higher (Flag Mountain site, QU-903). The data are also within the range of stable isotopic compositions of snow in the Taos Ski Valley area, which represent winter precipitation at elevations above 10,000 ft (Drakos et al., 2018; P. Drakos, personal commun., 2018). Mixing lines can be drawn through the samples plotting between the two meteoric water lines. This suggests most of the sampled water can be explained as recharge from a mixture of (1) precipitation above the valley floor in the elevation range of the three precipitation collectors used to the define the LMWL (ranging 7,500 to 8,900 ft) and (2) high-elevation winter precipitation.

These data imply that little groundwater is derived solely from precipitation in the valley itself, i.e., areal recharge across the valley is negligible. This conclusion is consistent with results of MacDonald and Stednick (2003), who showed that very little recharge in southern Colorado and northern Arizona occurs below the elevation of the 46 cm (18.1 inch) precipitation isohyet, which lies above the valley floor in the Sunshine Valley region. Similarly, Anderholm (1994) showed that there is no significant recharge in the Española Basin around Santa Fe outside of the channels of the major drainages that experience infiltration from snowmelt runoff and flooding during summer storms.

An evaporation trend can be projected from the February 2008 stream sample for Costilla Creek (Fig. 17). The evaporation effect shown by the May 2018 Costilla Creek sample is reasonable as this sample was collected downstream of the earlier sample and later in the year. The groundwater samples defining the evaporation trend are all in the vicinity of the southwest branch of the Cerro Canal that carries water from Costilla Creek for irrigation (Fig. 1). TDS of some "downstream" groundwaters are noticeably higher than groundwater samples near Sunshine, probably as a result of evaporative concentration (Fig. 15). These waters reflect the effects of partial evaporation of the creek water during flow-and-flood irrigation and/or possibly reinfiltration of partially evaporated groundwater, which is pumped to supply irrigation systems in the area. The pumped water itself is likely sourced in part from infiltrated irrigation water. The sampled wells comprising this trend range from 27 to over 600 feet deep and have high tritium values indicating recent recharge. This illustrates the potential for relatively rapid migration of surface water to depths of several hundred feet, and the importance of infiltration of surface water through the bottoms of channels and irrigation ditches. The latter is consistent with observations in the Santa Fe area (Anderholm, 1994).

Age of Recharge, Mixing, and Potential Irrigation Return

Tritium is produced naturally in the atmosphere by cosmic radiation and is incorporated directly into water molecules by reaction with oxygen. The tritium signal in groundwater is produced when precipitation infiltrates through the unsaturated zone to the water table and becomes groundwater. The ^{14}C signal in groundwater recharge is largely acquired in the soil, which has a large reservoir of ^{14}C from plant respiration and decay (Clark and Fritz, 1997). Five samples have tritium values of >5 TU and percent modern carbon (pMC) values of >90; this correspondence of

the two dating methods confirms modern recharge within the last 10 years (Clark and Fritz, 1997, fig. 19). An additional nine samples have tritium of 3.9 to 6.2 TU with 72 to 99 pMC. These waters are a mix of mostly modern recharge with some older water, perhaps up to a few thousand years old. The remaining ten samples for which both age-dating analyses are available have TU of ~0 to 2, and pMC ranging from 25 to 98, indicating mixing of a small component of modern recharge with water recharged prior to 1952, to old water with "dead" tritium that may be hundreds to a few thousand years old. These groups of mixed waters are not spatially distinct or clearly associated with faults, indicating variable mixing of old and young recharge waters across the study area. However, inspection of Figure 18A indicates that the highest tritium values (>4 TU) are spatially associated with the Cerro Canal southwest of Costilla Creek and the Llano Ditch, supporting active recharge of young waters from the irrigation ditches.

Waters with high tritium values, indicating modern recharge, exist at depths of up to 600 feet (Fig. 19) and overall there is no distinct trend of tritium with depth. The pMC value does tend to increase with depth, but there are exceptions, which also indicate relatively rapid migration of young waters to depths of several hundred feet. There is no consistent trend of TDS with depth and in fact the highest TDS waters are at shallow depths, and have some of the youngest ages. A simple uniform recharge process of steady downward percolation of water accompanied by progressive ion exchange and hydrolysis of silicates should result in a trend of increasing age and TDS with depth. The situation is clearly more complex in Sunshine Valley. The age-depth relations indicate, at least locally, the existence of pathways of high vertical permeability to allow deep migration and subsequent mixing of young recharge with older waters. Similarly, the highest TDS values are in part the result of mixing of calcium sulfate waters from the mountain block with fresher waters in the Sunshine Valley aquifer.

Tritium values tend to decrease from east to west, away from recharge areas in the mountains. With one exception, tritium values in the gorge springs are negligible, indicating pre-1952 recharge. Spring water samples in the lower Red River canyon also have pre-1952 ages or are a mix of old water and more recent recharge (Robinson, 2018). The spring age-dating data suggests residence time on the order of 60 years or more for most water moving through the Sunshine Valley aquifer from recharge areas to discharge at the springs. Spring sample TS-029bA has a modern tritium age (4.5 TU, Fig. 18). It may discharge from a very permeable zone such as a lava tube or highly porous interflow breccia allowing rapid travel times across the valley, or from areas where surface water irrigation is extensive. In addition, cascading wells can allow shallow, young water to rapidly reach deeper levels that would otherwise require longer travel times.

The occurrence of very old tritium and young or modern ^{14}C in the same sample can be an indication of recycling of water into the aquifer via irrigation return. Return of old groundwater (with little or no tritium) pumped from the aquifer for irrigation via infiltration can result in a resetting of the ^{14}C signal to a young age (high pMC value), but will result in no change in the tritium value if no recent precipitation is added (Clark and Fritz, 1997, Rawling, 2016). Delineating this process in detail requires the use of multiple environmental tracers that vary in degree of potential atmospheric re-equilibration (Cook and Dogramici, 2019) and was beyond the scope of this study. Nevertheless, there are six samples in this study that have $^{14}C > 80$ pMC and $^{3}H < 2$ TU (Fig. 18). We may conservatively assume that these samples potentially represent groundwater that is influenced by some degree of irrigation return. Spatially, they do not show an association with the areas of extensive irrigation northeast of Sunshine and north of Cerro (Fig. 18), and none of them are samples comprising the Costilla Creek evaporation trend. The evaporation trend samples have tritium values ranging from a mix of recent water with water up to 60 years old, to recent recharge (3.94 to 5.99 TU). The ^{14}C values of the evaporation trend are all recent (98.9 to 112.6 pMC). This suggests that the evaporation trend is largely due to evaporation of surface water prior to infiltration, and any component of recycled ground water is secondary. However, the influence of irrigation return on the aforementioned six samples is possible, or their age dating results may be another indication of the mixing of waters of different ages and sources in the aquifer.

Temperature and Mixing of Hydrothermal Waters

Thermal profiles from deep wells near Questa are compared to the data gathered during this study in Figure 25 (see Figs. 1, 4). Geothermal gradients measured in three drillholes in and near the Questa Molybdenum Mine within the recharge area in the Sangre de Cristo Mountains are low (1.0 to 1.5°F/

100 ft) (Reiter et al., 1975; Edwards et al.,1978). Two drillholes in the high country within the mine, Questa 2 and Questa 3, have concave-up profiles and thus appear to record downward groundwater flow, which is to be expected in a recharge region. The thermal profile of the third well located in Red River Canyon, Questa East, is linear, and slight changes in gradient appear to be related to changes in lithology (Figs. 4, 25); basement rock in this particular well must have low permeability because the temperatures record conductive rather than convective heat transfer. Although detailed lithologic logs were not available for these wells, the Questa drillholes likely penetrate volcanic rock from the Latir volcanic field and underlying Proterozoic basement rock. A well logged by Edwards et al. (1978) near San Cristobal, located 7.5 miles southwest of Questa, has a more complex thermal signature (Figs. 4, 25). The temperature of the warm water entering alluvial-fan deposits at 305 ft is similar to temperatures measured in the Johnson–Dimmett well in northern Sunshine Valley. The gradient in the San Cristobal well is linear (2.0°F/100 ft) through a thick Servilleta basalt flow. At the bottom of the well, water flows upwards from the basal screened interval in the underlying Santa Fe Group.

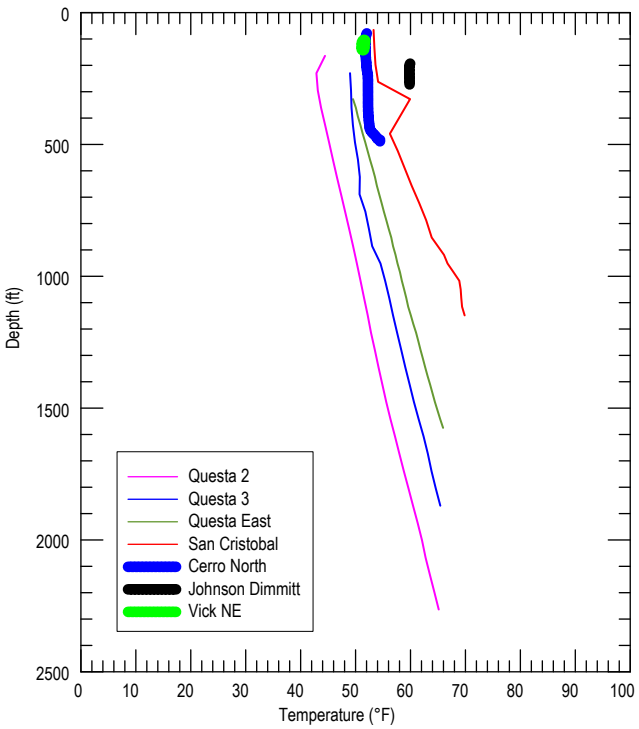

Figure 25. Temperature logs measured by Reiter et al. (1975) and Edwards (1978) south of Sunshine Valley and temperatures in wells logged during this study (thicker lines; locations shown in Fig. 1–4).

The Johnson–Dimmett well in the northern part of Sunshine Valley is 3 mi west of well TC-431, which has the warmest discharge temperature of the wells sampled during this study, and TC-434, which is also warm (Fig. 20, and see following discussion). This suggests that there may be higher geothermal potential west and southwest of the village of Costilla.

Water discharge temperature tends to increase with well depth and vertical distance of springs below the gorge rim, but there is significant variability and two distinct trends (Figs. 7, 19). The value of 43.9°F at 196 ft (well QU-177) is a notable outlier and may be in error. Well QU-168 at 509 ft with a temperature of 51.7°F is comparable to many wells with a depth of less than 300 ft, suggesting rapid downward flow of cool water from shallower depths in the vicinity of this well. This may occur along the faults at the foot of the range front immediately to the east of the well. Conversely, well TC-431 is 617 ft deep and is about 20°F warmer than the other sampled wells. Well TC-434 is 200 ft deep and a half mile to the southeast of TC-431. The discharge temperature in well TC-434 is about 10°F warmer than other wells in the study of comparable depth. The warmer temperature in these two wells suggests upwelling of warm water in the vicinity.

The other water discharge temperatures samples defining the trend in the ellipse around sample TC-434 in Figure 19D are springs in the gorge and two deep wells (415 and 550 ft deep) near the confluence of the Rio Grande and Red River. These warm temperatures may reflect long residence times in the aquifer at relatively large depths and/or upwelling of warm water along the Gorge and Red River fault zones (Fig. 4). Johnson and Bauer (2012) identified warmer waters in spring and well samples along the trend of the Red River fault zone.

Figure 26 shows silica, boron, lithium, and fluorine versus temperature. These chemical parameters have been shown to be elevated in hydrothermal waters relative to low-temperature groundwater (Hounslow, 1995). Silica and lithium concentrations found in samples from this study tend to increase with temperature, whereas boron and fluorine show no trend. Samples from the previously described warm wells TC-431 and TC-434 do not have the highest values of any of these parameters, and have modern tritium and ^{14}C pMC values (Fig. 18). These observations can be explained by rapid circulation of young meteoric water to depth where it is warmed, but undergoes no significant temperature-enhanced water-rock interaction or mixing with hydrothermal fluids. However, in Figure 23, sample TC-431 plots

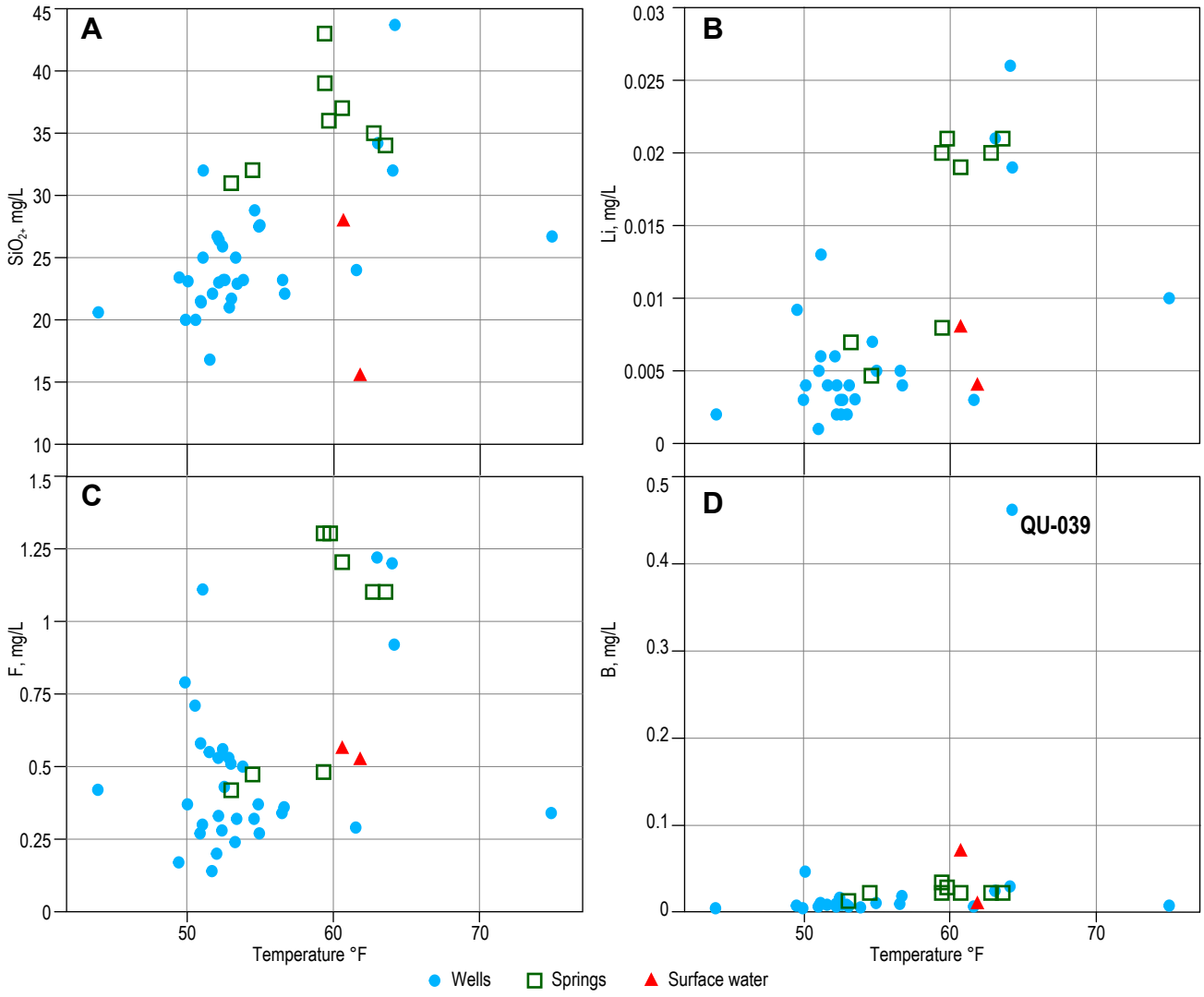

Figure 26. Parameters plotted against temperature. **A**—Silica. **B**—Lithium. **C**—Fluorine. **D**—Boron. Well samples are blue, springs green, and surface water is red.

similarly to the Rio Grande water sample, indicating a high degree of ion exchange. In this case the warming of the rapidly circulating water may have promoted the ion exchange process without altering other chemical parameters.

The Rio Grande Gorge springs, and samples from wells TC-249 and QU-039 in the southwest portion of the study area, have the highest values of the aforementioned hydrothermal-associated chemical parameters, along with submodern tritium values and ^{14}C values of 24–82 pMC. These sites also comprise the warmer, "upper" trend of temperature versus depth in Figure 19. The temperature and chemical trends for these sites may in part be due to their older ages and longer flowpaths in the Sunshine Valley aquifer. Robinson (2018) argued that the anomalously high level of boron in well QU-039 (Fig. 26), and generally high hydrothermal-associated chemical parameters, implied mixing of a component of hydrothermal fluid. An alternative explanation for the high level of boron is due to contamination from the old, splintered reinforced fiberglass casing of the well (J. Marcoline, personal commun., 2019). The water sample from this well was collected at a depth of 970 feet, the deepest well sample in the study, at an elevation below the level of the Rio Grande directly to the west. The well is located along a dike interpreted to be intruded into a fault (Robinson, 2018). Using a mixing model and silica geothermometry, Robinson (2018) estimated the hydrothermal fluid component for the QU-039A sample at 3–5%. In turn, the QU-039A water sample was used as an end-member for a second, regional, mixing model to explain groundwater chemistry variations around Questa. All of Robinson's (2018) sample sites west and southwest of well QU-039 included

a component of this water in the regional mixing model. Johnson and Bauer (2012) also argued for upwelling of warmer, possibly hydrothermal-sourced water in the southwest portion of the present study area. Thus is it probable that there is a contribution of deep-sourced, hydrothermal fluid upwelling and mixing with shallower groundwater near and southwest of Guadalupe Mountain, but it only represents a few percent of the total volume of water discharging from the wells and springs in this area.

Subsurface Interpretations from TEM Surveys

As noted previously, the 17 TEM soundings record the presence of a flat-lying resistive layer at a depth of 210 to 215 feet that appears to be underlain by more conductive material. The Cerro North monitoring well, RG-13887, reported to have a depth of 500 ft (152 m), is located between TEM stations 803/804 and 805/806/807 (Fig. 8). Although no driller's log is available for this well, information from screened intervals at 134–239, 276–328, and 459–469 ft (41–73, 84–100, and 140–143 m) provides some data on the location of water-bearing intervals in the well. Depth to water is about 77 ft (23 m). Garrabrandt (1993) determined geochemistry of the groundwater from this well to be quite fresh, with a TDS of 73 mg/L.

The lack of a driller's log for the deep Cerro North well hinders identification of the rock type forming the resistive layer, but two logical choices are basalt or a sand or gravel aquifer containing fresh water. Basalt is present at 212 ft in a deep well located about 1 mi west of TEM site 906 (i.e., Chiflo dam-site test hole R-5 of Winograd, 1959) (Fig. 8). The 2019 survey area, however, is located 0.6 mi to the east of the east-down Sunshine Valley fault zone (Figs. 1, 4). Based on the muted nature of the aeromagnetic anomalies to the east of the Sunshine Valley fault zone (Bankey et al., 2005), and a cross section passing through the study area (presented in Ruleman et al., 2013; C–C', Figs. 4, 27), the basalt found in well R-5 has likely dropped down to the east across the fault zone to depths greater than 213 ft (65 m). Thus, the resistive layer is likely a sand and/or gravel interval filled with fresh water. Interestingly, 213 ft (65 m) roughly coincides with a small jump in geothermal gradient from 223–226 ft (68–69 m) in the Cerro North well (Fig. 20), suggesting an influx of slightly warmer water near the base of the upper screen within the resistive unit.

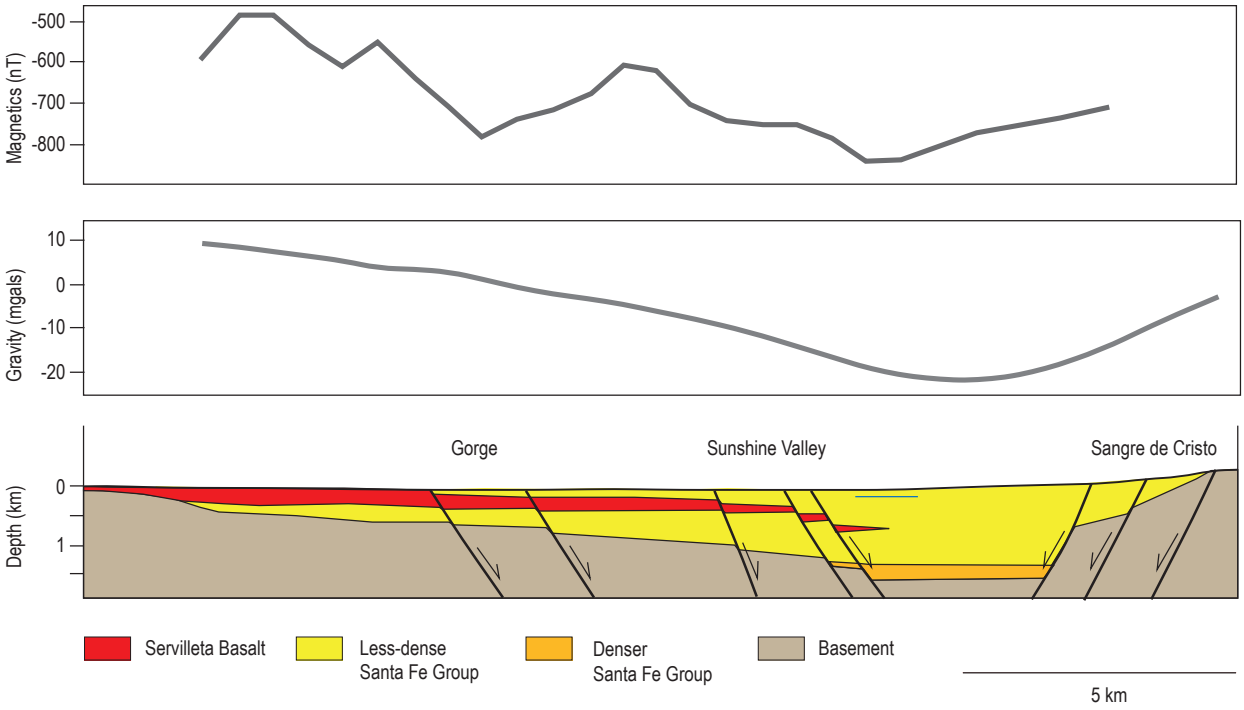

Figure 27. Cross-section C-C' in Fig. 4, modified from Ruleman et al. (2013). The blue horizontal line represents the aquifer mapped during the TEM survey. See text for discussion.

Temperature logging the Vick NE well. The Sangre de Cristo Mountains are in the background.

X. HYDROGEOLOGIC CONCEPTUAL MODEL

Figure 28 illustrates the conceptual model of the hydrogeology of Sunshine Valley based on the data and interpretations in this report and the work of Winograd (1959). The aquifer is laterally and vertically complex, with layers of sand and gravel overlying and interbedded with fractured, highly transmissive basalt flows that thin and pinch out to the east. Low-permeability lake beds are interpreted to be present in the central portion of the valley and lead to both "semi-perched" and "subartesian" conditions locally. Interbedded sediments and basalt flows of the Santa Fe Group, overlain by surficial deposits, constitute the upper "alluvial" part of the aquifer, and fractured, highly transmissive basalt flows with minor interbedded sediments comprise the lower "basalt" portion of the aquifer. However, overall, the Sunshine Valley aquifer is one continuous system with variable vertical and horizontal permeability. The only true perched zones probably exist under the mouths of the major drainages entering from the east and are likely dependent on the variations of streamflow and local irrigation intensity.

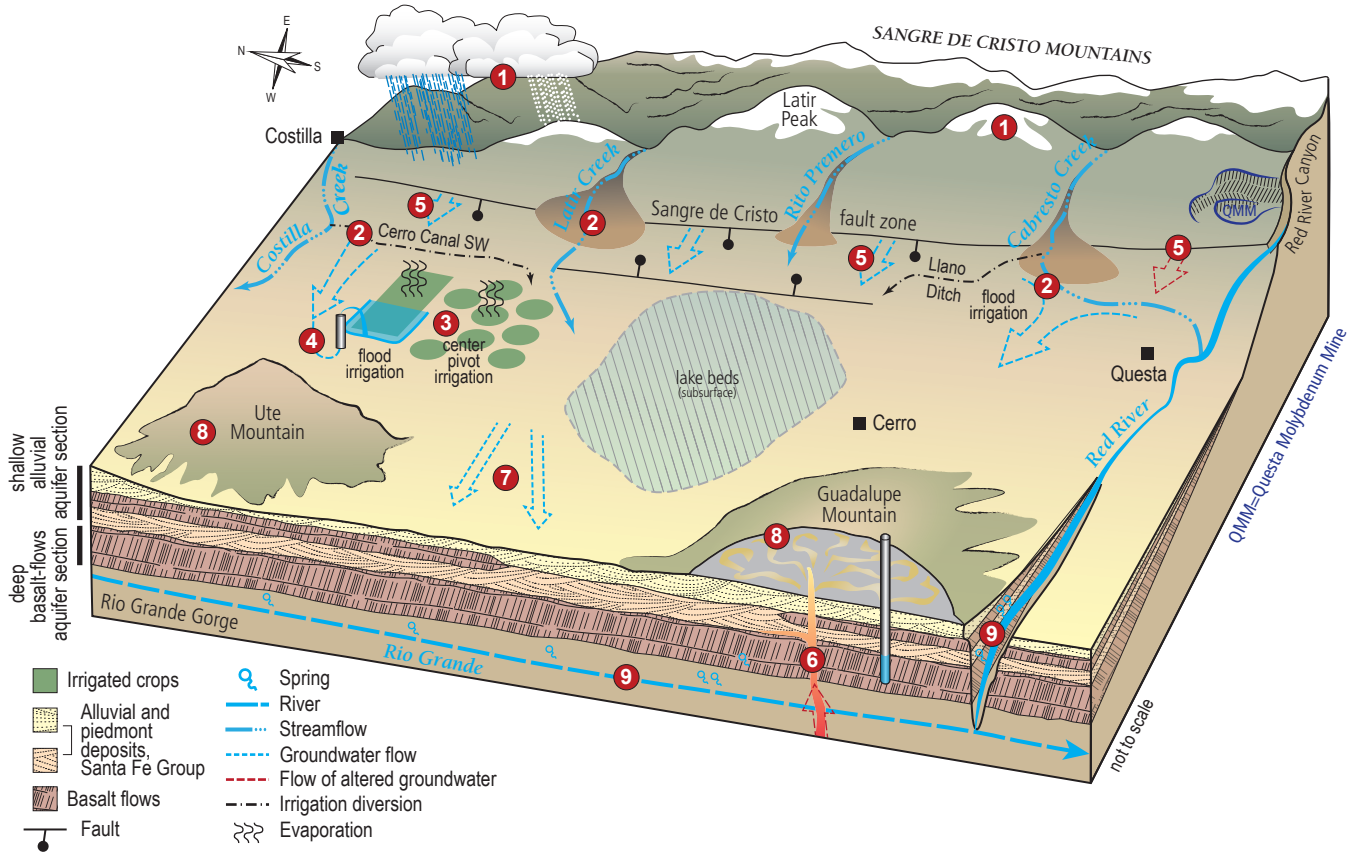

Figure 28. A conceptual model of hydrogeology of the Sunshine Valley region. **1**—Recharge is derived from high-elevation winter precipitation. **2**—Surface water enters the aquifer via infiltrating streams and irrigation diversions, and is locally recycled via shallow groundwater pumping for irrigation. **3**—These processes develop an evaporation signal that is noticeable in and to the southwest of Costilla Creek. **4**—Young water infiltrates to several hundreds of feet in the northern valley and is warmed before discharge via wells. **5**—Groundwater moves westward into the aquifer from the mountain block. Near Cerro and Questa, this water has high sulfate content. **6**—Deep below Guadalupe Mountain, small amounts of hydrothermal water upwell and mix into the aquifer. **7**—Groundwater moves from east to west under low gradients through transmissive basalt flows and sand and gravel beds, such as those identified in the TEM surveys. **8**—The fractured volcanic rocks of the buried basalts and Ute and Guadalupe Mountains act as drains for the shallow alluvial aquifer. **9**—The aquifer discharges to the Rio Grande and Red River via springs and seepage.

Cold-season precipitation and melting of snowpack are the sources of most recharge (1, numbers in parentheses here refer to Figure 28). Surface water enters the aquifer vertically as infiltration of streamflow and irrigation water, and is locally recycled via shallow groundwater pumping for irrigation (2). Several water samples along Costilla Creek and southwest of the mouth of Costilla Canyon constitute an evaporation trend, which is apparent both in the stable isotopic compositions and in the general chemistry of groundwater (3). This illustrates the importance of both streamflow and irrigation return in recharging the aquifer and their impact to the water budget.

Water-level, water-chemistry, water-temperature, and age-dating data all point to locally high vertical permeability allowing very young water to descend several hundreds of feet within the aquifer (4). These waters are rapidly warmed but are not associated with distinct geochemical anomalies. The young faults along the range front and in the central part of the valley probably facilitate this vertical movement, as they have offset some of the youngest deposits in the valley and may force upwelling by both offsetting low-permeability units at depth and by providing high permeability vertical pathways (4).

Groundwater enters the Sunshine Valley aquifer laterally from the mountain block to the east (5). The highest sulfate values measured were in wells around Cerro. These sites are affected by groundwater that has interacted with hydrothermally-altered volcanic rocks in the Questa caldera, and subsequently moved west into the aquifer from the mountains, crossing the range-front faults in the process. Steep caldera-margin faults oriented normal to the range front, abundant fracturing of the basement rocks, and brecciation and hydrothermal alteration associated with the caldera all likely facilitate movement of groundwater from the mountain block to the Sunshine Valley aquifer (5). The water sample from the well on Guadalupe Mountain has geochemical constituents indicative of a component of deep-sourced hydrothermal water (6, Robinson, 2018), as do other water samples in the vicinity as reported by Johnson and Bauer (2012).

The fractured, buried basalt flows transmit water to the west and southwest under low gradients, reflecting their high transmissivity (7). The resistive layer identified in the TEM survey is most likely a coarse sand or gravel bed and is an example of one of the water-bearing zones in this complex aquifer.

The volcanic edifices of Ute and Guadalupe mountains act as drains for the aquifer. On the north flank of Guadalupe Mountain, water levels in the shallow aquifer are 300 to 400 feet above the occurrence of water affected by deep-sourced hydrothermal fluids (8). Springs and seepage into the Rio Grande and Red River constitute discharge from the Sunshine Valley aquifer (9).

XI. WATER BUDGET

Components of the Water Budget

The importance of the Sunshine Valley region as a contributor of water to the Rio Grande was known prior to the work of Winograd (1959). His study was motivated in part by the recognition that the onset of intensive groundwater irrigation in the 1950s could potentially affect streamflow in the Rio Grande. The regional hydrological importance of Sunshine Valley has not waned and in fact has been recently reemphasized with the water rights transfer out of Sunshine Valley as part of the Aamodt settlement (Aamodt Settlement Agreement, 2018). The detailed accretion survey of Kinzli et al. (2011) quantified the groundwater inflows to the Rio Grande in the reach adjacent to Sunshine Valley. This work, along with the compilation of new and historical water chemistry data in the present study allows for a more comprehensive assessment of the water budget of Sunshine Valley using the chloride mass-balance method (CMB). This method was used to estimate recharge to the aquifer through infiltration of surface water and subsurface inflow sourced from the Sangre de Cristo Mountains. A water budget was calculated with inflows to the aquifer compared to outflows in the form of discharge to the Rio Grande and Red River via spring flow and seepage.

The area of interest for the water budget is larger than previously considered in this report and extends southward of the broad divide between Guadalupe Mountain and the Sangre de Cristo range front. The region addressed by the water budget also includes the area around Questa, eastward to the mountain front and southward to the Red River (Fig. 29). This additional area was excluded from the previous discussion because of potential complications in water chemistry interpretation due to the presence of the large tailing impoundments related to the Questa Molybdenum Mine and the fact that recently Robinson (2018) investigated the hydrogeology of the Questa area in great detail. However, water-level elevation contours (Fig. 6), indicate that the groundwater flows south and southwest out of Sunshine Valley into the Questa area and beneath Guadalupe Mountain, ultimately to discharge at the numerous springs along the lower Red River and in the Rio Grande Gorge west and southwest of Guadalupe Mountain (Fig. 28). This area must be included to correctly assess the water budget. Vail Engineering (1993) argued that the majority of spring flow and seepage to the Red River in the Questa area is sourced from the north, so the Red River was chosen as the southern boundary of the Sunshine Valley–Questa flow system. Several additional water samples from wells in the Questa area reported in Robinson (2018) were added to the dataset for the chloride mass-balance analysis, along with streamflow data for Cabresto Creek and the Red River (Table 1, Fig. 29). The northern boundary of the water-budget area is the New Mexico–Colorado state line. As discussed below, surface water entering Colorado is accounted for, and the geometry of the water-level elevation surface indicates that little groundwater flows from New Mexico into Colorado (Fig. 6).

A general water budget for an aquifer is described by the following equation:

$$\Delta S = \mathbf{GW}_{in} - \mathbf{GW}_{out} + \mathbf{P} - \mathbf{ET} + \mathbf{SW}_{inf} - \mathbf{SW}_{dis} - \mathbf{Irr}_{pump} + \mathbf{Irr}_{return} - \mathbf{Spring}_{dis} \quad (1)$$

The components of the budget are the following:

ΔS = change in storage of groundwater in the aquifer;

$\mathbf{GW}_{in}$; $\mathbf{GW}_{out}$ = subsurface groundwater flow into and out of the aquifer, respectively;

P = precipitation on the aquifer;

ET = evapotranspiration from the land above the aquifer;

$\mathbf{SW}_{inf}$; $\mathbf{SW}_{dis}$ = surface water infiltration into the aquifer and surface water discharge from the study area. The infiltration includes surface water diverted for irrigation that is not lost to evapotranspiration;

$\mathbf{Irr}_{pump}$; $\mathbf{Irr}_{return}$ = Groundwater pumped for irrigation use and reinfiltration of irrigation water derived from groundwater that is not evapotranspired;

$\mathbf{Spring}_{dis}$ = discharge of groundwater from springs and diffuse groundwater seepage into streams.

Table 1. Chloride mass-balance calculations and streamflow corrections for water budget.

Drainage basin	*From PRISM an81 dataset* **average total precipitation** (af/yr)	**Average total precipitation minus 30% canopy interception** (af/yr)	*From USGS gauges* **average annual streamflow** (af/yr)	**Corrected annual streamflow** (af/yr)	**Nature of streamflow correction**
RECHARGE SCENARIO 1 - Chloride mass-blance calculations using 69 samples. Removed three samples with Cl = 0					
Costilla Creek	296,369	207,458	37,494	23,246	subtract portion lost to CO
Latir Creek	31,356	21,949	3,952	3,952	
Urraca Canyon and Ute Mountain	24,060	16,842	0	0	
Rito Primero	11,754	8,228	0	1,403	add annual flow in Llano Ditch
Cabresto Creek	53,572	37,500	10,480	4,192	subtract 60% of flow below Llano Ditch (see text)
Total	**417,111**	**291,978**	**53,329**	**32,793**	
				Total streamflow contribution to groundwater (af/yr) 14,675	subtract (Costilla$_{TFWSW}$ + 0.75*Cerro–Questa$_{TFWSW}$)
Cl_{eff} in precipitation (mg/L) 0.5	**mean Cl_{gw}** (mg/L) 4.05	**median Cl_{gw}** (mg/L) 2.45	**Cl_{sw}** (mg/L) 1.5	**effective Cl in SW infiltration** (mg/L) 3.35 = 1.5*(32,793/14,675)	**mass Cl deposited over basin** (af/yr)*(mg/L) 145,989 = 0.5*291,978
	Total MFR from mean Cl_{gw} (af/yr) 36,047=291,978*(0.5/4.05)	**Total MFR from median Cl_{gw}** (af/yr) 59,587=291,978*(0.5/2.45)			
Estimation of groundwater component of mountain front recharge (af/yr)					
1. Using effective Cl in infiltrating surface water			**2. Using volume of infiltrating surface water from NMOSE data**		
Using mean Cl_{gw} 23,901=(145,989–3.35*14,675)/4.05	**Using mean Cl_{gw}** 39,510=(145,989–3.35*14,675)/2.45		**Using mean Cl_{gw}** 21,371=36,046-14,675	**Using mean Cl_{gw}** 44,912=59,587-14,675	
% MFR from groundwater 66	**% MFR from groundwater** 66		**% MFR from groundwater** 59	**% MFR from groundwater** 75	
RECHARGE SCENARIO 2 - Chloride mass-balance calculations using 25 samples. Removed samples with Cl=0, Br=0, Cl/Br molar >294.75, and samples possibly affected by irrigation return based on age-dating results					
Costilla Creek	296,369	207,458	37,494	23,246	subtract portion lost to CO
Latir Creek	31,356	21,949	3,952	3,952	
Urraca Canyon and Ute Mountain	24,060	16,842	0	0	
Rito Primero	11,754	8,228	0	1,403	add annual flow in Llano Ditch
Cabresto Creek	53,572	37,500	10,480	4,192	subtract 60% of flow below Llano Ditch (see text)
Total	**417,111**	**291,978**	**53,329**	**32,793**	
				Total streamflow contribution to groundwater (af/yr 14,675	subtract (Costilla$_{TFWSW}$ + 0.75*Cerro–Questa$_{TFWSW}$)
Cl_{eff} in precipitation (mg/L) 0.5	**mean Cl_{gw}** (mg/L) 4.44	**median Cl_{gw}** (mg/L) 3.2	**Cl_{sw}** (mg/L) 1.5	**effective Cl in SW infiltration** (mg/L) 3.35 = 1.5*(32,793/14,675)	**mass Cl deposited over basin** (af/yr)*(mg/L) 145,989 = 0.5*291,978
	Total MFR from mean Cl_{gw} (af/yr) 32880=291978*(0.5/4.44)	**Total MFR from median Cl_{gw}** (af/yr) 45622=291978*(0.5/3.20)			
Estimation of groundwater component of mountain front recharge (af/yr)					
1. Using effective Cl in infiltrating surface water			**2. Using volume of infiltrating surface water from NMOSE data**		
Using mean Cl_{gw} 21801=(145989-3.35*14675)/4.44	**Using mean Cl_{gw}** 30250=(145989-3.35*14675)/3.20		**Using mean Cl_{gw}** 18205=32880-14675	**Using mean Cl_{gw}** 30947=45622-14675	
% MFR from groundwater 66	**% MFR from groundwater** 66		**% MFR from groundwater** 55	**% MFR from groundwater** 68	

MFR=mountain front recharge; af/yr=acre-feet per year; TFWSW=total farm withdrawal, surface water; eff=effective ; gw=groundwater; sw=surface water

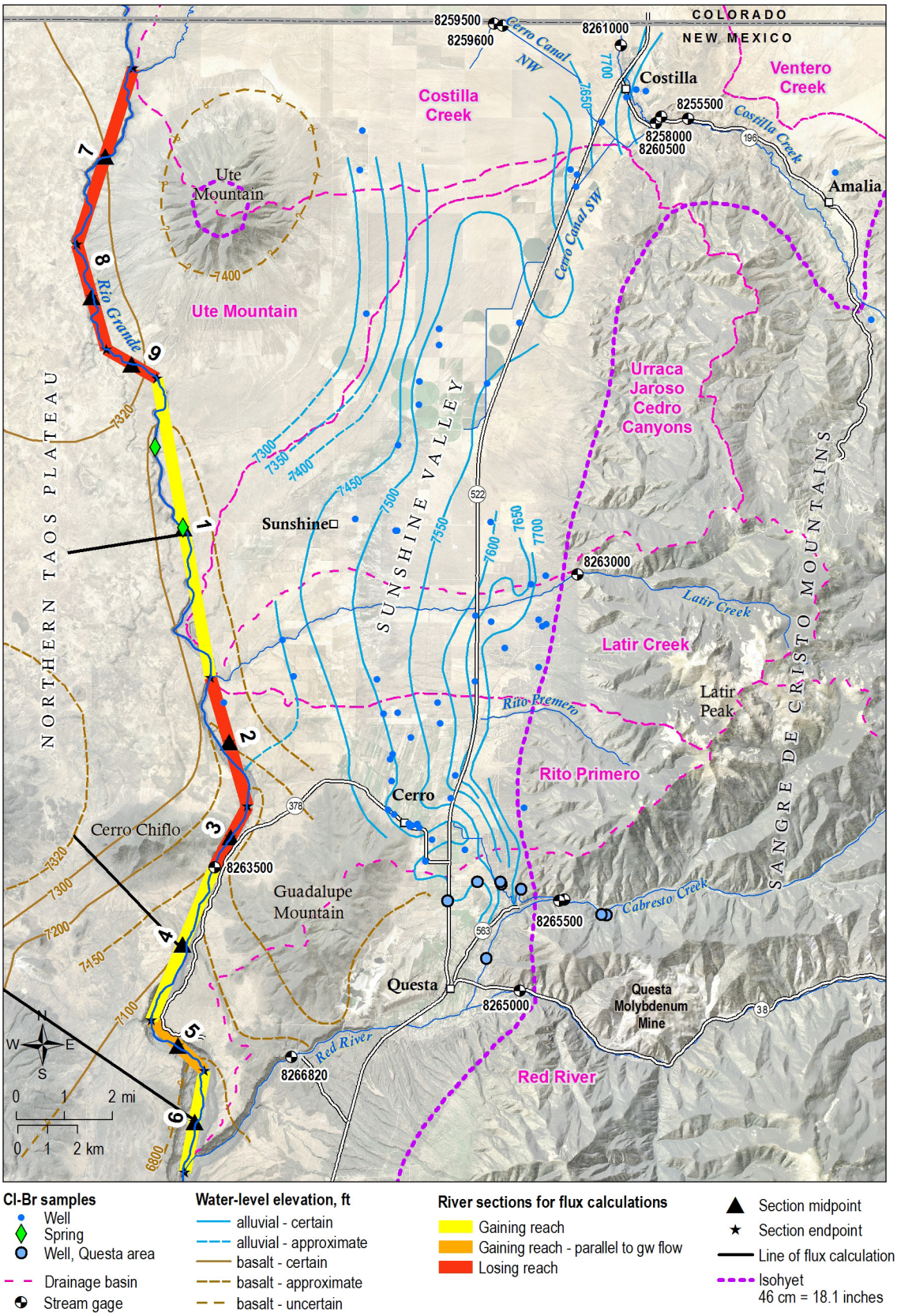

Figure 29. Map showing samples used in CMB recharge analysis, stream gauges used with USGS identification number, sections for analysis of groundwater flux into the Rio Grande from the west, and lines along which Dupuit approximation for groundwater flux was performed. The west ends of these lines are constrained by wells with water level measurements in Johnson and Bauer (2012).

If inflows to the aquifer equal outflows, the change in storage (ΔS) will be zero, the system is in equilibrium, and water levels will be stable over time. If outflows exceed inflows, water levels will drop over time and the storage term will be negative. Conversely, if inflows exceed outflows, water levels will rise over time and the storage term will be positive. Calculating the water budget involves quantification of each term, and/or determining whether one or more of the terms is negligible and can be ignored. An assessment must also be made of the reliability of each term of the equation—in a complicated natural system such as a regional aquifer, all of the components of the equation must be derived from a variety of data types, each with varying accuracy, precision, and temporal and spatial resolution. It is unlikely that the storage term will balance out to exactly zero and thus hydrogeological reasoning must be used in interpretation of the results and their significance.

In Sunshine Valley, several of the terms can be combined or ignored. Macdonald and Stednick (2003) showed that in Colorado and northern Arizona, reducing forest canopy had no effect on water yields in areas where average annual precipitation was less than about 46 cm (18.1 inches). In other words, below this precipitation threshold, all precipitation is lost to evapotranspiration at the surface or in the root zone regardless of the vegetation type. These results should apply in the Sunshine Valley region due to similarities in climate, elevation and vegetation. This appears to be the case, as the stable isotopic compositions of the water samples imply that winter precipitation above the elevation of Questa and Taos Ski Valley (the latter above 10,000 ft) is the dominant recharge source (Fig. 17). The 46-cm (18.1 inch) precipitation isohyet is shown in Figure 29. Everywhere in Sunshine Valley proper is below this isohyet, so it is assumed that precipitation (P) is balanced by evapotranspiration (ET), and there is effectively no areal recharge from precipitation. Thus, these two terms can be removed from the water budget equation. The effect of evapotranspiration on surface water and irrigation water will be addressed below.

Costilla Creek, Latir Creek, Rito Primero, and the Llano Ditch diversion from Cabresto Creek are the main surface water drainages entering Sunshine Valley north of the divide that runs east of Guadalupe Mountain. Rarely do these drainages flow to the Rio Grande (Winograd, 1959), so the $\mathbf{SW}_{dis}$ term is assumed to be zero. All of the water from the Llano Ditch is used for irrigation in the study area. These waters are all sourced in the Sangre de Cristo Mountains, and all of the combined flow is assumed to either infiltrate into the Sunshine Valley aquifer or be consumed by evapotranspiration. Some of the flow of Costilla Creek enters Colorado either in the main channel or in irrigation diversions and this must be taken into account.

Assuming flow perpendicular to water-level elevation contours, groundwater moves west and southwest from the Sangre de Cristo Mountains towards the Rio Grande. In the southern portion of the valley, near Cerro and the low surface water divide, groundwater flows towards Questa and the Red River (Fig. 6). West of Costilla, the water-level elevation contours are not well constrained for the 1950s, 1980s, or 2010s (Fig. 6), but flow appears to be west and southwest towards Ute Mountain. Little or no groundwater appears to flow north into Colorado and in fact groundwater may actually flow into New Mexico. The local drain effect of the highly fractured volcanic rocks of Ute and Guadalupe Mountains was described earlier. Water that descends into these features will likely emerge at the springs in the deeply incised gorges of the Rio Grande and lower Red River because these streams define the local base level and act as regional drains. The Rio Grande and Red River define the western and southern boundaries of the Sunshine Valley flow system. Thus the $\mathbf{GW}_{out}$ term in the water budget is assumed to be negligible. However, discharge to the Rio Grande and Red River is significant and occurs as spring flow and seepage though the river beds. These terms can be combined as $\mathbf{Spring}_{dis}$.

Irrigated agriculture using both surface and groundwater occurs throughout Sunshine Valley and the Questa area. The Office of the State Engineer (OSE) uses various approximations to estimate the irrigation withdrawals of groundwater and surface water separately at five-year intervals (Longworth et al., 2008, 2013). These results can be evaluated as consumptive use ($\mathbf{Irr}_{cug}$, $\mathbf{Irr}_{cus}$), which is the net loss of water from the land due to evapotranspiration. For groundwater, $\mathbf{Irr}_{cug}$, this quantity represents the difference between $\mathbf{Irr}_{pump}$ and $\mathbf{Irr}_{return}$. For surface water, $\mathbf{Irr}_{cus}$, this quantity represents the surface water lost to evapotranspiration during irrigation.

With these considerations, the water budget for Sunshine Valley can be formulated as follows:

$$\Delta S = \mathbf{GW}_{in} + \mathbf{SW}_{inf} - \mathbf{Irr}_{cug} - \mathbf{Irr}_{cus} - \mathbf{Spring}_{dis} \quad (2)$$

$\mathbf{GW}_{in} + \mathbf{SW}_{inf}$ is the total contribution of groundwater and surface water to the Sunshine Valley aquifer. This is estimated using the chloride

mass-balance method. The groundwater component is water that has migrated laterally in the subsurface from the Sangre de Cristo Mountains. Together these two components are known as "mountain front recharge" (Wilson and Guan, 2004), because, as noted above, there is little or no direct recharge to the valley from precipitation, so all of the recharge water comes from the mountain block. $\mathbf{Irr}_{cug}$ and $\mathbf{Irr}_{cus}$, are taken from Longworth et al. (2008, 2013). $\mathbf{Spring}_{dis}$ is the total discharge of groundwater to surface water in the Rio Grande and Red River drainages and is taken from Kinzli et al. (2011) and Vail Engineering (1993). Streamflow data are from the USGS National Water Information System website for surface water in New Mexico (USGS NWIS, 2018).

Chloride Mass Balance

The chloride mass-balance method (CMB) is a widely used approach for estimating groundwater recharge over spatial scales comparable to the Sunshine Valley study area (Anderholm, 1994; Wood and Sanford, 1995; Wood, 1999; Zhu et al., 2003). Atmospheric chloride (Cl) present as dust is used as a tracer. Differences between the average Cl concentration in surface infiltration and Cl concentrations in groundwater are due to the removal of water by evapotranspiration. The quantity of surface infiltration that enters the saturated zone of the aquifer is estimated as:

$$\mathbf{R} = \mathbf{P}^*(\mathbf{C}_{eff}/\mathbf{C}_{gw}) \quad (3)$$

where **R** is recharge, **P** is average annual precipitation $\mathbf{C}_{gw}$ is the Cl concentration in groundwater and $\mathbf{C}_{eff}$ is the effective Cl concentration. The latter results from both wet deposition dissolved in precipitation and dry deposition (dust) leached into the ground during infiltration.

Several assumptions must be realized to apply the CMB method:

1. Cl in groundwater originates from precipitation;
2. Cl is conservative in the aquifer;
3. The Cl mass flux has not changed over time;
4. There is no recycling or concentration of Cl in the aquifer.

Assumptions 1, and 2 are likely valid due to the highly soluble nature of Cl, and the lack of natural sources (halite) in the Sunshine Valley aquifer and the adjacent bedrock of the Sangre de Cristo Mountains (Feth 1981; Anderholm, 1994). Zhu et al. (2003) assumed different steady-state precipitation and Cl fluxes for the late Pleistocene and Holocene climate regimes. All of the samples used in the CMB analysis have Holocene ^{14}C ages thus steady-state Cl flux was assumed.

Hydrothermal waters may have enhanced Cl contents (Feth, 1981). One of the end-member water compositions in the mixing model for groundwater in the Questa area developed by Robinson (2018) was sample QU-039B from the well on Guadalupe Mountain (Figure 7). Robinson (2018) interpreted this water composition itself to be a mix of various water types, including 3 to 8% deep-sourced hydrothermal water. His mixing model identified all wells and springs west and south of the QU-039 well site as having a component of the QU-039B end-member. Due to this potential of a hydrothermal source, none of the wells and springs in this area were used in the CMB analysis.

Leakage from the tailing ponds near Questa is a potential source of anthropogenic contamination. Vail Engineering (1993) documented the effects of leakage on shallow groundwater and spring flow in the Questa area. Robinson (2018) also identified a tailing-leakage water component in some water samples collected around Questa. Care was taken to exclude these in selecting additional Questa-area samples for the CMB analysis (Fig. 29).

Chloride/bromide (CI/Br) molar ratios are useful in identifying the source of salinity in groundwater and are plotted against Cl in Figure 30. Typical values of the ratio for high-altitude continental precipitation and recharge waters range from 400–500 (Alcala and Custodio, 2008). Use of halite in the home, as a road de-icer, and in many industrial processes can lead to groundwater contamination with Cl. Because of the high Cl/Br ratio in halite (up to 40,000), even a small amount of anthropogenic Cl contamination can cause a large increase in the measured Cl/Br ratio of groundwater. Evapotranspiration increases both Cl and Br concentrations and will not change the ratio.

Alcala and Custodio (2008) reported examples of groundwater affected by leaching of garbage, solid waste, septic, and urban runoff wastewater as having Cl/Br ratios of 463 to over 1000. Of the 33 samples with analyzed Br, all but one have Cl/Br ratios of <400. The exception is <600, but this sample does not have elevated Cl. In particular, the highest Cl samples do not have elevated Cl/Br ratios. There are no strong grounds for removing any of the samples based on this criterion and it is possible all of the Cl/Br versus Cl data can be explained by natural geologic variation and evapotranspiration. However, the four samples with

the highest Cl/Br molar ratios (>294. 75) do comprise a statistically different population based on the t-test (Appendix D), which could be due to a small degree of anthropogenic contamination (Fig. 30).

The Costilla Creek evaporation trend was identified from the stable isotopic compositions of water samples (Fig. 17). Evaporative concentration of Cl in water prior to infiltration and recharge will not negatively affect the results of the recharge analysis. This may happen during normal streamflow and when surface water is used for irrigation. However, evaporative concentration during recycling of groundwater via pumping for irrigation and subsequent reinfiltration violates assumption 4 in the above list. As described above, the age-dating data suggests that the influence of groundwater recycling via irrigation return is of secondary importance in the Costilla Creek evaporation trend samples. However, there are six samples for which possibility of groundwater being recycled should be considered based on the age-dating results, four of which are in the CMB dataset.

With these issues in mind, two CMB recharge analysis scenarios were performed (Table 1). Recharge Scenario 1 used all groundwater samples excluding those with Cl=0. This scenario uses all data available for which the CMB analysis can be performed. Recharge Scenario 2 used only those samples with Br analyses for which the Cl/Br molar ratio < 294.75 and also excludes the samples with age-dating results suggesting the possibility of groundwater recycling via irrigation return. The second scenario is more conservative and eliminates samples in which there is the possibility for Cl concentration by processes other than natural evapotranspiration prior to infiltration and aquifer recharge. Calculations were also performed for a third scenario in which the samples comprising the Costilla Creek evaporation trend were removed from the Recharge Scenario 2 dataset, but the results were not significantly different and are not presented here.

Dry deposition of Cl as dust in New Mexico is significant and is much larger than wet deposition, which is only the Cl dissolved in precipitation. This can be seen when the Cl concentration is measured in bulk deposition (wet plus dry) and compared to the Cl concentration in wet deposition alone. Popp et al. (1984) reported average concentrations of Cl in bulk and wet deposition of 3.4 mg/L and 0.8 mg/L at Socorro in central New Mexico and 8.4 mg/L in bulk and 2.9 mg/L in wet at Raton in northern New Mexico. Lewis et al. (1984) recorded Cl of 0.71 mg/L in bulk deposition in southern Colorado, whereas Anderholm (1994) recorded Cl in bulk deposition of 0.29 mg/L at Santa Fe. Lewis (2018) reported volume weighted Cl in precipitation in the upper Santa Fe River watershed of 0.18 to 0.24 mg/L. The results of CMB recharge analyses are highly sensitive to the value used for C_{eff}, which clearly varies widely. No atmospheric Cl data were collected in this study; rather the average of the results of Lewis et al. (1984)

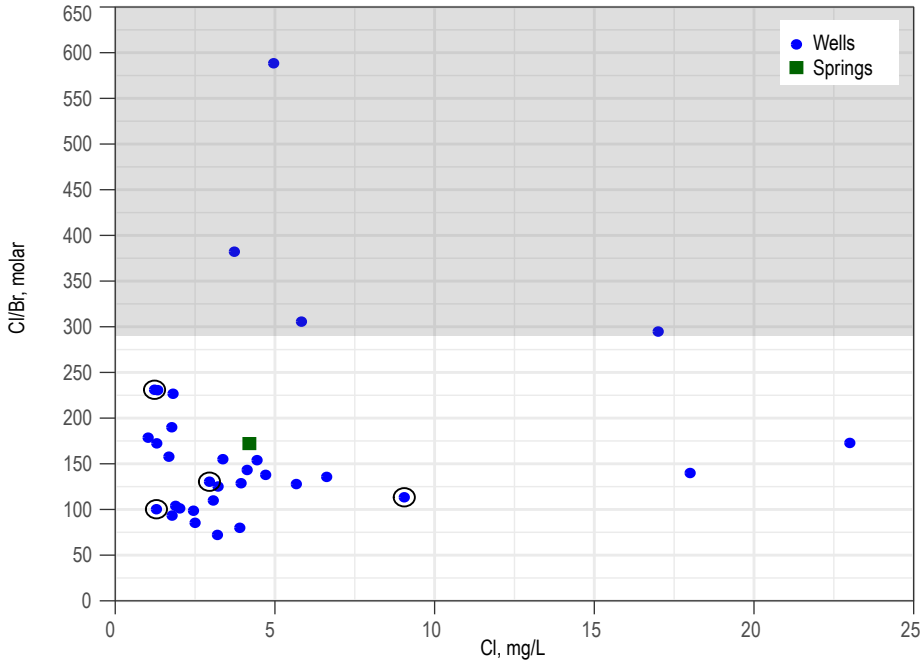

Figure 30. Plot of Cl/Br molar ratio against chloride concentration. Grey area highlights samples with ratios >294.75. Black circles highlight four samples that may be affected by irrigation return flow, as discussed in text and shown in Fig. 18.

and Anderholm (1994) of 0.5 mg/L was chosen as the value for bulk Cl deposition.

The value of C_{gw} was taken as both the average and the median of the Cl values in the analyzed groundwater samples for both scenarios and recharge was calculated using both (Table 1). Precipitation input was the PRISM *an81* dataset, the 30-year average annual precipitation over the drainage basins that discharge into the expanded Sunshine Valley–Questa study area (PRISM Climate Group, 2018). The *an81* annual precipitation data are calculated on an 800 x 800-m (2,624 x 2,246-ft) grid. The Sangre de Cristo Mountains are heavily forested and the recharge estimates include a canopy interception factor of 30% (Table 1). This is intermediate between the maximum value of 40% determined by Canaris et al. (2011) in the Sacramento Mountains of south-central New Mexico and the value of 28% determined by MacDonald and Stednick (2003) in southern Colorado (Rawling and Newton, 2016).

The total amount of mountain-front recharge to the Sunshine Valley aquifer calculated using equation (3) is presented in Table 1 and Figure 31. Using the full dataset of 69 samples (Recharge Scenario 1, Table 1A), the recharge is 36,047 acre-feet/year (af/yr) using the mean C_{gw} of 4.05 mg/L and 59,587 af/yr using the median C_{gw} of 2.45 mg/L. These recharge values are 8% and 14% of the average annual precipitation, respectively. Using the 25 samples in Recharge Scenario 2 (Table 1B), the recharge is 30,541 af/yr using the mean C_{gw} of 4.44 mg/L and 48,501 af/yr using the median C_{gw} of 3.20 mg/L. These recharge values are 8% and 11% of the average annual precipitation, respectively.

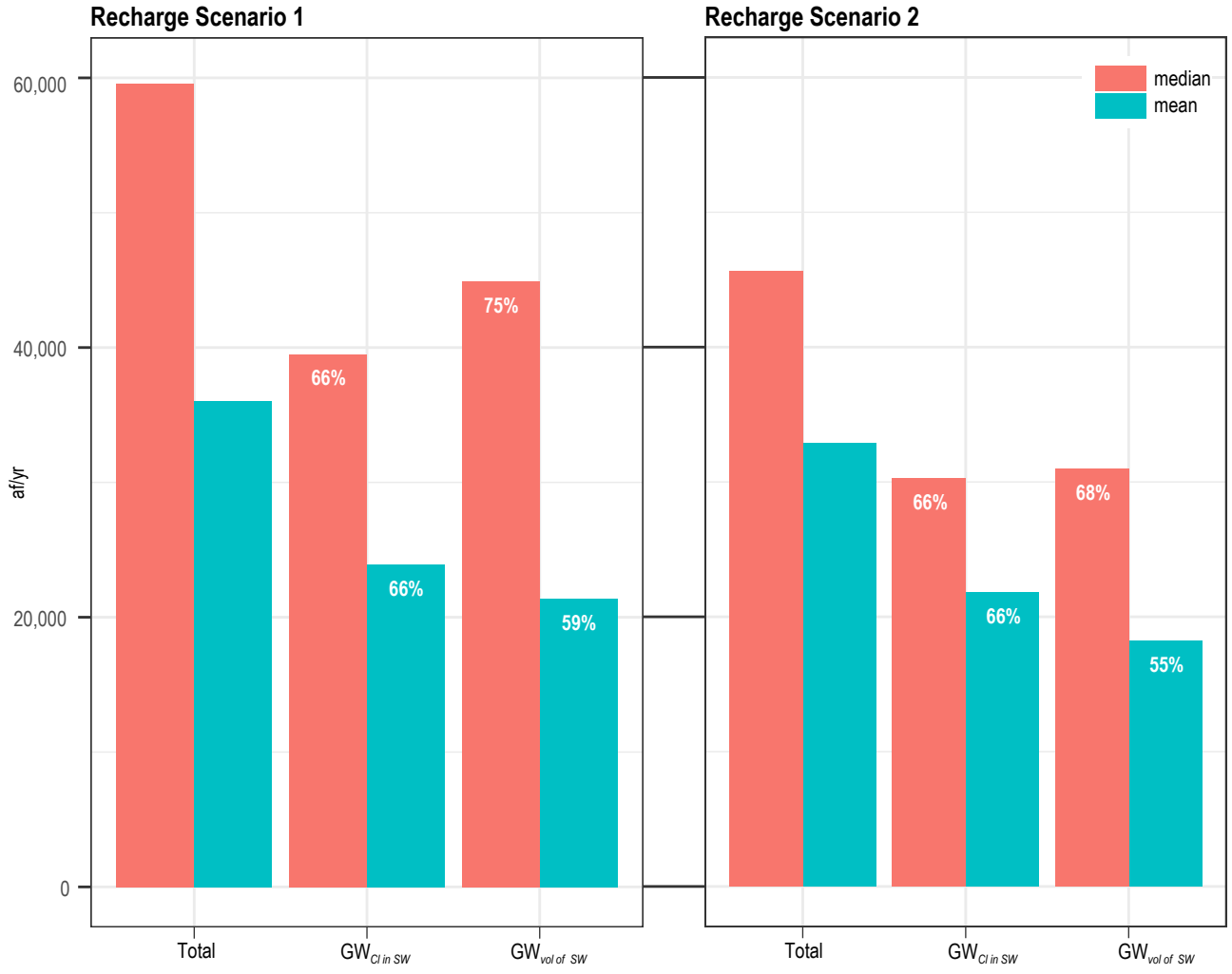

Figure 31. **A**—Recharge Scenario 1. **B**—Recharge Scenario 2. Recharge estimates are shown using the median and mean Cl value for each scenario. $GW_{Cl\ in\ SW}$ is the estimate of the groundwater fraction of the mountain front recharge derived from the estimate of Cl in infiltrating surface water. $GW_{vol\ of\ SW}$ is the estimate of the groundwater fraction of the mountain front recharge derived from the estimate of the volume of infiltrating surface water based on NMOSE data.

Inflow from Streams

Equation 2 illustrates that streamflow is an important component of the water budget as both inflows to and outflows from the aquifer. Streamflow data from USGS gauges were compiled to assess the quantity of surface water entering Sunshine Valley that can enter the aquifer (Fig. 29, Appendix C). If available, streamflow data from 1981 to the present were used, consistent with the time interval covered by the PRISM *an81* dataset (PRISM Climate Group, 2018). Many sites did not have data within this time range. In those cases, streamflow data were used regardless of the timeframe (Appendix C). Several corrections and/or approximations to the streamflow data were needed to estimate the quantity of streamflow available for infiltration (Tables 1–2).

First, the amount of flow in Costilla Creek that exits the study area and flows into Colorado was estimated by subtracting the flow at Costilla Creek near Garcia, Colorado (gauge 08261000), from the flow in Costilla Creek downstream of the irrigation diversion at Costilla (gauge 08260500). Flow in the Cerro Canal that enters Colorado at the State Line gauge near Jaroso, Colorado (gauge 08259600), was subtracted from flow in the Cerro Canal.

Second, the amount of flow in Cabresto Creek below the Llano ditch that does not reach the Red River but infiltrates as groundwater recharge was estimated as follows. In April 1993, Vail Engineering (1993) estimated the gain in the Red River from the gauge at Questa (gauge 08265000) to the Fish Hatchery west of Questa (gauge 08266820) at 5,140 af/yr, excluding springflow and seepage from tailing impoundments. In April 1993, the average flow in Cabresto Creek below the Llano Ditch (gauge 08266000) was 9,701 af/yr. The difference between these two values is 4,561 af/yr, and is assumed to be the quantity of water in Cabresto Creek below the Llano Ditch diversion (gauge 08265500) that did not reach the Red River. In other words, 9,701–5140 = 4561 af/yr was lost to groundwater along Cabresto Creek between the Llano Ditch and the confluence with the Red River. This is about 47% of the flow below the Llano Ditch. Detailed springflow and tailing seepage estimates do not exist outside of the April 1993 period when the Vail Engineering survey was performed. During the summer monsoon season when flows are higher, more water may reach the Red River. A value of 40% was thus taken as an estimate of the typical loss from Cabresto Creek to groundwater in the Questa area.

Third, the amount of surface water entering Sunshine Valley that is lost to evapotranspiration during irrigation was estimated from NMOSE reports on consumptive use (Longworth et al., 2008, 2013). For surface water, values are reported as TFWSW and CLSW, which are "total farm withdrawal, surface water," and "conveyance losses, surface water," respectively. The latter is leakage from unlined ditches and canals and becomes groundwater recharge with minimal evapotranspiration losses. The former is derived from the consumptive irrigation requirement for crops and is the quantity lost to evapotranspiration. The streamflow values that are assumed to infiltrate into the Sunshine Valley aquifer should be reduced by an amount equal to TFWSW.

In the Sunshine Valley region, Longworth et al. (2008, 2013) report TFWSW for the Costilla area and the Cerro-Questa area. The average of the values in the two reports was used here. It is straightforward to subtract the amount of TFWSW for the Costilla area from the average annual streamflow for Costilla Creek. In the Cerro–Questa area it is necessary to estimate what proportion of the TFWSW is associated with irrigation diversions from Cabresto Creek, which contributes water to the Sunshine Valley aquifer, as opposed to the Red River, which does not.

The only available estimate for irrigation diversions from the Red River is that from the Vail Engineering survey in April 1993, at 2,172 af/yr (Vail Engineering, 1993). It is assumed that this is a typical quantity, and that 40% of the Cabresto Creek streamflow below the Llano ditch is lost to irrigation or natural infiltration before the Red River confluence, as calculated above. Then the average streamflow lost to groundwater from Cabresto Creek below the Llano Ditch for the month of April from 1981 to 1995 is 0.4*11,595 = 4,638 af/yr (Appendix C). The average diversion to the Llano ditch in April for the years in which there are data is 1,368 af/yr. Then, average total irrigation diversions for the month of April in the Cerro–Questa area are estimated as 2,172 + 4,638 + 1,368 = 8,178 af/yr. The fraction of this amount sourced from Cabresto Creek is (4,638 + 1,368)/8178 or about 75%. It is assumed that this percentage is typical for the whole irrigation season. If so, then 75% of the total TFWSW quantity for the Cerro–Questa area represents water lost to evapotranspiration from the Cabresto Creek drainage.

Inflow into Sunshine Valley from streamflow and groundwater can also be assessed via the CMB analysis, as parts of the total mountain front recharge (Anderholm, 1994; Table 1). The total mass of Cl deposited annually over the drainage basin

contributing recharge to the Sunshine Valley aquifer can be calculated from the PRISM *an81* average annual precipitation data combined with the C_{eff} value. The two measured values of Cl in Costilla Creek streamflow (1.0 and 1.5 mg/L) are consistent with Anderholm's (1994) preferred value for average Cl in streamflow in the Santa Fe River of 1.5 mg/L. The actual Cl concentration in infiltrating surface water will be increased in the ratio calculated as the total volume of streamflow entering Sunshine Valley divided by the volume of infiltrating water. The denominator term here is smaller due to ET losses during irrigation. This assumes that all Cl left behind in the soil during ET is ultimately flushed into the aquifer by subsequent applications of irrigation water. If 1.5 mg/L is assumed for Cl concentration in streamflow exiting the mountains, then the effective Cl in infiltrating streamflow is 3.35 mg/L. From this value and the total mass of Cl, the proportion of groundwater in the total amount of mountain front recharge can be estimated (Table 1 and Fig. 31).

The groundwater component of the mountain front recharge can be calculated independently without reference to the Cl concentration in surface water by subtracting the estimated quantity of surface water that infiltrates as recharge from the total amount of mountain front recharge (Table 1 and Fig. 31). The results from the two calculations agree fairly well and indicate that approximately 65 ±5% of the mountain front recharge to the Sunshine Valley aquifer occurs as subsurface flow from the mountain block.

Table 2. Discharge from and recharge to Sunshine Valley

Discharges from Sunshine Valley	af/yr	notes
Total river gain, Lobatos gauge to Red River, occurs in NM	**41,569**	from Kinzli et al. (2011)
Estimated inflow from west side of river	**7,760**	from Dupuit approximation
Net river gain from Sunshine Valley	**33,809**	
Cold spring discharge and "field flow" to Red River	**3,540**	from Vail Engineering (1993)
Warm spring discharge in lower Red River gorge	**4,743**	from Vail Engineering (1993)
Consumptive groundwater use (Irr_{cug})		
Costilla	**492**	mean of 2005 and 2010, Longworth et al (2008, 2013)
Cerro and Questa	**668**	mean of 2005 and 2010, Longworth et al (2008, 2013)
Sum of Discharges	**43,252**	
Recharge to Sunshine Valley (GW_{in} + SW_{inf} - Irr_{cus})		
Recharge Scenario 1		
MFR from mean Cl_{gw}	**36,047**	
MFR from median Cl_{gw}	**59,587**	
Recharge Scenario 2		
MFR from mean Cl_{gw}	**32,880**	
MFR from median Cl_{gw}	**45,622**	

MFR = mountain front recharge, which implicitly includes the effect of Irr_{cus}, the surface water water lost to evapotranspiration during irrigation.

Outflow to Streams

The main discharge from the Sunshine Valley aquifer is springflow and seepage discharge to the Rio Grande and Red River. Kinzli et al. (2011) showed that the Rio Grande gains a significant amount of water (accretion) in the reach of the Rio Grande adjacent to Sunshine Valley from the Lobatos gauge in Colorado to the mouth of the Red River. To determine the amount of water entering from Sunshine Valley, the amount entering from the west side of the river in this reach was estimated and subtracted from the gains in flow measured by Kinzli et al. (2011). The remainder is assumed to be sourced from the Sunshine Valley aquifer to the east. To this end, the Rio Grande Gorge was divided into a series of linear segments and the water table map and water-level data from Johnson and Bauer (2012) were used to estimate groundwater flow using the Dupuit approximation for unconfined flow (Fetter, 2001) (Table 3, Figs. 29, 32). For accretion to the Red River, the data in Vail Engineering (1993) were used to quantify spring flow and diffuse groundwater accretion (their "field flow," Table 2). The resulting estimated accretions from Sunshine Valley to the Rio Grande and Red River are 33,809 af/yr and 8,283 af/yr, respectively (Table 2, Fig. 33). Winograd (1959) estimated these same quantities as 20,270 af/yr and 6,000 af/yr, although he did not provide details of the procedure used to reach those values.

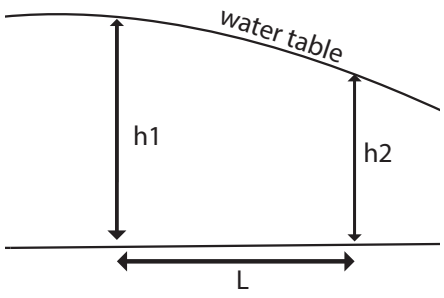

Figure 32. Geometry of the Dupuit approximation for unconfined groundwater flow. Parameters h1, h2, and L are enumerated in Table 3.

Table 3. Estimation of groundwater flux into the Rio Grande from the northern Taos Plateau. Flow is west to east along line segments perpendicular to river sections as shown in Figure 29. See Figure 32 for geometry of Dupuit approximation for unconfined flow; $q' = 0.5*K*(h_1^2-h_2^2)/L$. Calculations use geometric mean of basalt hydraulic conductivity reported in Drakos et al. (2004)

River Section 1		notes	River Section 4		notes
length, m	10,191.7		length, m	5,514.6	
water level at river (h2), ft	7,299	assumed to be at river level	water level at river (h2), ft	7,098	estimated from contours
river elevation, ft	7,299	from DEM	river elevation, ft	7,047	from DEM
h2, m	0		h2, m	15.54	
water level at h1, to west, ft	7,312	well TC209, Johnson and Bauer (2012)	water level at h1, to west, ft	7,319	well TC207, Johnson and Bauer (2012)
h1, m	3.96		h1, m	82.91	
L, from river to h1, m	3,961		L, from river to h1, m	5,211	
q` m^2/s	7.08E-08		q` m^2/s	2.27E-05	
volumetric flow, m^3/s	7.21E-04		volumetric flow, m^3/s	0.13	
volumetric flow, af/yr	18		volumetric flow, af/yr	3,204	
River Section 6		**notes**	**River Section 5**		**notes**
length, m	3,475		Segment is subparallel to flow-lines, so unit width perpendicu-lar to flow is ~ 0		
water level at river (h2), ft	7,077	estimated from contours	Water table is poorly con-strained west of river, cannot estimate possible flow to NE into river with Dupuit approximation		
river elevation, ft	6,614	from DEM	Assume Darcian flow thorough riverbed; q' = - Kh(dh/dl)		
h2, m	141.12		Estimate of river width is 75 m from satellite image in Figure 1		
water level at h1, to west, ft	7,305	well TC202, Johnson and Bauer (2012)	length m	2,459	length section 5
h1, m	210.62		dh	0.02	Change in water table elvation, upstream to downstream
L, from river to h1, m	8,640		h	42.37	Elevation of midpoint above downstream end
				2.61E-05	
q` m^2/s	5.05E-05		q` m^2/s	1.96E-03	
volumetric flow, m^3/s	0.18		volumetric flow, m^3/s	50	roughly 80 times less than Sections 4 and 6
volumetric flow, af/yr	4488		volumetric flow, af/yr		
River Sections 2, 3, 7, 8, and 9					

These sections are above the water table (Winograd, 1959, and this study) and/or identified as losing reaches by Kinzli et al (2011).

Discussion

A summary of the water budget and the components of Equation 2 is presented in Table 2 and Figure 33. If all inflows and outflows have been identified and quantified accurately, inflows should equal outflows if the aquifer system is in equilibrium and no water is being gained or lost from storage. The estimate of discharges, 43,252 af/yr, is intermediate between the total mountain front recharge quantities calculated using mean and median Cl values for both Recharge Scenarios 1 and 2. It is not a clear *a priori* whether results using the mean Cl value should be preferred over results using the median Cl value. The means are affected by the samples with Cl >15. If these were due to a spatially or temporally localized evapotranspiration process atypical of most of the natural recharge, then the calculations using the median values would be preferred. The three highest Cl samples are located adjacent to irrigated fields, so locally enhanced evapotranspiration is a possibility, but evapotranspiration of irrigation water prior to infiltration is accounted for in the CMB analysis. If the recharge calculations using the mean and median values are viewed as lower and upper bounds on the total quantities of mountain front recharge, then it is encouraging that the estimate of discharge is intermediate between the two bounds. Within the limits of this analysis alone, inflows approximately balance outflows and the Sunshine valley aquifer does not appear to be drastically out of equilibrium.

Anderholm (1994) estimated the contribution of groundwater flow to mountain front recharge in the Santa Fe area to be negligible. This is in strong contrast to the Sunshine Valley area, where more than half of the mountain front recharge constitutes groundwater flow, as estimated by the CMB analysis. Significant groundwater flow from the mountains is also indicated by the addition of sulfate-rich water in the southern portion of Sunshine Valley. There are distinct geologic differences between the Sunshine Valley and Santa Fe areas that can explain this contrast. Santa Fe is located along the east side of the west-tilted Española Basin of the Rio Grande rift, where rift-filling sediments of the Santa Fe Group thin and onlap onto igneous and metamorphic basement rocks of the Sangre de Cristo Mountains. Fault offsets along the mountain front are modest (Koning and Read, 2010). Sunshine Valley lies on the east side of the east-tilted San Luis basin, where rift-filling sediments and interlayered basalts are juxtaposed against the mountain front by west-side down normal faults with thousands of feet of vertical displacement and Holocene movement (Ruleman et al., 2013). There is much greater relief between the valley floor and the mountains to the east than in the Santa Fe area, which causes a strong hydraulic head gradient between the mountains and the aquifer in the valley. The range-front faults bounding Sunshine Valley also crosscut the Questa caldera (Lipman and Reed, 1989) and faults, fractures, and hydrothermal alteration associated with the caldera can facilitate westward movement of groundwater from the mountains to the valley aquifer. The warmer temperatures in the Johnson–Dimmitt well near one of the strands in Sunshine Valley fault zone and elevated discharge temperatures in wells TC-431 and TC-434 (Figs. 4, 19–20) near a splay of the Sangre de Cristo fault zone are consistent with a process of groundwater circulating deeply in the mountain block and discharging in the vicinity of youthful faults near the mountain front. Use of the CMB approach to document the contribution of significant quantities of deeply-circulated mountain block recharge to extensional basins could prove to be a useful geothermal exploration tool.

In Figure 9, it is clear that during both the 1950s–1980s and 1980s–2010s time intervals, water-level changes were varied with areas of increase and decrease across the study area. The changes in well networks over time results in variable robustness of the estimates of water level change. Nevertheless, there is not a spatial pattern of region-wide rise or fall of water levels over either time interval. The mean value of water level changes from the 1950s to the 1980s is -3.8 feet; the median is -2.3 feet. The mean value of the water level changes from the 1980s to the 2010s decade is -8.6 feet, and the median is -1.5 feet.

These water-level statistics imply net water-level declines and a net loss in storage. This can be roughly estimated with a few simple calculations. The loss from storage can be estimated first using an intermediate, uniform water-level decline value of 2 feet per year for the period of the 1950s to the 2010s, and a specific yield value of 0.15 (Rinehart et al., 2016) over the total area of surficial and valley-fill deposits in Sunshine Valley (363 km^2) (Fig. 4 and 6). This is assumed to represent the surface area of the shallow alluvial aquifer. Over 60 years from the 1950s to the 2010s, the total estimated amount of water lost from storage is ~26,900 acre-feet, or an average of 448 acre-feet/year.

Alternatively, using the same assumed specific yield value of 0.15, the net volume of water gained/lost from storage can be estimated in the regions where water levels rose/declined over the two 30 year time intervals shown in Figure 9. From the 1950s to the 1980s, losses outpaced gains by 28,380 acre-feet, or an average of 946 acre-feet/year. For the 1980s to the 2010s losses outpaced gains by 57,143 acre-feet, or an average of 2,065 acre-feet /year. Comparing the 1950s to the 2010s decades directly, the total loss from storage was 73,487 acre-feet, or an average of 1124 acre-feet/year over 60 years.

Rinehart et al. (2016) calculated water-level and groundwater-storage changes in alluvial basins of the Rio Grande rift, including the Sunshine Valley region. From the 1950s to the 1990s, Rinehart et al. (2016) indicated a similar pattern of variably rising and falling water levels across much of Sunshine Valley, as illustrated in Figure 9. Their interpolations covered a larger area than the water-level surfaces in the present study, so for comparison, the storage changes of Rinehart et al. (2016) were recalculated within the area of the 1980s water-level surface presented here. Within that area, the estimated yearly change in water in storage over the 40 year interval is 3,600 acre-feet/year. This is larger than the values calculated herein by about a factor of three when compared to the 1950s–2010s results shown above.

The three water-level surfaces in the present study are probably somewhat more accurate than those calculated by Rinehart et al. (2016) because more data was used, although some of it was of lesser quality (the static water levels reported on well logs). Water-level contours in the present study were hand-drawn, and roughly modelled after the original

work of Winograd (1959), whereas Rinehart et al. (2016) used an automated kriging procedure. Overall, it seems reasonable to conclude that the present study and the work of Rinehart et al. (2016) are in general agreement that an average of 1,000 to 3,000 acre-feet of storage has been lost per year over the past 30 to 40 years.

The few thousand acre-feet of storage lost per year represents the ΔS term in equation 2 and indicates that there has been a progressive net loss of water from the Sunshine Valley aquifer for some time. The uncertainty in the quantity of mountain-front recharge is large enough that this loss cannot be independently assessed by comparing inflows and outflows in this equation. A serious limitation to the water budget analysis is that discharge and spring-flow data do not all span the same time period, and in some cases we are limited to only one-time measurements, such as the data from Vail Engineering (1993) (Appendix C). A groundwater flow model based on detailed subsurface geology, quantification of hydrologic properties, and the spatial variability of both is probably required to improve on these results, but would still be hampered by the basic data constraints. These types of data limitations are not unique to this study or area, and are a fundamental issue going forward as more in-depth studies are required to better understand hydrologic systems and develop management policies (e.g., Grafton et al., 2018).

Some insight into the storage changes and the equilibrium state of the aquifer can be gained from the temporal trends in precipitation, air temperature, and water use. The smoothed trend of yearly precipitation in Figure 3 shows fluctuations around a fairly stable trend of 12–13 inches per year in Cerro from the 1940s to the 1990s, and then a slight decline to the present (2015 is the most recent year with complete data). The smoothed trend for Red River

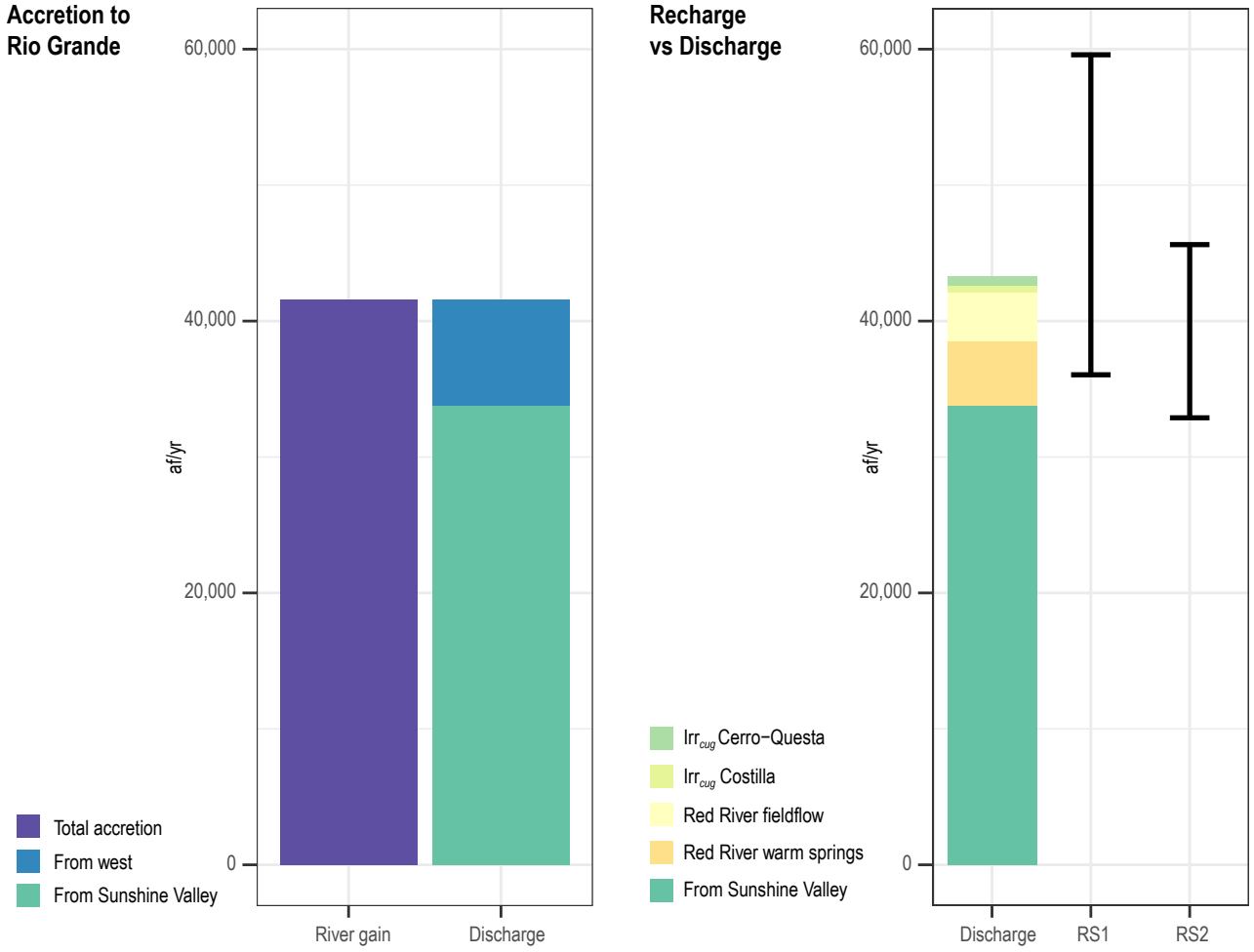

Figure 33. Summary of the water budget for the Sunshine Valley aquifer. RS1 and RS2 are chloride mass-balance Recharge Scenarios 1 and 2, respectively. Vertical black bars connect the mean- and median-Cl estimates for each scenario. Irr_{cug} is groundwater consumptive use as reported by the New Mexico Office of the State Engineer (2018).

shows an increasing trend from the mid-1950s to the 1990s, followed by a distinct decreasing trend from the mid-1990s to the present. The regional drought of the 1950s (Thomas et al., 1963; Nace and Pluhowski, 1965) is evident in the Red River precipitation trend; this is also the time period that intensive irrigation began in Sunshine Valley. Winograd (1959) estimated groundwater pumping in Sunshine Valley in 1955 to total 3,500 acre-feet (Fig. 2). Declining water levels in the 1950s reflect these two factors (Fig. 10). Water levels recovered in the following decades coincident with increases in mountain precipitation.

The average and median consumptive use of groundwater in the Sunshine Valley region from the 1950s to the 2010s were 2,160 and 1,280 acre-feet/year, respectively. The median value is comparable to the estimates of losses from storage calculated in this study. Yet groundwater pumping for irrigation has dropped by about half since 1980, while surface water use has increased (Fig. 2). Spreading of surface water across fields during irrigation increases evapotranspiration losses compared to the same amount of water infiltrating in stream channels; thus more potential recharge from streams is likely lost with increased surface water irrigation.

Figure 3 shows yearly total streamflow summed from the monthly averages for the Red River and Costilla Creek from 1980 to 2010. Even with the high variability, streamflow shows declines since 1980. Based on a linear fit to the Costilla Creek data the average yearly flow was roughly 10,000 acre-feet (~25%) less in 2010 than in 1980. The nonlinear curve fit shows a distinct decline in streamflow in the early 2000s and an increase in streamflow in the latter part of the decade. The streamflow declines from about 1990 are correlated in time with decreases in precipitation and increases in temperature at the towns of Cerro and Red River.

Udall and Overpeck (2017) illustrated the effect that increasing temperatures since 2000 have had on decreasing flow in the Colorado River. Increased precipitation is required to keeps flows stable with increasing temperature. For example, for the entire Colorado River basin, a 25% potential loss in flow due to increased temperatures requires an approximately 10% increase in precipitation to keep actual flows stable. Increasing temperatures will also increase ET demand. Thus larger irrigation diversions will be required to sustain the same crops and acreage.

The streamflow declines are significant and will greatly affect recharge to the Sunshine Valley aquifer because very little of the flow from the drainages entering Sunshine Valley ever travels to the Rio Grande. From the CMB analysis it was estimated that about 66% of the mountain-front recharge occurs as groundwater flow moving laterally from the Sangre de Cristo range; obviously declining precipitation and increasing temperature will decrease this quantity as well. It is probable that the losses from storage in Sunshine Valley are the combined effect of decreased precipitation and increased temperatures over the past 20 to 30 years with the additional influence of increased evapotranspiration due to larger surface water diversions for irrigation.

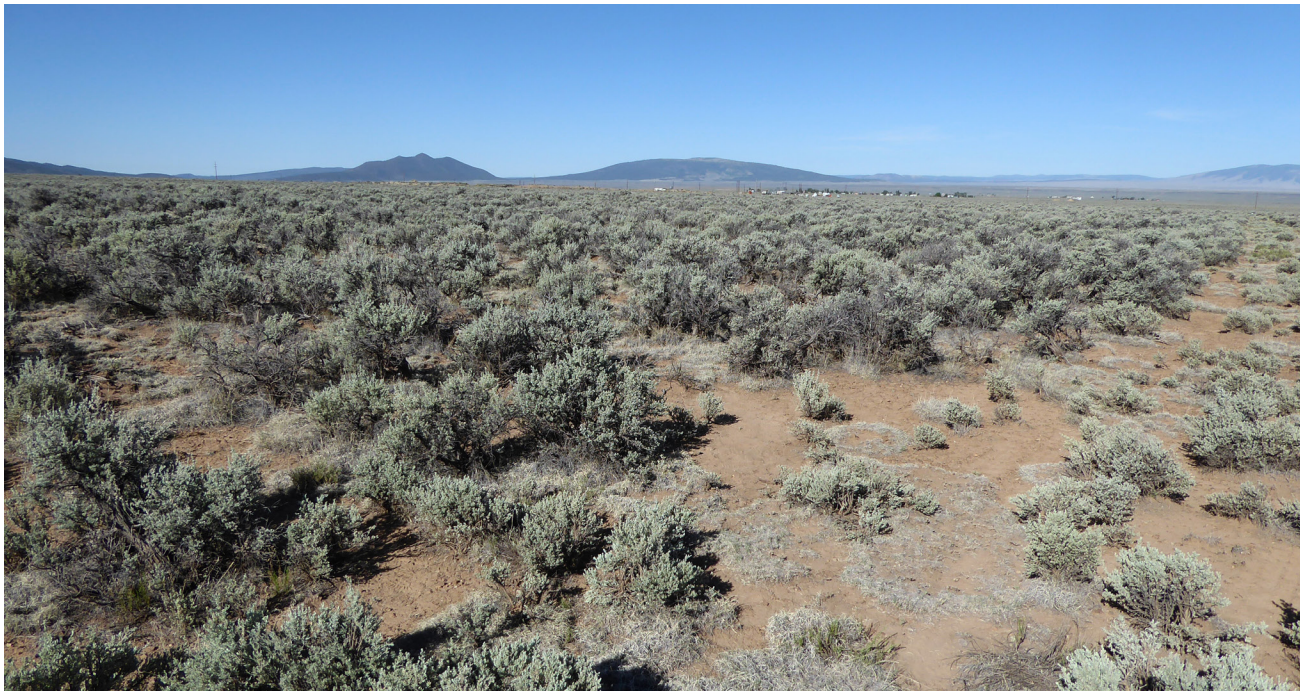

View to the west across Sunshine Valley.

XII. CONCLUSIONS

The Sunshine Valley aquifer is laterally and vertically heterogeneous, with sand and gravel layers overlying and interbedded with fractured and highly transmissive basalt flows. Low-permeability, clay-rich lake bed deposits in the central valley cause local semi-perched and semi-artesian conditions, as defined and described by Winograd (1959). The TEM survey did not identify the shallow clay-rich deposits, but did locate a resistive layer at a depth of 210–215 feet that is apparently underlain by a more conductive unit. The resistive layer is interpreted to be a fresh water aquifer in sand and gravel.

Groundwater recharge occurs in the Sangre de Cristo Mountains to the east of the valley, largely sourced from high-elevation winter precipitation. Little or no areal recharge occurs across the valley floor. Recharge arrives in the valley aquifer as infiltrating streamflow and irrigation water derived from streamflow. More than half of the recharge occurs as groundwater underflow into the aquifer directly from the mountain block, resulting in locally elevated discharge temperatures and perturbations in thermal profiles in wells near youthful faults. The very steep range front and extreme relief from the valley floor to the adjacent peaks, recently-active range-front faults, and abundant faults, fractures, and hydrothermal alteration in the mountain block associated with the Questa caldera all play a role in the large amount of lateral groundwater movement into the aquifer. As a consequence, previously unrecognized geothermal resources may be present beneath Sunshine Valley, particularly in an area a few miles south of Costilla.

Groundwater storage changes calculated from sequential water-level elevation surfaces indicate average groundwater storage losses of 1,000 to 3,000 acre-feet per year since the 1980s. These storage changes correspond to average water-level declines of a few feet per year across the region. The water budget calculations results yield estimated discharges falling between the estimated upper and lower bounds of recharge inputs. However, the water budget analysis is constrained by fundamental data limitations and is neither accurate nor precise enough to independently confirm or refute the groundwater storage losses based on the sequential water-level elevation surfaces.

Reduction of groundwater pumping due to the Aamodt settlement water-rights transfer can ultimately result in additional water flowing through the Sunshine Valley aquifer to discharge in the Rio Grande and Red River. The time scale for this to occur is on the order of several tens of years at least. Current levels of groundwater withdrawals for irrigation do not appear likely to be the main cause of the storage changes since the 1980s. Trends in regional precipitation, temperature, and surface-water use are more likely factors affecting the amount of water in storage in the Sunshine Valley aquifer and the discharge amounts. Regardless of the amount of groundwater pumping, continued declines in annual precipitation and streamflow and increases in mean annual temperature will decrease the amount of recharge to and discharge from Sunshine Valley.

ACKNOWLEDGMENTS

We thank the Healy Foundation, Aquifer Mapping Program, and the New Mexico Bureau of Geology and Mineral Resources for funding this research. Previous work by Kylian Robinson supplemented this project. Ginger McLemore provided many references pertaining to the Questa region and the Molycorp Molybdenum Mine. Scott Christenson assisted in sample collection and water-level measurements. Ethan Mamer assisted with temperature measurements and the TEM surveys. Kitty Pokorny provided database support. Bernie Torres of Costilla, New Mexico, was invaluable in facilitating contact with landowners, to whom we are grateful for providing access to their property and wells. Constructive reviews by Joe Marcoline, Talon Newton, and Stacy Timmons improved this report. Production editing was done by Jennifer Eoff and Belinda Harrison.

REFERENCES

Aamodt Settlement Agreement, 2018, https://www.santafecountynm.gov/public_works/utilities/aamodt (accessed November 2018).

Alcala, F.J., and Custodio, E., 2008, Using the Cl/Br ratio as a tracer to identify the origin of salinity in aquifers in Spain and Portugal: Journal of Hydrology, v. 359, p. 189–207.

Anderholm, S. K., 1994, Ground-water recharge near Santa Fe, north-central New Mexico: U.S. Geological Survey Water-Resources Investigation Report 94-4078, 68 p.

Baldridge, W.S., Dickerson, P.W., Riecker, R.E., and Zidek, J., eds., 1984, Rio Grande rift (northern New Mexico): New Mexico Geological Society Fall Field Conference Guidebook 35, 379 p.

Bankey, V., Grauch, V.J.S., Webbers, A., and PRJ, Inc., 2005, Digital data and derivative products from a high-resolution aeromagnetic survey of the central San Luis Basin, covering parts of Alamosa, Conejos, Costilla, and Rio Grande Counties, Colorado, and Taos County, New Mexico: U.S. Geological Survey Open-File Report 2005-1200: http://pubs .usgs.gov/of/2005/1200/.

Bankey, V., Grauch, V.J.S., Drenth, B., and Geophex, Inc., 2006, Digital data from the Santa Fe East and Questa–San Luis helicopter magnetic surveys in Santa Fe and Taos Counties, New Mexico, and Costilla County, Colorado: U.S. Geological Survey Open-File Report 2006-1170: http://pubs.usgs.gov/of/2006/1170/.

Bauer, P.W., Lucas, S.G., Mawer, C.K., and McIntosh, W.C., eds., 1990, Tectonic development of the southern Sangre de Cristo Mountains, New Mexico: New Mexico Geological Society Fall Field Conference Guidebook 41, 450 p.

Bauer, P.W., Johnson, P.S., and Timmons, S.W., 2007 (updated 2017), Springs of the Rio Grande gorge, Taos County, New Mexico: Inventory, data report, and preliminary geochemistry: New Mexico Bureau of Geology and Mineral Resources Open-File Report 506, 54 p.

Best, M.G., 1982, Igneous and metamorphic petrology: San Francisco, California, W.H. Freeman and Company, 630 p.

Brister, B., Bauer, P.W., Read, A.S., and Leuth, V.W., eds., 2004, Geology of the Taos region: New Mexico Geological Society Fall Field Conference Guidebook 55, 440 p.

Bliss, J.H., and Osgood, E.P., 1928, Seepage study on Rio Grande between State Line Bridge, Colorado, and Embudo, New Mexico, and between Alamosa, Colorado, and Embudo, New Mexico: New Mexico State Engineer 9th Biennial Report, 1928–1930, p. 27–40.

Canaris, N., Kludt, T., and Newton, B.T., 2011, Canopy interception loss for a mixed coniferous forest in southern New Mexico prior to tree-thinning treatment: New Mexico Geological Society Annual Spring Meeting, New Mexico Tech, Socorro, New Mexico, April 2011, Abstracts, p. 14.

Clark, I., and Fritz, P., 1997, Environmental isotopes in hydrogeology: New York, Lewis Publishers, 328 p.

Cook, P.G., and Dogramici, S., 2019, Estimating recharge from recirculated groundwater with dissolved gases: An end-member mixing analysis: Water Resources Research, v. 55, doi:10.1029/2019WR025012.

Craig, H., 1961, Isotopic variations in meteoric water: Science, v. 133, p. 1702–1703.

Darr, M.J., 2011, Hydrogeology of southeast Sunshine Valley, New Mexico, *in* Koning, D.J., Karlstrom, K.E., Kelley, S.A., Lueth, V.W., and Aby, S.B., eds., Geology of the Tusas Mountains and Ojo Caliente: New Mexico Geological Society Fall Field Conference Guidebook 62, p. 329–338.

Drakos, P., Lazarus, J., White, B., Banet, C., Hodgins, M., Riesterer, J., and Sandoval, J., 2004, Hydrologic characteristics of basin-fill aquifers in the southern San Luis Basin, New Mexico, *in* Brister, B., Bauer, P.W., Read, A.S., and Leuth, V.W., eds., Geology of the Taos region: New Mexico Geological Society Field Conference Guidebook 55, p. 391–404.

Drakos, P., Tahoya, A.J., Lazarus, J., and Riesterer, J., 2018, Alpine hydrology of Phoenix Spring and Lake Fork of the Rio Hondo, Taos Ski Valley, NM: New Mexico Geological Society Annual Spring Meeting, New Mexico Tech, Socorro, New Mexico, April 2018, Abstracts, p. 25.

Drenth, B.J., Grauch, V.J.S., and Rodriguez, B.D., 2013, Geophysical constraints on Rio Grande rift structure in the central San Luis Basin, Colorado and New Mexico, *in* Hudson, M.R., and Grauch, V.J.S., eds., New perspectives on Rio Grande rift basins: From tectonics to groundwater: Geological Society of America Special Paper 494, p. 75–99, doi:10.1130/2013.2494(04).

Dungan, M.A., Muehlberger, W.R., Leininger, L., Peterson, C., McMillan, N.J., Gunn, G., Lindstrom, M., and Haskin, L., 1984, Volcanic and sedimentary stratigraphy of the Rio Grande gorge and the late Cenozoic geologic evolution of the southeastern San Luis Valley, *in* Baldridge, W.S., Dickerson, P.W., Riecker, R.E., and Zidek, J., eds., Rio Grande rift: Northern New Mexico: New Mexico Geological Society Fall Field Conference Guidebook 35, p. 157–170.

Edwards, C.L., Reiter, M., Shearer, C., and Young, W., 1978, Terrestrial heat flow and crustal radioactivity in northeastern New Mexico and southeastern Colorado: Geological Society of America Bulletin, v. 89, p. 1341–1350.

Emery, P.A., Boettcher, A.J., Snipes, R.J., and McIntyre, H.J., Jr., 1971, Hydrology of the San Luis Valley, south-central Colorado: U.S. Geological Survey Hydrologic Atlas 381, 2 plates.

Feth, J.H., 1981, Chloride in natural continental water—A review: U.S. Geological Survey Water-Supply Paper 2176, 30 p.

Fetter, C.W., 2001, Applied hydrogeology: Upper Saddle River, New Jersey, Prentice-Hall, 598 p.

Garrabrandt, L.A., 1993, Water resources of Taos County: U.S. Geological Survey Water-Resources Investigation Report 93-4107, 86 p.

Grafton, R.Q., Williams, J., Perry, C.J., Molle, F., Ringler, C., Steduto, P., Udall, B., Wheeler, S.A., Wang, Y., Garrick, D., and Allen, R.G., 2018, The paradox of irrigation efficiency: Science, v. 361, p. 748–750, doi:10.1126/science.aat9314.

Hearne, G.A., and Dewey, J.D., 1988, Hydrologic analysis of the Rio Grande basin north of Embudo, New Mexico, Colorado and New Mexico: U.S. Geological Survey Water Resources Investigation Report 86-4113, 251 p.

Hacker, L.W., and Carleton, J.O., 1982, Soil survey of Taos County and parts of Rio Arriba and Mora Counties, New Mexico: Washington, D.C., U.S. Government Printing Office, 220 p.

Hem, J.D., 1985, Study and interpretation of the chemical characteristics of natural water: U.S. Geological Survey Water Supply Paper 2254, 218 p.

Hounslow, A.W., 1995, Water quality data: Analysis and interpretation: New York, CRC Press, 397 p.

Ingersoll, R.V., Cavazza, W., Baldridge, W.S., and Shafiqullah, M., 1990, Cenozoic sedimentation and paleotectonics of north-central New Mexico: Implications for initiation and evolution of the Rio Grande rift: Geological Society of America Bulletin, v. 102, p. 1280–1296.

Jochems, A.P., Haller, K.M., and Koning, D.J., 2016, An updated map of Quaternary faults and folds in New Mexico: Geological Society of America Abstracts with Programs, v. 48, no. 7, doi:10.1130/abs/2016AM-280631.

Johnson, P.S., 1998, Surface-water assessment, Taos County, New Mexico: New Mexico Bureau of Geology and Mineral Resources Open-File Report 440, 332 p.

Johnson, P.S., Bauer, P.W., and Felix, B., 2016, Hydrogeologic investigation of the southern Taos Valley, Taos County, New Mexico: New Mexico Bureau of Geology and Mineral Resources Open-File Report 581, 101 p.

Johnson, P.S., and Bauer, P.W., 2012, Hydrogeologic investigation of the northern Taos Plateau, Taos County, New Mexico: New Mexico Bureau of Geology and Mineral Resources Open-File Report 544, 96 p.

Kelson, K.I., and Bauer, P.W., 2013, Geologic map of the Questa 7.5-minute quadrangle, Taos County, New Mexico: New Mexico Bureau of Geology and Mineral Resources Open-File Geologic Map OF-GM-247, scale 1:24,000.

Kelson, K.I., Bauer, P.W., and Thompson, R.A., 2008, Geologic map of the Guadalupe Mountain 7.5-minute quadrangle map, Taos County, New Mexico: New Mexico Bureau of Geology and Mineral Resources Open-File Geologic Map OF-GM-168, scale 1:24,000.

Kinzli, K.D., Shafike, N., Bauer, P., Lundahl, A., Schmidt-Petersen, R., Harris, S., Lewis, G., Johnson, P., and Timmons, M., 2011, Quantifying river accretion in the upper Rio Grande gorge, New Mexico, by using an acoustic Doppler current profiler: River Research and Applications, v. 29, p. 4–16, doi:10.1002/rra.1581.

Koning, D.J., and Read, A.S., 2010, Geologic map of the southern Española Basin: New Mexico Bureau of Geology and Mineral Resources Open-File Report 531, scale 1:48,000.

Kurylyk, B.L., Irvine, D.J., and Bense, V.F., 2018, Theory, tools, and multidisciplinary applications for tracing groundwater fluxes from temperature profiles: WIREs Water, e1329, doi:10.1002/wat2.1329.

Lewis, A.C., 2018, Monitoring effects of wildfire mitigation treatments on water budget components: A paired basin study in the Santa Fe watershed, New Mexico: New Mexico Bureau of Geology and Mineral Resources Bulletin 163, 52 p.

Lewis, W.M., Grant, M.C., and Saunders, J.F., 1984, Chemical patterns of bulk atmospheric deposition in the State of Colorado: Water Resources Research, v. 20, p. 1691–1704.

Lipman, P.W., and Mehnert, H.H., 1979, The Taos Plateau volcanic field, northern Rio Grande rift, New Mexico, *in* Riecker, R.E., ed., Rio Grande rift: Tectonics and magmatism: Washington, D.C., American Geophysical Union, p. 289–311.

Lipman, P.W., and Reed, J.C., 1989, Geologic map of the Latir volcanic field and adjacent areas, northern New Mexico: U.S. Geological Survey Miscellaneous Investigations Series Map I-1907, 2 sheets.

Longworth, J.W., Valdez, J.M., Magnuson, M.L., Albury, E.S., and Keller, J., 2008, New Mexico water use by categories 2005: New Mexico Office of the State Engineer Technical Report 52, 122 p.

Longworth, J.W., Valdez, J.M., Magnuson, M.L., and Richard, K., 2013, New Mexico water use by categories 2010: New Mexico Office of the State Engineer Technical Report 54, 144 p.

Ludington, S., Plumlee, G., Caine, J., Bove, D., Holloway, J., and Livo, E., 2005, Geologic influences on ground and surface waters in the Red River watershed, New Mexico: U.S. Geological Survey Scientific Investigations Report 2004-5245, 41 p.

Macdonald, L.H., and Stednick, J.D., 2003, Forests and water: A state of the art review for Colorado: Colorado Water Resources Research Institute Completion Report 196, 75 p.

Machette, M.N., Coates, M.M., and Johnson, M.L., eds., 2007, Quaternary geology of the San Luis Basin of Colorado and New Mexico, *in* Rocky Mountain Section Friends of the Pleistocene Field Trip, September 2007: U.S. Geological Survey Open-File Report 2007-1193, 197 p.

Machette, M.N., Thompson, R.A., Marchetti, D.W., and Smith, R.S.U., 2013, Evolution of ancient Lake Alamosa and integration of the Rio Grande during the Pliocene and Pleistocene, *in* Hudson, M.R., and Grauch, V.J.S., eds., New perspectives on Rio Grande rift basins: From tectonics to groundwater: Geological Society of America Special Paper 494, p. 1–20, doi:10.1130/2013.2494(01).

Maest, A.S., Nordstrom, D.K., and LoVetere, S.J., 2004, Questa baseline and pre-mining ground-water quality investigation 4: Historical surface-water quality for the Red River valley, New Mexico, 1965 to 2001: U.S. Geological Survey Scientific Investigations Report 2004-5063, 160 p.

Nace, R.L., and Pluhowski, E.J., 1965, Drought of the 1950's with special reference to the midcontinent: U.S. Geological Survey Water Supply Paper 1804, 93 p.

New Mexico Bureau of Geology and Mineral Resources, 2003, Geologic Map of New Mexico, scale 1:500,000, 2 sheets.

Nordstrom, D.K., 2008, Questa baseline and pre-mining ground-water quality investigation 25: Summary of results and baseline and pre-mining groundwater geochemistry, Red River valley, Taos County, New Mexico, 2001–2005: U.S. Geological Survey Professional Paper 1728, 111p.

Parkhurst, D.L., and Appelo, C.A.J., 1999, User's guide to PHREEQC (Version 2)—A computer program for speciation, batch-reaction, one-dimensional transport, and inverse geochemical calculations: U.S. Geological Survey Water-Resources Investigations Report 99-4259, 310 p.

Plumlee, G.S., Ludington, S., Vincent, K.R., Verplanck, P.L., Caine, J.S., and Livo, K.E., 2006, Questa baseline and pre-mining ground-water quality investigation 7: A pictorial record of chemical weathering, erosional processes, and potential debris-flow hazards in scar areas developed on hydrothermally altered rocks: U.S. Geological Survey Open-File Report 2006-1205, 19 p.

Popp, C.J., Ohline, R.W., Brandvold, D.K., and Brandvold, L.A., 1984, Nature of precipitation and atmospheric particulates in central and northern New Mexico, in Hicks, B.B., ed., Deposition both wet and dry: London, Butterworth Publishers, p. 79–95.

PRISM Climate Group, 2018, 30-year average precipitation data for New Mexico: http://www.prism.oregonstate.edu/ (accessed October 2018).

Rawling, G.C., 2016, A hydrogeologic investigation of Curry and Roosevelt Counties, New Mexico: New Mexico Bureau of Geology and Mineral Resources Open-File Report 580, 48 p.

Rawling, G.C., and Newton, B.T., 2016, Quantity and location of groundwater recharge in the Sacramento Mountains, south-central New Mexico (USA), and their relation to the adjacent Roswell Artesian Basin: Hydrogeology Journal, v. 24, p. 757–786, doi:10.1007/s10040-016-1399-6.

Reiter, M., Edwards, C.L., Hartman, H., and Weidman, C., 1975, Terrestrial heat flow along the Rio Grande rift, New Mexico and southern Colorado: Geological Society of America Bulletin, v. 86, p. 811–818.

Rinehart, A.J., Mamer, E., Kludt, T., Felix, B., Pokorny, C., and Timmons, S., 2016, Groundwater level and storage changes in alluvial basins in the Rio Grande basin, New Mexico: New Mexico Water Resources Research Institute Technical Completion Report, 41 p.

Robinson, K., 2018, Hydrogeology of the Questa area: End-member mixing analysis of shallow groundwater [M.S. Thesis]: New Mexico Institute of Mining and Technology, Socorro, New Mexico, 181 p.

Ruleman, C., Shroba, R., and Thompson, R., 2007, Quaternary geology of Sunshine Valley and associated neotectonics along the Latir Peaks section of the Southern Sangre de Cristo fault zone, *in* Machette, M.N., Coates, M.M., and Johnson, M.L., eds., Quaternary geology of the San Luis Basin of Colorado and New Mexico, Rocky Mountain Section Friends of the Pleistocene Field Trip, September 2007: U.S. Geological Survey Open-File Report 2007-1193, p. 111–133.

Ruleman, C., Thompson, R.A., Shroba, R.R., Anderson, M., Drenth, B.J., Rotzien, J., and Lyon, J., 2013, Late Miocene–Pleistocene evolution of a Rio Grande rift subbasin, Sunshine Valley–Costilla Plain, San Luis Basin, New Mexico and Colorado, *in* Hudson, M.R., and Grauch, V.J.S., eds., New perspectives on Rio Grande rift basins: From tectonics to groundwater: Geological Society of America Special Paper 494, p. 47–73, doi:10.1130/2013.2494(03).

Saar, M.O., 2011, Review: Geothermal heat as a tracer of large-scale groundwater flow and as a means to determine permeability fields: Hydrogeology Journal, v. 19, p.31–52, doi:10.1007/s10040-010-0657-2.

Summers, W.K., and Hargis, L.L., 1984, Hydrogeologic cross section through Sunshine Valley, Taos County, New Mexico, *in* Baldridge, W.S., Dickerson, P.W., Riecker, R.E., and Zidek, J., eds., Rio Grande rift (northern New Mexico): New Mexico Geological Society Fall Field Conference Guidebook 35, p. 245–248.

Thomas, H.E., and others, 1963, Drought in the southwest 1942–56: Effects of drought in the Rio Grande basin: U.S. Geological Survey Professional Paper 372-D, 59 p.

Thompson, R.A., Turner, K.J., Shroba, R.R., Cosca, M.A., Ruleman, C.A., Lee, J.P., and Brandt, T.R., 2014a, Geologic map of the Sunshine 7.5-minute quadrangle, Taos County, New Mexico: U.S. Geological Survey Scientific Investigations Map 3283, scale 1:24,000.

Thompson, R.A., Turner, K.J., Shroba, R.R., Cosca, M.A., Ruleman, C.A., Lee, J.P., and Brandt, T.R., 2014b, Geologic map of the Ute Mountain 7.5-minute quadrangle, Taos County, New Mexico, and Conejos and Costilla Counties, Colorado: U.S. Geological Survey Scientific Investigations Map 3284, scale 1:24000.

Udall, B., and Overpeck, J., 2017, The twenty-first century Colorado River hot drought and implications for the future: Water Resources Research, v. 53, p. 2404–2418, doi:10.1002/2016WR019638.

USGS NWIS, 2018, Surface water data for New Mexico: U.S. Geological Survey National Water Information System: https://waterdata.usgs.gov/nm/nwis/sw (accessed September 2018).

Vail Engineering, 1993, Analysis of tailing pond seepage flow to the Red River: Unpublished report to Molycorp, Inc., 24 p.

Wade, S.C., and Reiter, M., 1994, Hydrothermal estimation of vertical ground-water flow, Cañutillo, Texas: Groundwater, v. 32, p. 735–742, doi:10.1111/j.1745-6584.1994.tb00914.x.

Western Regional Climate Center, 2018: Reno, Nevada: https://wrcc.dri.edu/ (accessed November 2018).

Winograd, I.J., 1959, Ground-water conditions and geology of Sunshine Valley and western Taos County, New Mexico: New Mexico Office of the State Engineer Technical Report 12, 86 p.

Winograd, I.J., 1985, Hydrogeologic cross section through Sunshine Valley, Taos County, New Mexico: Comment: New Mexico Geology, v. 7, p. 54–55.

Wilson, J.L, and Guan, H., 2004, Mountain-block hydrology and mountain front recharge, *in* Hogan, J.F., Phillips, F.M., and Scanlon, B.R., eds., Groundwater recharge in a desert environment: Washington, D.C., American Geophysical Union, p. 113–137.

Wood, W.W., 1999, Use and misuse of the chloride-mass balance method in estimating groundwater recharge: Groundwater, v. 37, p. 2–3.

Wood, W.W., and Sanford, W.E., 1995, Chemical and isotopic methods for quantifying ground-water recharge in a regional, semiarid environment: Groundwater, v. 33, p. 458–468.

Zhu, C., Winterle, J.R., and Love, E.I., 2003, Late Pleistocene and Holocene groundwater recharge from the chloride mass balance method and chlorine-36 data: Water Resources Research, v. 39, p. 1182 (unpaginated, 15 pages), doi:10.1029/2003WR001987.

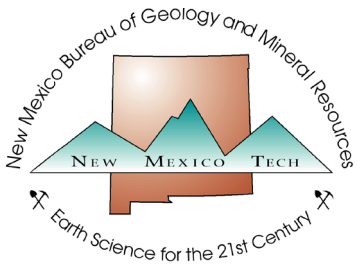

New Mexico Bureau of Geology and Mineral Resources

A Research Division of New Mexico Institute of Mining and Technology

Socorro, NM 87801
(575) 835 5490
www.geoinfo.nmt.edu